LIFE
Climate Change Mitigation

<u>Deliverable C.2:</u> Projections of future climatic conditions for tree crop categories in S. Europe

Month Year

Deadline of deliverable: 31/01/2018

LIFE CLIMATREE (LIFE14 CCM/GR/ 000635)

A novel approach for accounting and monitoring carbon sequestration of tree crops and their potential as carbon sink areas

The **LIFE CLIMATREE** project "A novel approach for accounting and monitoring carbon sequestration of tree crops and their potential as carbon sink areas" (LIFE14 CCM/GR/000635) is co-funded by the EU Environmental Funding Programme **LIFE Climate Change Mitigation**.

Implementation period: 16.7.2015 until 28.6.2019

Project budget: Total budget: 1,931,447 €
EU financial contribution: 1,158,868 €

Participating Beneficiaries:

University Research Institute
urban environment human resources Panteion University, Athens

ΓΕΩΠΟΝΙΚΟ ΠΑΝΕΠΙΣΤΗΜΙΟ ΑΘΗΝΩΝ
AGRICULTURAL UNIVERSITY OF ATHENS

UNIVERSITY OF WESTERN MACEDONIA

ferra nova

UNIVERSITÀ DEGLI STUDI DELLA BASILICATA

CSIC
CONSEJO SUPERIOR DE INVESTIGACIONES CIENTÍFICAS

Table of Contents

Summary **3**

1. Introduction **7**

2. Methods **9**

2.1. General Circulation Model 9

2.2. Regional Climate Model - Downscaling 10

3. Results **11**

3.1. General Circulation Model 11

3.2. Regional Climate Model - Downscaling 19

4. Conclusion **29**

References **30**

Annex 1: Seasonal global average GCM parameters and their change for RCP8.5 **35**

Annex 2: Seasonal global average GCM parameters and their change for RCP4.5 **55**

Annex 3: Monthly average temperature change for RCP8.5 **75**

Annex 4: Monthly average precipitation change for RCP8.5 **81**

Annex 5: Monthly average temperature change for RCP4.5 **87**

Annex 6: Monthly average precipitation change for RCP4.5 **93**

Summary

BACKGROUND: During the last years there is an increasing interest related to the climate change over Mediterranean. Mediterranean area is one of the most vulnerable regions of the globe given that large climate shifts have been observed in the past. As a result, Mediterranean has been identified as one of the most prominent "Hot-Spots" in future climate change projections. It is located in a transition zone between the arid climate of northern Africa and the wet climate of central Europe and even a minor change in large scale climatic factors might impose large impacts on the climatic conditions of different Mediterranean areas. Furthermore, the complex topography and the vast coastlines suggest a fine scale spatial variability of the climatic conditions.

Tree crops cultivation is affected by parameters related to climatic conditions. Therefore, future climate will affect tree crops cultivation conditions in S. Europe, suggesting changes in the carbon balance of tree-ecosystem for the future years. The objective of this Action is to estimate the changes in the climatic conditions affecting tree crops cultivation. For this reason, the NASA GISS GCM ModelE2 is used to simulate current and future climate under two different Representative Concentration Pathways: the RCP8.5 and the RCP4.5. However, the outputs from the GCM are relatively coarse (i.e., $1^{\circ} \times 1.25^{\circ}$) for applications to regional and local scales. The need for regional climate projections in a finer grid size (i.e., 9 Km x 9 Km) is assessed, here, using the Weather Research and Forecasting (WRF) model to dynamically downscale GCM simulations. The goal is to generate more locally relevant projections of long-term weather patterns over S. Europe.

RESULTS: General Circulation Model: Global average temperature for historical years (i.e., 1981-2010) is estimated at 14.2 °C, while an increase of 1.3 °C and 1 °C for RCP8.5 and RCP4.5 is assessed, respectively, confirming the increasing trend in future temperature (i.e., 2031–2060). This trend is also noticed in the domain of our interest. Global average precipitation rate for the historic period is estimated at 3 mm/day while under RCP8.5 and RCP4.5 an increase of 0.1 mm/day is noted suggesting an almost stable precipitation rate on average over globe. However, precipitation is very location dependent suggesting regions with increasing or decreasing trends in the precipitation rates. As such, the need for regional climate projections in a finer grid size is necessary, as mentioned above. Global average relative humidity (RH) for the historic

period is estimated at 74%. RH is not zonally uniform, presenting centers of various intensities at all latitudes. Under RCP8.5 and RCP4.5 an increase of 0.2% is noted suggesting an almost stable RH on average over globe. Although on average RH presents a modest increase, GISS-E2-R simulates a land–ocean contrast in response to the larger warming seen over land than over ocean. Compared to the historic data, RH tends to slightly increase over oceans but decrease over significant part of the land. The annual average solar radiation incident at the Earth's surface or downward solar radiation is 192 W/m2 for the historical years. As expected higher values are seen in the region between mid-latitudes. The simulation for the future indicate that the downward solar radiation remains stable, presenting though local variations that range between -21.4 W/m2 and 17.5 W/m2 under RCP8.5 and between -21.6 W/m2 and 13.8 W/m2 under RCP4.5.

Regional Climate Model – Downscaling: Temperature changes between current (i.e., 2008 – 2012) and future years (i.e., 2048-2052) for RCP8.5 over Greece, Italy and Spain is estimated in the range of 0.0 - 0.5 degrees, 0.25 - 1.25 degrees and 0.5 - 1.5 degrees, respectively. The maximum increase up to 1.5 degrees is estimated over north – northeastern Spain while the minimum increase up to 0.25 degrees is estimated over eastern Greece. Temperature increase has been found over Greece, Italy and Spain for all seasons with an exception for Greece during spring where a small reduction (i.e., up to 0.5 degrees) is found. The maximum increase for Greece is estimated up to 1 degrees during winter, autumn and summer while the maximum increase for Italy and Spain is estimated 2 degrees during winter and 2.5 degrees during summer, respectively. Precipitation change is very location and seasonal dependent presenting a mixed trend. Annual precipitation is estimated to be lower all over Spain (up to 60%, locally). Annual precipitation change over Italy is estimated in the range of ±40% where decreases are found to the north and increases to the south. Annual precipitation change over Greece is estimated in the range of ±20%. During winter the general trend presents a decrease in the precipitations rates over the continental regions. During spring reduction in precipitation rates over Spain and Italy is dominant. Over Greece precipitation is estimated to decrease only over the northern part. During summer precipitation rates over Spain are estimated to decrease mainly at the south of the country, while there are regions mainly at the north where precipitation is found to increase. This is not the case for the other two countries where reduction is dominant

over Italy and increase is dominant over Greece. During autumn reduction in the precipitation rates over Spain is dominant. Over Italy precipitation is estimated to increase at the south and to decrease at the north. Over Greece higher precipitation rates are estimated for most of the country.

Temperature change between current (i.e., 2008 – 2012) and future years (i.e., 2048-2052) for RCP4.5 is estimated to be higher over Spain and northern Italy and lower over southern Italy and Greece. Over Spain annual temperature is found higher in the range 0.0 - 1.0 degrees. Over Italy an increase in the range of 0.0 - 0.5 degrees is estimated at the north and a decrease up to 0.25 degrees is estimated at the south. Over Greece annual temperature is estimated lower in the range 0.0 - 0.5 degrees. The maximum increase for Spain is estimated up to 1.25 degrees during autumn while the maximum increase for Italy is estimated up to 1.75 degrees during winter. The maximum increase for Greece is estimated up to 0.25 degrees during autumn while the maximum decrease is estimated up to 1 degree during spring. Precipitation change is very location and seasonal dependent. Annual precipitation is estimated to be lower over Spain (up to 40%) except the coastal regions where increases are found (up to 60% south and up to 20% north). Annual precipitation over Italy is estimated to be higher up to 40% except the north region and west Sicily where a decrease up to 20% is found. Annual precipitation change over Greece is estimated in the range of ±20% for most of the country, where decreases are found over the Aegean Sea, the north-eastern continental land and Attica region. During winter precipitation rates are estimated to be lower for the major part of Spain. Over Italy a decrease in precipitation rates is found at the central part of the country. For the rest parts of Italy an increase is found. The general trend over Greece is a decrease in the precipitation rates. During spring reduction in precipitation rates is dominant over Spain. Over Italy an increase is found in the precipitation rates except the northern regions. Over Greece increases in precipitation rates are found for most of the country with an exception at the south Aegean Sea. During summer precipitation rates over Spain are estimated to increase at the south coastal zone, the east border and at the central of the country. Over Italy increases at the precipitation rates are found over north Italy and decreases are found at the south. Over Greece decreases in the precipitation rates are found for most of the country with an exception of the western Greece, Peloponnesus and south Crete. During autumn decreases in precipitation rates are dominant over Spain and Italy. Over

Greece increases at the precipitation rates are found over west and north regions of the country as well as at the central Aegean Sea.

CONCLUSION: Climatic and meteorological parameters affecting tree crops are assessed in S. Europe for future years under two different RCPs in order the related uncertainties to be assessed. Moreover simulations produced by the GISS-WRF provide high-resolution results. Comparison between the RCP8.5 and RCP4.5 outputs suggests an increase in the annual temperature all over the domain according to RCP8.5 while the RCP4.5 estimates an increase only in the western part. Both RCPs suggest an increase in the annual temperature over Spain, where RCP8.5 suggest more than 0.5 degrees higher increases compare to RCP4.5. Over Italy RCP8.5 estimates an increase all over the country while RCP4.5 estimates a small decrease at the central and south parts. In general, annual temperature over Italy under RCP8.5 is 1.0 degree higher compared to RCP4.5. Over Greece RCP8.5 estimates an increase in the annual temperature while RCP4.5 estimates a decrease. In general, annual temperature over Greece under RCP8.5 is 0.75 degrees higher compared to RCP4.5. Annual precipitation over Spain is estimated to decrease up to 40% for both of RCPs with an exception of the coastal zone where RCP4.5 suggests an increase up to 80% for the south coast. Over Italy both RCPs agree to the annual precipitation reduction up to 20-40% over the northern part of the country while it is estimated to increase up to 20-40% at the south. For the central part of the country RCP8.5 suggests a decrease in precipitation up to 40% while RCP4.5 suggests an increase up to 40%. Over Greece precipitation for both RCPs is estimated to change ±20%. The general trend for both RCPs is a precipitation increase over the land and a decrease over the sea. However, deviations from this trend is found, locally.

1. Introduction

Climate change is a major environmental problem having effects both globally and locally. Extreme weather events, heat weaves, floods, sea level rise, heat stress, water and soil salinization, ecosystem and economic disruption, vector-borne disease, food and waterborne diseases and the mass population movement are among the impacts caused by climate (Patz et al. 2000; Frumkin et al. 2008; IPCC 2013). The globally-averaged combined land and ocean surface temperature data show a warming of 0.85 [0.65 to 1.06] °C, over the period 1880 to 2012 (IPCC 2013). General Circulation Models (GCMs) are the most advanced tools currently available for simulating the response of the global climate system to increasing greenhouse gas concentrations. GCMs estimate that the global mean surface temperature change for the mid-21st century (i.e., for the period 2046-2065 relative to 1986-2005) will likely be in the range of 0.4°C to 2.6°C while globally-averaged precipitation increases with global mean surface temperature at about 1 to 3% $°C^{-1}$ are projected. However, the minimum and the maximum estimated changes cover a wide range of values for all geographical regions (IPCC 2013). For example, under the RCP4.5 (Representative Concentration Pathways) scenario (van Vuuren et al. 2011), annual temperatures for northern, central, and southern Europe are estimated to be modified in the range of -0.5°C to 3.8°C, 0.4°C to 3.2°C and 0.7°C to 3.1°C, respectively, while annual precipitation rates are estimated to be modified in the range of -5% to 17%, -6% to 9%, and -14% to 3%, respectively for the period 2046-2065 relative to 1986-2005 (IPCC 2013). Although the outputs from the GCM are very useful, they are relatively coarse for applications to regional scales. To increase their spatial resolution the coarse resolution data of the GCM are used as initial and boundary conditions by a regional climate model (RCM) (dynamical downscaling). The purpose of doing this is to add-up more detail from local topography, coastline and land use/land cover to obtain high resolution data in the area of interest.

Addressing the importance of climate change for Europe, there are studies assessing the climatic changes either over the entire continent or focusing on specific European regions (e.g., Kyselý and Beranová 2009; Pavlik et al. 2012; van Vliet et al. 2012; Gonçalves et al. 2014, Jacob et al. 2014). PESETA (Christensen et al. 2012) and ENSEMBLES (van der Linden and Mitchell 2009) are among the recent projects that examine the impact of climate change in Europe at high spatial resolution. In the

PESETA project two future periods (i.e., 2011-2040 and 2071-2100) are assessed at a spatial resolution of 50 km by 50 km using two global and three regional climate models under the IPCC A2 and B2 emissions scenarios. Spatial distribution plots suggest warming in all European regions during both winter and summer months. However, the choice of regional model plays a more significant role mainly for summer. Precipitation is a more variable parameter than temperature and the choice of the regional model is much more important for the summer period than for the winter one, to an even greater extent than what is seen for temperature. There is a transition between increase at the north and decrease at the south, with the position of the boundary to depend on the season (Christensen et al. 2012). In the ENSEMBLE project future climate over Europe in 2021-2050 relative to 1961-1990 is assessed, using fifteen different Regional Climate Models at 25 km spatial resolution with boundary conditions from seven different GCMs, under the IPCC A1B emissions scenario. The climate-change signal for the annual near-surface temperature suggests a warming all over Europe up to 2 °C. For precipitation, Europe can be divided into two regimes with increased precipitation at the north and decreased precipitation at the south. However, while all of the models agree on an increasing precipitation signal for the north part of Europe, up to one fourth of the models disagree with the decrease predicted for the south part (van der Linden and Mitchell 2009).

During the last years there is an increasing interest related to the climate change over Mediterranean (e.g., Gaertner et al. 2007; Goubanova et al. 2007; Giorgi and Lionello 2008; Boberg and Christensen 2012; Hertig and Jacobeit 2008; Somot et al. 2008; Senatore et al. 2011; Krichak et al. 2010; Kysely et al. 2012; Lelieveld et al. 2012; Lionello et al. 2014; Seubert et al. 2014). Mediterranean area is one of the most vulnerable regions of the globe given that large climate shifts have been observed in the past (Luterbacher et al. 2006). As a result, Mediterranean has been identified as one of the most prominent “Hot-Spots” in future climate change projections (Giorgi 2006). It is located in a transition zone between the arid climate of northern Africa and the wet climate of central Europe and even a minor change in large scale climatic factors might impose large impacts on the climatic conditions of different Mediterranean areas. Furthermore, the complex topography and the vast coastlines suggest a fine scale spatial variability of the climatic conditions (Gao and Giorgi 2008).

Tree crops cultivation is affected by parameters related to climatic conditions. Therefore, future climate will affect tree crops cultivation conditions in S. Europe,

suggesting changes in the carbon balance of tree-ecosystem for the future years. The objective of this work is to estimate the changes in the climatic conditions affecting tree crops cultivation.

2. Methods

2.1. General Circulation Model

The NASA GISS GCM ModelE2 (Schmidt et al., 2014) is used to simulate current and future climate. ModelE2, the latest generation of the NASA Goddard Institute for Space Sciences (GISS) coupled general circulation model (CGCM), is a state-of- the-art and widely used global climate model. We have used the GISS-E2-R configuration of ModelE2 with physics_version=1, where aerosols and ozone are read in via pre-computed transient aerosol and ozone fields and the aerosol indirect effect is parameterized, to simulate global climate. The version of ModelE2 that is used has horizontal resolution 1° × 1.25° latitude by longitude and 40 vertical layers (from surface to 0.1 hPa). The surface is split into four types: open water (including lakes and oceans), ice-covered water (again including lake ice and sea ice areas), ground (including bare soil and vegetated regions), and glaciers. Within each type there are further subdivisions (fraction of burned area, fraction of plant functional types, fractional snow cover, melt pond fraction over sea ice, etc.). The model accounts for both the seasonal and diurnal solar cycles in its temperature calculations. It simulates the emissions, transport, chemical transformation and deposition of several chemical tracers. Sea surface temperatures (SST) are calculated online using the dynamic Russell Ocean model that is coupled to the GCM. Large-scale and convective cloud covers are predicted, and precipitation is generated whenever supersaturated conditions occur. Vegetation is divided into 10 different vegetation types with different spectral and masking depth properties, and an explicit dependence of vegetation spectral albedos on leaf area index and solar zenith angle dependence. More than one vegetation type can be assigned to each grid box. The model involves parameterization to account for the relative contribution of transpiration and soil evaporation for vegetated areas.

In the present study the uncertainties due to uncertainties in climate projection is assessed using the Representative Concentration Pathways 4.5 (RCP4.5) and 8.5

(RCP8.5) from the CMIP5 set to cover lower to median range of emissions expected according to IPCC AR5 (IPCC, 2013). The simulations cover the period from 1880 to 2060. The beginning of the simulations is chosen prior to significant anthropogenic forcing and climate change. The main perturbation to climate over the historic period (up to 2008) is the change in atmospheric composition: primarily the increasing concentration of greenhouse gases and aerosols. Greenhouse gas concentrations up to 2008 are prescribed using ice-core measurements (Schmidt et al. 2011). For the period 2009-2060 the GHG levels are supplied from the two RCPs (i.e., RCP4.5 and RCP8.5). All the technical parameters of the model are consistent with those originally proposed, allowing the repeatability of the simulations.

2.2. Regional Climate Model - Downscaling

The outputs from the GCM are relatively coarse (i.e., $1^{\circ} \times 1.25^{\circ}$) for applications to regional and local scales. The need for regional climate projections in a finer grid size will be assessed, here, using the Weather Research and Forecasting (WRF) (http://www.wrf-model.org/index.php) model to dynamically downscale GCM simulations. The goal is to generate more locally relevant projections of long-term weather patterns over Mediterranean. WRF is a state-of-the-art atmospheric modeling system that is applicable for both meteorological research and numerical weather prediction (http://www.wrf-model.org/index.php). For the set of physics options we used the following modules: the WRF Single-Moment 3-class scheme for microphysics, the Rapid radiative transfer model (RRTM) for long-wave radiation, the Dudhia scheme for short-wave radiation, the Monin-Obukhov with Carslon-Boland viscous sub-layer for surface layer options, the 5-layer thermal diffusion for land surface options, the Yonsei University scheme for the planetary boundary layer and the Kain-Fritsch scheme for the cumulus cloud option. WRF is applied here using a multi - nested grid approach. The initial and time-evolving lateral boundary conditions at six-hourly instantaneous intervals for the physical parameters necessary to drive WRF (i.e., temperature, relative humidity, wind components, soil temperature and moisture at different soil depths, sea surface temperature, surface pressure, ice fraction and snow water equivalent) is obtained from the corresponding simulations carried out with the NASA GISS GCM ModelE2. The innermost domain has 9 Km horizontal grid spacing (Figure 1). Meteorological conditions in the finer grid size is simulated for five current

years around 2010 (i.e., 2008-2012) and five future years around 2050 (i.e., 2048-2052).

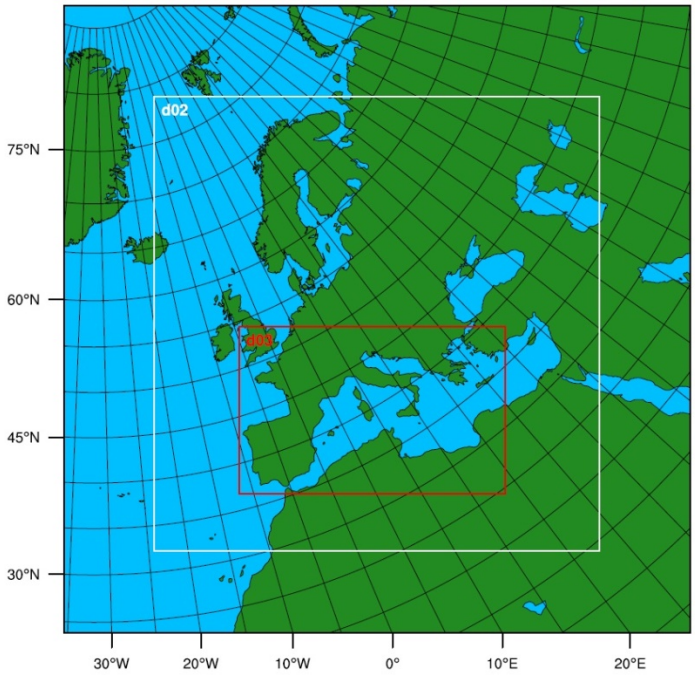

Figure 1: Modeling domains used in WRF simulations (the innermost domain has 9 Km horizontal grid spacing).

3. Results

3.1. General Circulation Model

Annual average surface air temperature from the GISS-E2-R outputs is presented in Figure 2 for the historical simulation (i.e., 1981-2010) and the differences for 2031–2060 minus the corresponding historical simulation for RCP4.5 and RCP8.5 are presented in Figures 3a and 3b respectively. Global average temperature for historical years is estimated at 14.2 °C (Figure 1), while an increase of 1.3 °C and 1 °C for RCP8.5 and RCP4.5 is assessed, respectively, confirming the increasing trend in future temperature. This trend is also noticed in the domain of our interest.

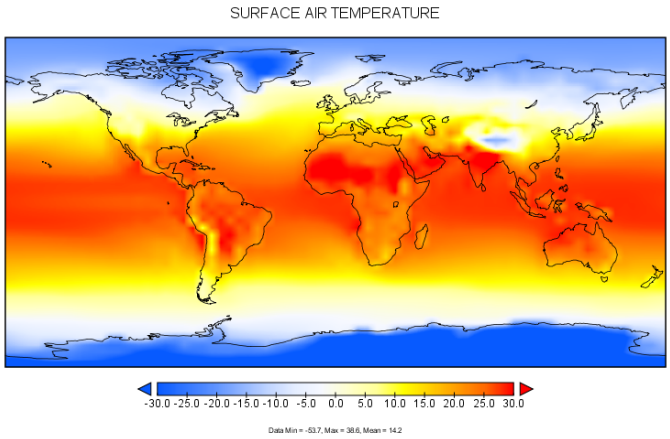

Figure 2: Annual average surface air temperature for the 1981-2010 historical simulations

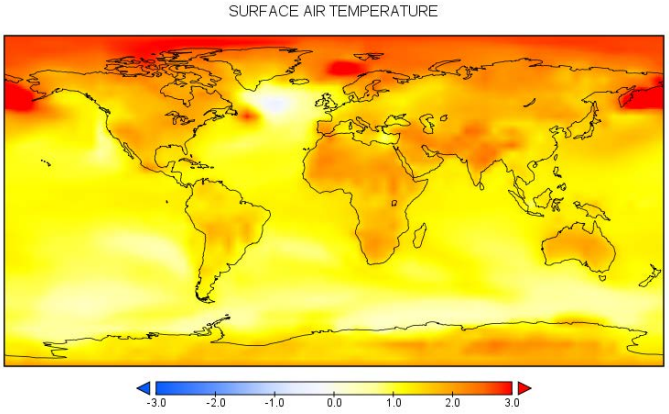

(a)

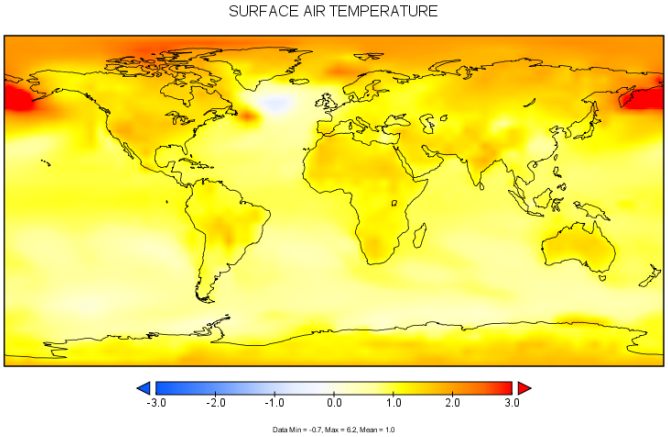

(b)

Figure 3: Surface annual average air temperature differences (°C) for 2031–2060 minus 1981–2010 of the corresponding historical simulation for (a) RCP8.5; (b) RCP4.5

Seasonal global average surface air temperature for the historical simulations and the related changes for the two RCP scenarios are presented in Annexes 1 and 2. The seasonal results are in agreement with the increasing trend simulated for the whole year.

While mean surface air temperature is generally used as an indicator for climate change, as a metric alone is not enough to reflect the complicated variations of climate. In fact, trends in mean surface temperature are often due to changes in daily maximum and minimum temperatures [Sun et al., 2006]. As a result, the diurnal temperature range (DTR) is also an important indicator for climate change studies [Braganza et al., 2004] and its implications for agriculture. DTR ranges between 4 and 18 °C over land, with a global average of 4°C (Figure 4) for the historical simulation (i.e., 1981-2010). DTR remains steady on average under RCP8.5 and RCP4.5. However, as can be seen by the spatial distribution plots (Figures 5a and 5b) there is a mixed trend, with some regions facing up to 0.9 °C increase (e.g., Mexico, Georgia, China, etc.) in the DTR and other regions facing a decrease up to 0.7 °C (e.g., Norway, Sweden, Poland, etc.) under RCP8.5. The same spatial variation but of smaller magnitude is also profound under RCP4.5. The DTR increases up to 0.7 °C and decreases up to 0.4 °C.

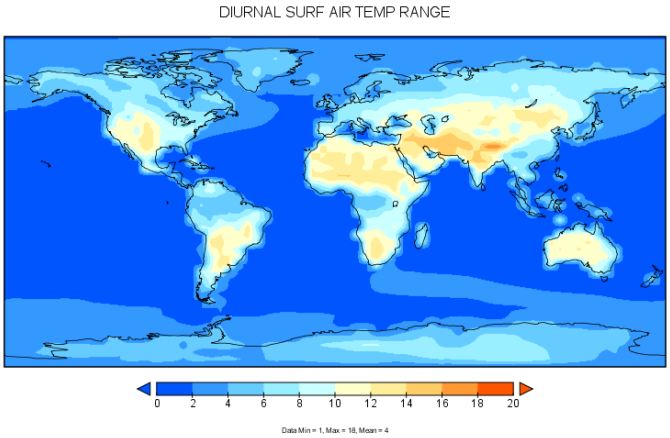

Figure 4: Annual average diurnal surface air temperature range (°C) for the 1981-2010 historical simulations

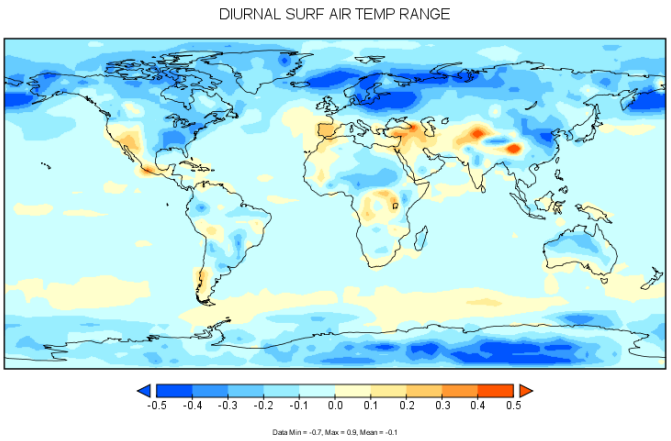

(a)

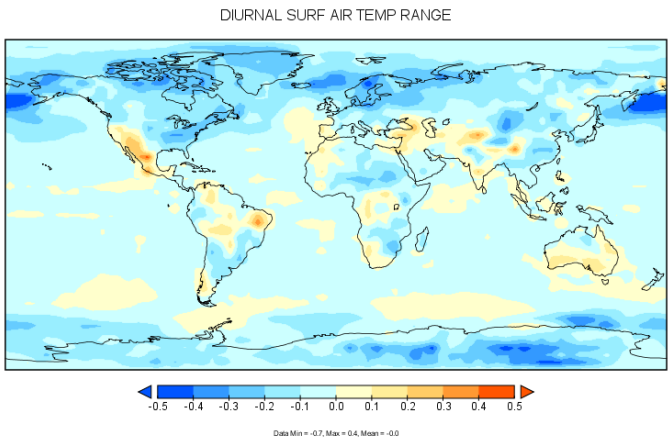

(b)

Figure 5: Diurnal surface air temperature range differences (°C) for 2031–2060 minus 1981–2010 of the corresponding historical simulation for (a) RCP8.5; (b) RCP4.5

Annual average precipitation is presented in Figure 6 for the historical simulation (i.e., 1981-2010) and the differences for 2031–2060 minus the corresponding historical simulation for RCP4.5 and RCP8.5 are presented in Figures 7a and 7b respectively. Global average precipitation rate for the historic period is estimated at 3 mm/day while under RCP8.5 and RCP4.5 an increase of 0.1 mm/day is noted suggesting an almost stable precipitation rate on average over globe. However, precipitation is very location dependent suggesting regions with increasing or decreasing trends in the precipitation rates (Figures 7a and 7b). As such, the need for regional climate projections in a finer grid size is necessary, as mentioned above.

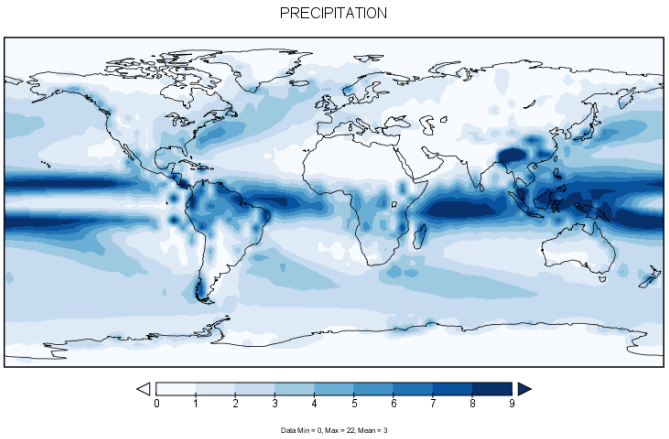

Figure 6: Annual average precipitation (mm/day) for the 1981-2010 historical simulations

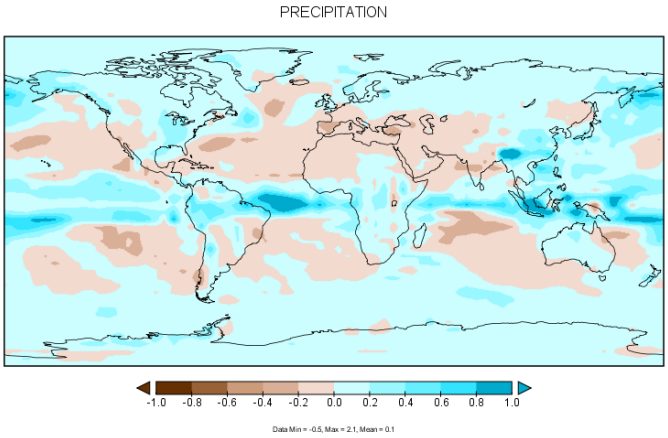

(a)

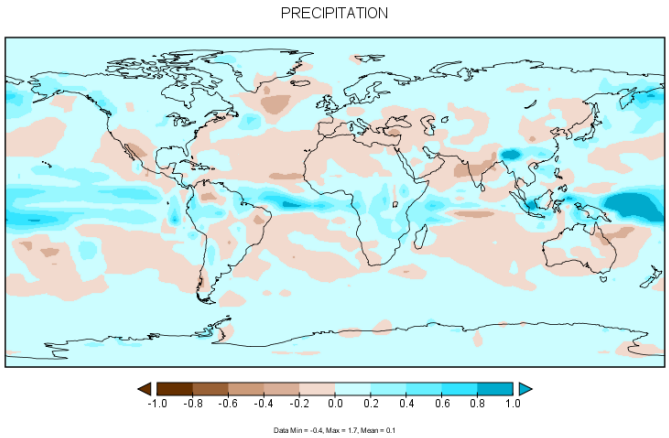

(b)

Figure 7: Precipitation differences (mm/day) for 2031–2060 minus 1981–2010 of the corresponding historical simulation for (a) RCP8.5; (b) RCP4.5

Another parameter of interest is relative humidity (RH). Annual average RH is presented in Figure 8 for the historical simulation (i.e., 1981-2010) and the differences

for 2031–2060 minus the corresponding historical simulation for RCP4.5 and RCP8.5 are presented in Figures 8a and 8b respectively.

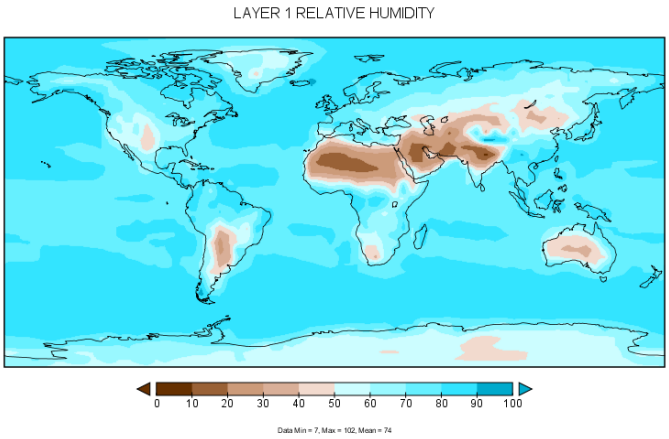

Figure 8: Annual average relative humidity (%) for the 1981-2010 historical simulations

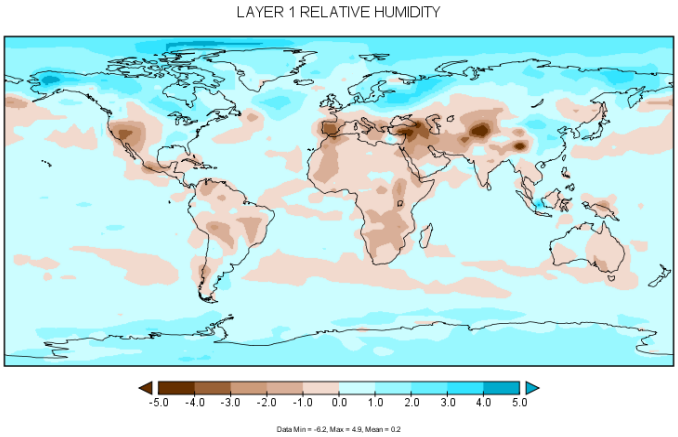

(a)

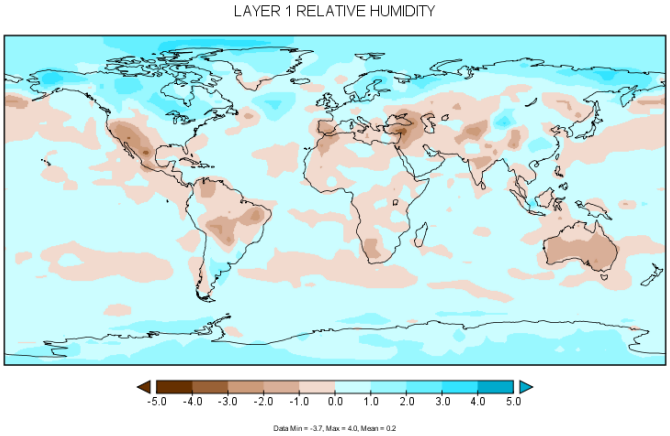

(b)

Figure 9: Relative humidity differences (%) for 2031–2060 minus 1981–2010 of the corresponding historical simulation for (a) RCP8.5; (b) RCP4.5

Global average RH for the historic period is estimated at 74%. RH is not zonally uniform, presenting centers of various intensities at all latitudes as can be seen in the spatial distribution plot. The global map shows maxima in the equatorial zone and minima in the dry subtropical regions around 30°N and 30°S over land. Under RCP8.5 and RCP4.5 an increase of 0.2% is noted suggesting an almost stable RH on average over globe. Although on average RH presents a modest increase, GISS-E2-R simulates a land–ocean contrast (Figures 9a and 9b) in response to the larger warming seen over land than over ocean (Figure 2). Compared to the historic data, RH tends to slightly increase over oceans but decrease over significant part of the land (Figures 9a and 9b).

Finally, the annual average solar radiation incident at the Earth's surface or downward solar radiation is presented in Figure 10. The historical (i.e., 1981-2010) mean is 192 W/m^2. As expected higher values are seen in the region between mid-latitudes. The simulation for the future indicate that the downward solar radiation remains stable, presenting though local variations that range between -21.4 W/m^2 and 17.5 W/m^2 under RCP8.5 and between -21.6 W/m^2 and 13.8 W/m^2 under RCP45 (Figures 11a and 11b).

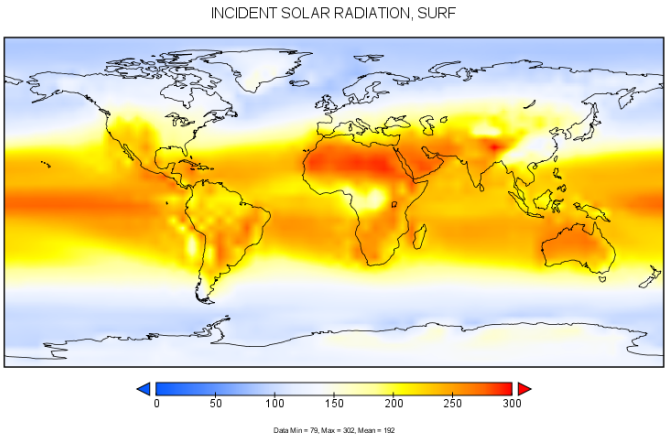

Figure 10: Annual average incident solar radiation at the surface (W/m^2) for the 1981-2010 historical simulations

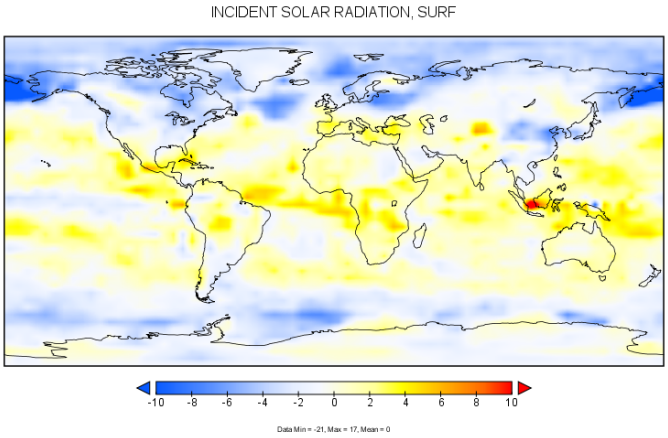

(a)

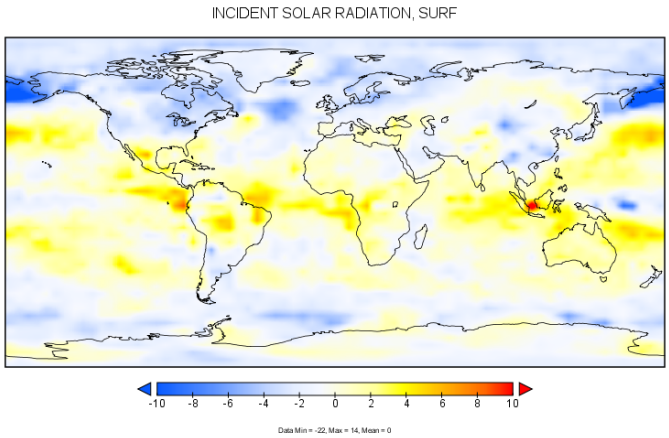

(b)

Figure 11: Incident solar radiation differences (W/m^2) for 2031–2060 minus 1981–2010 of the corresponding historical simulation for (a) RCP8.5; (b) RCP4.5

3.2. Regional Climate Model - Downscaling

Monthly average changes for temperature and precipitation in S. Europe between current (i.e., 2008 – 2012) and future years (i.e., 2048-2052) for RCP8.5 and RCP4.5 are presented in the Annexes 3-6. These plots illustrate the database for the meteorological parameters affecting tree cultivations in the domain of our interest. Below is discuss the annual and seasonal trend for temperature and precipitation for both RCPs as well as a comprehensive analysis of the two RCPs results.

Representative Concentration Pathways 8.5 (RCP8.5)

Annual temperature is estimated to be higher in the future all over the domain (Figure 12). Temperature changes over Greece, Italy and Spain is estimated in the range of 0.0 - 0.5 degrees, 0.25 - 1.25 degrees and 0.5 - 1.5 degrees, respectively. The maximum increase up to 1.5 degrees is estimated over north – northeastern Spain while the minimum increase up to 0.25 degrees is estimated over eastern Greece.

During winter temperature changes over Greece, Italy and Spain are estimated in the range of 0.25 - 1.0 degrees, 0.75 - 2.0 degrees and 0.5 - 1.25 degrees, respectively. The maximum change over Greece is found to the west region of the country, over Italy is found to the north and over Spain to the south.

During spring higher temperatures are estimated over Italy and Spain while a reduction is found over Greece. Temperatures changes over Greece, Italy and Spain are estimated in the range of -0.25 - -0.5 degrees, 0.0 - 1.25 degrees and 0.75 - 1.5 degrees, respectively. The maximum change over Greece is found over the Aegean Sea, while over Italy and Spain is found at the north.

During summer temperature changes over Greece, Italy and Spain are estimated in the range of 0.0 - 1.0 degrees, 0.25 - 1.25 degrees and 1.0 - 2.5 degrees, respectively. The maximum change over Greece is found to the south-west region of the country while over Italy and Spain is found to the north, north-east and east regions.

During autumn higher temperatures are estimated over Greece and Italy while a reduction is found over the south Spain. Temperature changes over Greece, Italy and Spain are estimated in the range of 0.25 - 1.0 degrees, 0.0 - 1.0 degrees and -0.25 - 1.0

degrees, respectively. The maximum change over Greece is found at the west region of the country over Italy is found at the south and over Spain at the north.

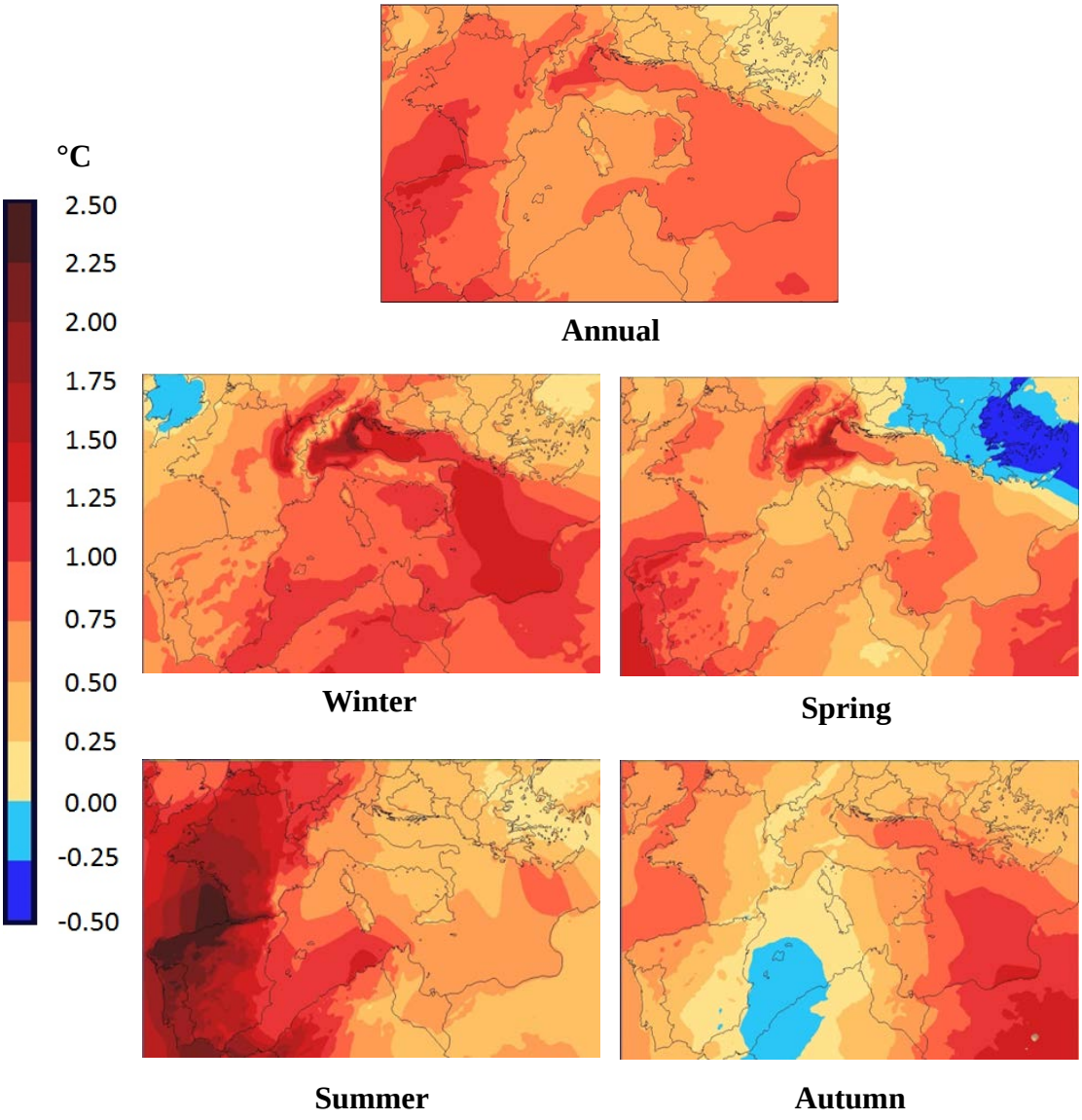

Figure 12: Annual and seasonal temperature change between future and current years (RCP8.5)

Precipitation change is very location dependent presenting a mixed trend (Figure 13). Annual precipitation is estimated to be lower all over Spain (up to 60%, locally). Annual precipitation change over Italy is estimated in the range of ±40% where decreases are found to the north and increases to the south. Annual precipitation change over Greece is estimated in the range of ±20%. Decreases are found mainly

over the islands in the Aegean Sea with an exception of the central part, north-eastern, central-eastern and parts of the south-western continental Greece.

During winter the general trend presents a decrease in the precipitations rates over the continental regions. Over Spain the decrease is simulated up to 60%, locally. However, an increase up to 100% is found over the south-eastern part of the country. A decrease up to 40% is simulated for the major part of Italy, with an exceptions the north-western region and few regions to the south where an increase up to 40% is found. Over Greece precipitation is estimated to decrease up to 60% almost everywhere with an exception of the north-central continental area and eastern Peloponnesus where an increase up to 20% is found.

During spring a reduction up to 60% in precipitation rates over Spain and Italy is dominant. However, there is a region to the south-eastern Spain where an increase up to 100% is found as well as over southern Italy, where an increase up to 20% is found. Over Greece precipitation is estimated to decrease up to 40% only over the northern part. For the rest of the country precipitation is found to increase where the highest rate increases (up to 100%) over the Aegean Sea and the south-western part of the continental land.

During summer precipitation rates over Spain are estimated in the range ±100%. Results are very location dependent. This is not the case for the other two countries where reduction up to 100% is dominant over Italy and increase up to 100% is dominant over Greece.

During autumn precipitation rates over Spain are estimated to decrease up 60% with an exception to the north-eastern part where an increase up to 100% is found. Over Italy precipitation is estimated to increase up to 80% mainly at the south. However a decrease up to 40% is found at the north. Over Greece higher precipitation rates are estimated for most of the country. The highest rates (up to 100%) are found over the north-central, west and south-west continental parts of the country as well as nor-east Aegean Sea. However a decrease up to 20% is found over south Aegean Sea and parts of the central continental area.

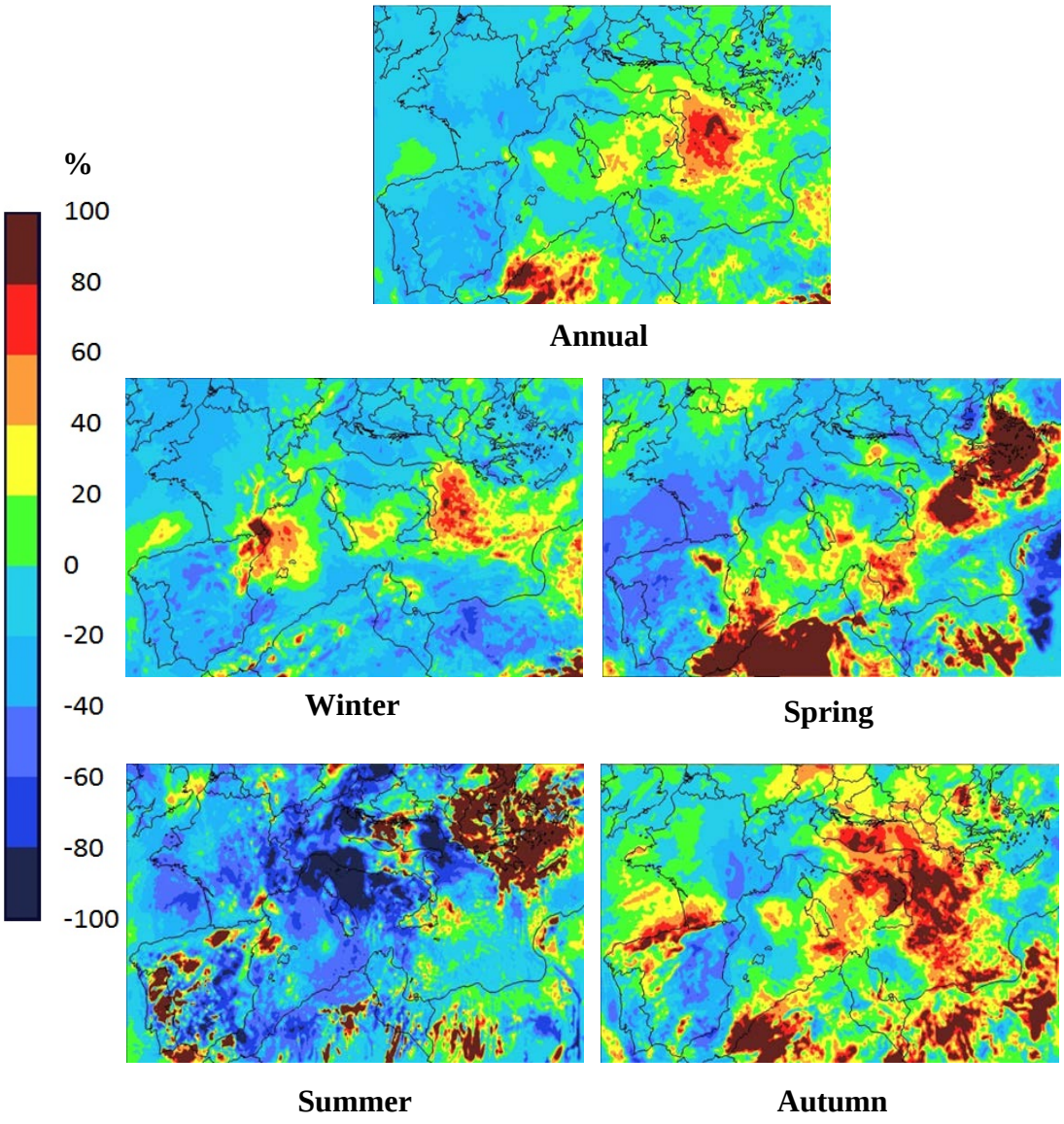

Figure 13: Annual and seasonal precipitation change between future and current years (RCP8.5)

Representative Concentration Pathways 4.5 (RCP4.5)

Annual temperature presents a gradually increase from the east to the west of the domain (Figure 14). It is estimated the annual temperature to be higher over Spain and northern Italy and lower over southern Italy and Greece. Over Spain annual temperature is found higher in the range 0.0 - 1.0 degrees. The west region of the Spain will have the highest increase while the south-east part of the country will have the minimum increase. Over Italy an increase in the range of 0.0 - 0.5 degrees is estimated at the north and a decrease up to 0.25 degrees is estimated at the south. However, a mix

trend is found over Sicily (i.e., ± 0.25 degrees). Over Greece annual temperature is estimated lower in the range 0.0 - 0.5 degrees. The lowest change is found over the west and north-east part of the country.

During winter a temperature increase up to 0.75 degrees is estimated over Spain. The highest increase is found over the south-west of the country. Over Italy an increase up to 1.75 degrees is found at the north part of the country while an increase up to 0.25 degrees is found at the south. Over Greece temperature is found lower up to 0.25 degrees for most of the country. However, a decrease up to 0.5 degrees and an increase up to 0.25 degrees is found at the central and northern part of the country, respectively.

During spring a reduction is estimated in the temperature for Greece, Italy and eastern Spain. Over Spain an increase up to 0.75 is found at the south-west and a decrease up to 0.5 degrees is found at the south-east. Over Italy a decrease up to 0.75 degrees is found for the major part of the domain. However, there are regions where a decrease up to 1.0 degree as well as an increase up to 0.25 degrees is found. Over Greece a decrease in the range 0.75 - 1.0 degrees is found for the major part of the country. However, a smaller decrease (0.25 - 0.75 degrease) is found at the south-west.

During summer the dominant trend suggests a reduction in the temperature, except the western Spain. Over Spain it is estimated an increase up to 1.0 degree over the west region of the country and a decrease up to 0.75 degrees at the south part. Over Italy a decrease in temperature is found in the range 0.75 - 1.0 degrees for the major part of the country. However, a smaller decrease is found at the south and north regions. Over Greece a reduction in the range 0 - 0.25 degrees is found for the major part of the country. However, a largest decrease (up to 0.5 degrees is found over a large continental part of the country. Small increases (up to 0.25 degrees) is found mainly at the south-eastern part.

During autumn temperature increase is estimated over Spain in the range 1.0 - 1.25 degrees for the major part of the country. However, smaller and higher increases are found locally. Over Italy the increase is dominant (0.0 - 0.5 degrees) with an exception at the north-eastern part of the country where a reduction up to 0.25 degrees is found. Over Greece, there is a mixing trend where an increase up to 0.25 degrees is

found over the central and western continental land. For the rest of the country a reduction is found up to 0.75 degrees at the south-eastern Aegean Sea.

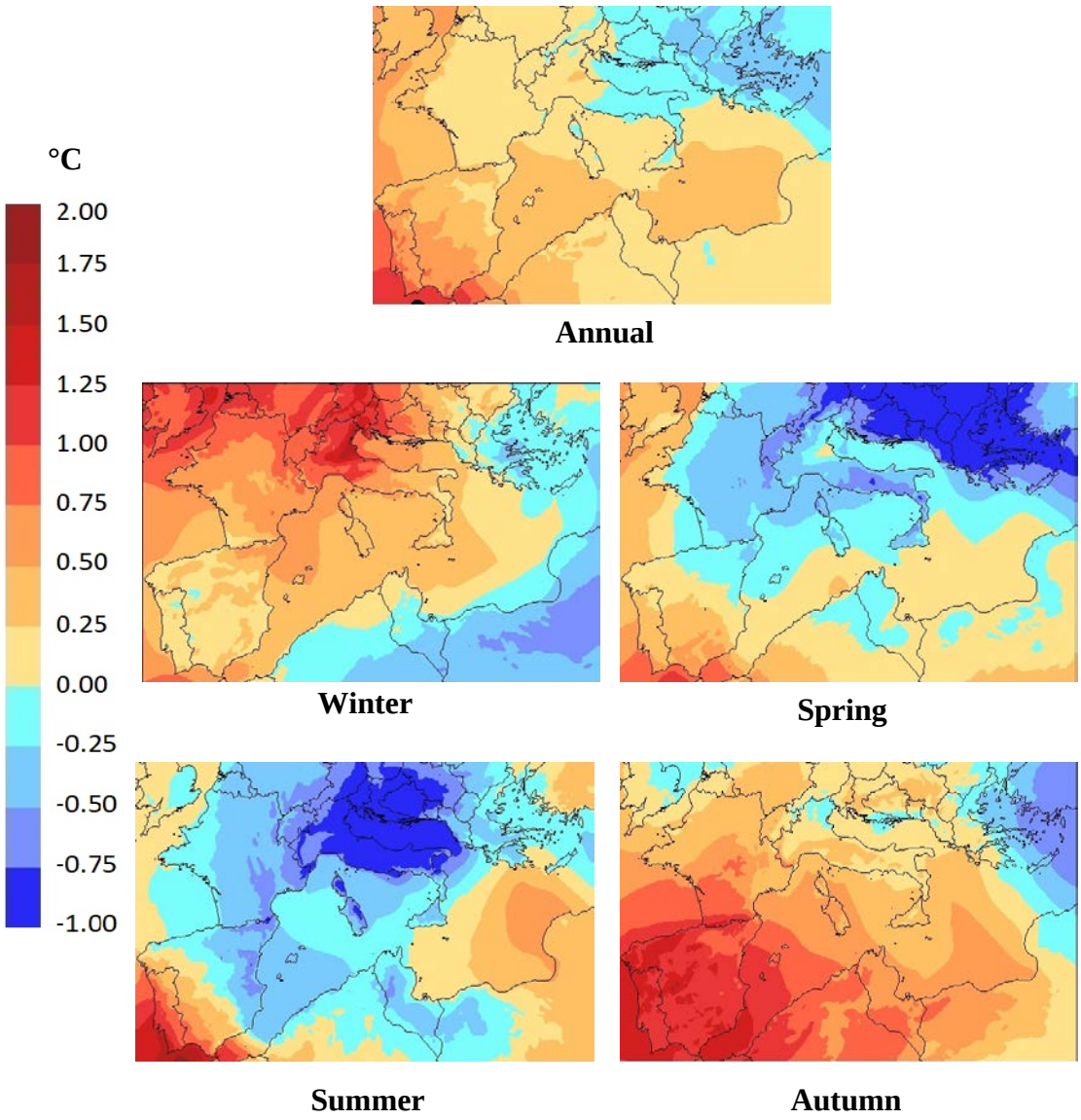

Figure 14: Annual and seasonal temperature change between future and current years (RCP4.5)

Precipitation change is very location dependent (Figure 15). Annual precipitation is estimated to be lower over Spain (up to 40%) except the coastal regions where increases are found (up to 60% south and up to 20% north). Annual precipitation over Italy is estimated to be higher up to 40% except the north region and west Sicily where a decrease up to 20% is found. Annual precipitation change over Greece is estimated in the range of ±20% for most of the country, where decreases are found over the Aegean Sea, the north-eastern continental land and Attica region. Decreases up to 40% are found at the north-eastern and south-eastern Aegean Sea. For the rest of

country (central, west, north-west, and Peloponnesus) an increase up to 20% is found, while locally it is up to 40%.

During winter precipitation rates are estimated to be lower up to 40% for the major part of Spain, except the south and south-eastern where an increase up to 100% is found, locally. Over Italy a decrease in precipitation rates up to 20% is found at the central part of the country. For the rest parts of Italy an increase up to 60% is found. The general trend for precipitation rates over Greece is a decrease almost everywhere with an exceptions for Crete and east Peloponnesus where an increase up to 40% is found locally. The highest decreases are found at the north-eastern Aegean Sea (up to 60%).

During spring reduction in precipitation rates are dominant over Spain (up to 60%, locally). However, increases are found at the coastal regions (up to 80% at the south and up to 20% at the north). Over Italy an increase is found in the precipitation rates except the northern regions where a decrease up to 60% is found. The highest increases (up to 100%) are found over the central part of the country. Over Greece increases in precipitation rates up to 100% are found for most of the country. However, a decrease up to 40% is found at the south Aegean Sea.

During summer precipitation rates over Spain will change in the range of ±100%. The highest increases are found at the south coastal zone, the east border and at the central of the country. The highest decreases are found near the west border and south-west coastal zone. Over Italy increases at the precipitation rates up to 100% are found over north Italy and decreases up to 80% are found at the south. A mixed trend is found over central Italy and Sicily. Over Greece decreases in the precipitation rates are found for most of the country with an exception of the western Greece and, Peloponnesus and south Crete, where an increase up to 100% is found. The highest decreases up to 100% are found over northern Aegean Sea.

During autumn precipitation rates are estimated to decrease over Spain up to 80%. However, an increase up to 80% is found over the coast. Over Italy the decrease in precipitation rates is dominant. The highest decrease is found at the north (up to 80%, locally). However, an increase up to 40% is found on a region at the central of the country. Over Greece increases at the precipitation rates are found over west and north regions of the country (up to 100%) as well as at the central Aegean Sea (up to

80%). For the rest of the country decreases are found (up to 80 % at the south Aegean Sea).

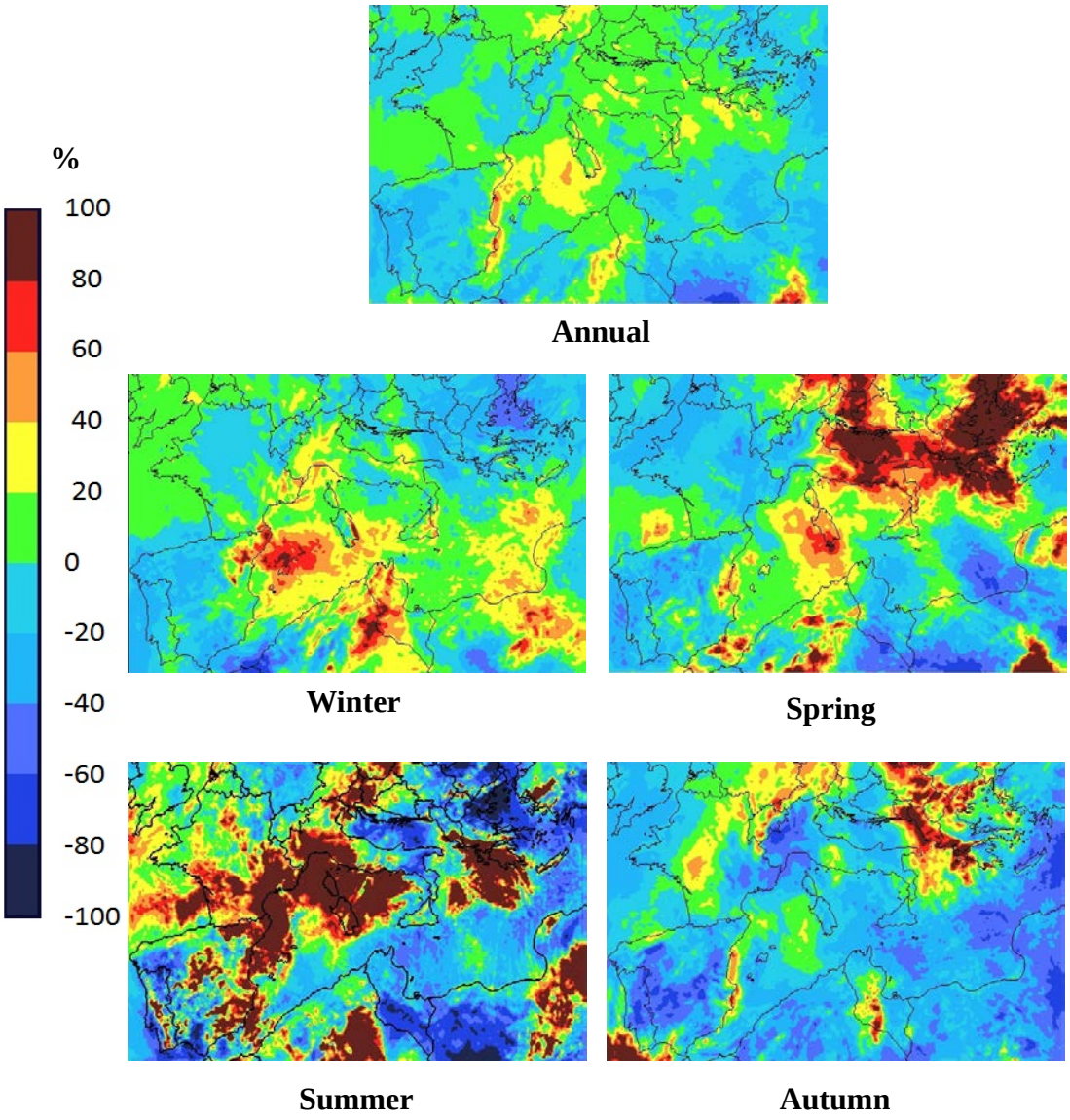

Figure 15: Annual and seasonal precipitation change between future and current years (RCP4.5)

Comparison between the RCP8.5 and RCP4.5 outputs

Temperature

Annual temperature is estimated to increase in the future all over the domain according to RCP8.5 while the RCP4.5 estimates an increase only in the western part. Both RCPs suggest an increase in the annual temperature over Spain, where RCP8.5

suggest more than 0.5 degrees higher increases compare to RCP4.5. Over Italy RCP8.5 estimates an increase all over the country while RCP4.5 estimates a decrease small at the central and south parts. In general, annual temperature over Italy under RCP8.5 is 1.0 degree higher compared to RCP4.5. Over Greece RCP8.5 estimates an increase in the annual temperature while RCP4.5 estimates a decrease. In general, annual temperature over Greece under RCP8.5 is 0.75 degrees higher compared to RCP4.5.

During winter temperature changes over Spain are estimated 0.5 - 1.25 degrees according to RCP8.5 while RCP4.5 estimates an increase up to 0.75 degrees. Spatially, the highest increases are found at the south according to RCP8.5 and at the south-east according to RCP4.5. Over Italy it is estimated an increase 0.5 - 2.00 degrees according to RCP8.5 while RCP4.5 estimates an increase 0.0 - 1.75 degrees. Spatially, the highest increases are found at the north for both RCPs.

During spring temperature changes over Spain are estimated 0.75 - 1.5 degrees according to RCP8.5 while RCP4.5 estimates a change -0.5 - 0.75 degrees. Spatially, the eastern part of the country is the most uncertain region since the increases found in RCP8.5 turn to decreases in RCP4.5. Over Italy the increases estimated in RCP8.5 (0.0 - 1.25 degrees) turn to decreases in RCP4.5 (up to 1.0 degree), except a small region at the south-east where a small increase is found. Over Greece the general trend of both RCPs suggest a reduction in the temperature where RCP8.5 estimates more than 0.5 degree more reduction compared to RCP4.5, locally.

During summer temperature changes over Spain are estimated 0.5 - 2.5 degrees according to RCP8.5, suggesting an increase all over the country. However, simulations using the RCP4.5 estimates an increase only at the west part of the country (up to 1.0 degree at the south-west) while at the east part of the country a decrease is estimated (up to 0.75 at the south-east). Over Italy the increase estimated in RCP8.5 (0.25 - 1.25 degrees) turn to decrease in RCP4.5 where in most of the country a temperature reduction -0.75 - -1.0 is found. A similar behavior with Italy is found for Greece, as well, where the increase 0.0 - 0.5 degrees estimated for most of the country in RCP8.5 turn to decrease in RCP4.5 up to -0.5 degrees.

During autumn RCP8.5 estimates a smaller temperature increase compared to RCP4.5 over Spain. Regions at the south of Spain where temperature increase is estimated up to 0.25 degrees in RCP8.5, is founded to have an increase up to 1.25 degrees according to RCP4.5. Over Italy, although the central part of the country is

estimated to have a similar increase for both of RCPs (i.e., an increase 0.25 - 0.5 degrees) for the northern and southern parts RCP8.5 estimates 0.25 and 0.5 degrees higher increases compared to RCP4.5. In addition, a small reduction in temperature is estimated at the north - east of the country according to RCP4.5. Over Greece both RCPs estimate a temperature increase over the west continental country where RCP8.5 estimates an increase up to 0.75 compared to RCP4.5. However, for the rest of the country differences are found between the two RCPs. RCP8.5 estimates an increase up to 1.0 degree while RCP4.5 estimates a decrease up to -0.75 degrees.

Precipitation

Annual precipitation over Spain is estimated to decrease up to 40% for both of RCPs with an exception of the coastal zone where RCP4.5 suggests an increase up to 80% for the south coast. Over Italy both RCPs agree to the annual precipitation reduction up to 20-40% over the northern part of the country while it is estimated to increase up to 20-40% at the south. For the central part of the country RCP8.5 suggests a decrease in precipitation up to 40% while RCP4.5 suggests an increase up to 40%. Over Greece precipitation for both RCPs is estimated to change ±20%. The general trend for both RCPs is a precipitation increase over the land and a decrease over the sea. However, deviations from this trend is found, locally.

During winter both RCPs estimate a reduction in precipitation over most of the Spain with an exception of the south-east part. The reduction is estimated up to 60% for the RCP8.5 and 40% for the RCP4.5 while the increase is estimated up to 100%. Over Italy both RCPs estimate a decrease for the central part of the country (40% in RCP8.5 and 20% in RCP4.5). However, for the rest of the country RCP8.5 estimates both reduction and increase in the range of ±20% while RCP4.5 estimates an increase up to 60%, locally. Over Greece the general trend suggests a reduction in precipitation for both RCPs (40% in RCP8.5 and 60% in RCP4.5). However, an increase mainly up to 20% is found locally for both RCPs.

During spring both RCPs estimate that reduction in precipitation is dominant over Spain (up to 60%), while increases are found over the coastal zone. Over Italy both RCPs estimate reduction in precipitation at the north (up to 60%) and increases at the south with the RCP8.5 to suggest up to 20% increase and the RCP4.5 to suggest up

to 60% increase. Differences are found for the central part of the country with the RCP8.5 to suggest reduction up to 40% and the RCP4.5 to suggest increase up to 100%. Over Greece RCP8.5 estimates precipitation reduction up to 40% only at the north-east region and increase up to 100% for the rest of the country, while RCP4.5 estimates reduction up to 60% only at the south Aegean Sea and increase up to 100% for the rest of the country.

During summer both RCPs estimate that precipitation rates will change in the range ±100%. Results are very location dependent presenting different trend for the two RCPs. RCP8.5 estimates a reduction at the south and an increase at the north of the country, while RCP4.5 estimates an increase at the south and a reduction at the north. Over central and north Italy RCP8.5 estimates a reduction in precipitation up to 100% while RCP4.5 estimates and increase up to 100%. For the south part of the country RCP8.5 estimates a mixed trend while RCP4.5 estimates reduction. Both RCPs estimate a mixed trend over Sicily. Over Greece both RCPs estimate an increase up to 100% over the west part of the country. However, RCP8.5 estimates increases for the rest of the country up to 100% while RCP4.5 estimates decreases up to 100%.

During autumn both RCPs estimate reduction in precipitation over the major part of the country (up to 60% for RCP8.5 and up to 80% for RCP4.5). However, RCP8.5 estimates increases at the north-eastern part up to 100% while RCP4.5 estimates increases over the coast up to 80%. Over Italy both RCPs estimate decrease in precipitation over north Italy (up to 40% for RCP8.5 and up to 80% for RCP4.5). For the rest of the country RCP8.5 estimates increases up to 80% while RCP4.5 decreases up to 40%. Over Greece both RCPs estimate precipitation increases at the west and north of the country as well as eastern Aegean Sea (up to 100%, locally) and decreases at the south Aegean Sea (up to 40% for RCP8.5 and up to 80% for RCP4.5). For the rest of the country RCP8.5 estimates increases up to 40% while RCP4.5 estimates decreases up to 40%.

4. Conclusion

Comparison between the RCP8.5 and RCP4.5 outputs suggest an increase in the annual temperature all over the domain according to RCP8.5 while the RCP4.5

estimates an increase only in the western part. Both RCPs suggest an increase in the annual temperature over Spain, where RCP8.5 suggest more than 0.5 degrees higher increases compare to RCP4.5. Over Italy RCP8.5 estimates an increase all over the country while RCP4.5 estimates a small decrease at the central and south parts. In general, annual temperature over Italy under RCP8.5 is 1.0 degree higher compared to RCP4.5. Over Greece RCP8.5 estimates an increase in the annual temperature while RCP4.5 estimates a decrease. In general, annual temperature over Greece under RCP8.5 is 0.75 degrees higher compared to RCP4.5. Annual precipitation over Spain is estimated to decrease up to 40% for both of RCPs with an exception of the coastal zone where RCP4.5 suggests an increase up to 80% for the south coast. Over Italy both RCPs agree to the annual precipitation reduction up to 20-40% over the northern part of the country while it is estimated to increase up to 20-40% at the south. For the central part of the country RCP8.5 suggests a decrease in precipitation up to 40% while RCP4.5 suggests an increase up to 40%. Over Greece precipitation for both RCPs is estimated to change ±20%. The general trend for both RCPs is a precipitation increase over the land and a decrease over the sea. However, deviations from this trend is found, locally.

References

1. Boberg, F., Christensen, J.H. (2012). Overestimation of Mediterranean summer temperature projections due to model deficiencies. Nature Climate Change, 2, 433-436.

2. Braganza, K., Karoly, D. J. and Arblaster J. M. (2004), Diurnal temperature range as an index of global climate change during the twentieth century, Geophys. Res. Lett., 31, L13217, doi:10.1029/2004GL019998.

3. Christensen, O.B., Goodess, C.M., Ciscar, J.C. (2012). Methodological framework of the PESETA project on the impacts of climate change in Europe, doi: 10.1007/s10584-011-0337-9.

4. Frumkin, H., Hess, J., Luber, G., Malilay, J., McGeehin, M. (2008). Climate Change: The Public Health Response. American Journal of Public Health, 98, 435-445.

5. Gaertner, M.A., Jacob, D., Gil, V., Domı´nguez, M., Padorno, E., Sanchez, E., Castro1, M. (2007). Tropical cyclones over the Mediterranean Sea in climate change simulations, doi:10.1029/2007GL029977

6. Gao, X., Giorgi, F. (2008). Increased aridity in the Mediterranean region under greenhouse gas forcing estimated from high resolution simulations with a regional climate model. Global Planet Change, 62, 195–209.

7. Giorgi, F. (2006). Climate change hot-spots. doi:10.1029/2006GL025734.

8. Giorgi, F., Lionello, P. (2008). Climate change projections for the Mediterranean region. Global Planet Change, 63, 90–104.

9. Gonçalves, M., Barrera-Escoda, A., Guerreiro, D., Baldasano, J.M., Cunillera, J. (2014). Seasonal to yearly assessment of temperature and precipitation trends in the North Western Mediterranean Basin by dynamical downscaling of climate scenarios at high resolution (1971–2050), doi: 10.1007/s10584-013-0994-y.

10. Goubanova, K., Li, L. (2007). Extremes in temperature and precipitation around the Mediterranean basin in an ensemble of future climate scenario simulations. Global Planet Change, 57, 27–42.

11. Hertig, E., Jacobeit, J. (2008). Downscaling future climate change: Temperature scenarios for the Mediterranean area. Global Planet Change, 63, 127–131.

12. Intergovernmental Panel on Climate Change (IPCC) (2013). Climate Change 2013: The Physical Science Basis. Contribution of Working Group I to the Fifth Assessment Report of the Intergovernmental Panel on Climate Change [Stocker TF, Qin D, Plattner GK, Tignor M, Allen SK, Boschung J, Nauels A, Xia Y, Bex V, Midgley PM (eds.)], Cambridge University Press, Cambridge, United Kingdom and New York, NY, USA.

13. Jacob, D., Petersen, J., Eggert, B., Alias, A., Christensen, O.B., Bouwer, L.M., et al. (2014). EURO-CORDEX: new high-resolution climate change projections for European impact research, doi: 10.1007/s10113-013-0499-2

14. Krichak, S.O., Alpert, P., Kunin, P. (2010). Numerical simulation of seasonal distribution of precipitation over the eastern Mediterranean with a RCM, doi 10.1007/s00382-009-0649-x

15. Kyselý, J., & Beranová, R. (2009). Climate-change effects on extreme precipitation in central Europe: uncertainties of scenarios based on regional climate model, doi: 10.1007/s00704-008-0014-8.

16. Kyselý, J., Beguería, S., Beranová, R., Gaál, L., López-Moreno, J.I. (2012). Different patterns of climate change scenarios for short-term and multi-day precipitation extremes in the Mediterranean. Global Planet Change 98–99, 63–72.

17. Lelieveld, J., Hadjinicolaou, P., Kostopoulou, E., Chenoweth, J., El Maayar, M., Giannakopoulos, C., Hannides, C., Lange, M.A., Tanarhte, M., Tyrlis, E., Xoplaki, E. (2012). Climate change and impacts in the Eastern Mediterranean and the Middle East, doi: 10.1007/s10584-012-0418-4

18. Lionello, P., Abrantes, F., Gacic, M., Planton, S., Trigo, R., Ulbrich, U. (2014). The climate of the Mediterranean region: research progress and climate change impacts, doi: 10.1007/s10113-014-0666-0.

19. Luterbacher, J., et al. (2006). Lionello, P., Malanotte-Rizzoli, P., Boscolo, R. (Eds.), Mediterranean climate variability over the last centuries: a review. Elsevier, Amsterdam, ISBN 9780444521705 - pp. 27.

20. Patz, J.A., McGeehin, M.A., Bernard, S.M., Ebi, K.L., Epstein, P.R., Grambsch, A., et al. (2000). The Potential Health Impacts of Climate Change Variability and Change for the United States: Executive Summary of the Report of the Health Sector of the U.S. National Assessment. Environmental Health Perspectives, 108, 367-376.

21. Pavlik, D., Sohl, D., Pluntke, T., Mykhnovych, A., Bernhofer, C. (2012). Dynamic downscaling of global climate projections for Eastern Europe with a horizontal resolution of 7 km, doi: 10.1007/s12665-011-1081-1.

22. Sun, D., Pinker, R.T., Kafatos, M. (2006) Diurnal temperature range over the United States: A Satellite View, Geophysical Research Letters, Vol. 33, L05705, 2006. doi:10.1029/2005GL024780

23. Schmidt, G.A., M. Kelley, L. Nazarenko, R. Ruedy, G.L. Russell, I. Aleinov, M. Bauer, S.E. Bauer, M.K. Bhat, R. Bleck, V. Canuto, Y.-H. Chen, Y. Cheng, T.L. Clune, A. Del Genio, R. de Fainchtein, G. Faluvegi, J.E. Hansen, R.J. Healy, N.Y. Kiang, D. Koch, A.A. Lacis, A.N. LeGrande, J. Lerner, K.K. Lo, E.E. Matthews, S. Menon, R.L. Miller, V. Oinas, A.O. Oloso, J.P. Perlwitz, M.J. Puma, W.M. Putman, D. Rind, A. Romanou, M. Sato, D.T. Shindell, S. Sun, R.A. Syed, N. Tausnev, K. Tsigaridis, N. Unger, A. Voulgarakis, M.-S. Yao, and J. Zhang, 2014: Configuration and assessment of the GISS ModelE2 contributions to the CMIP5 archive. J. Adv. Model. Earth Syst., 6, no. 1, 141-184, doi:10.1002/2013MS000265.

24. Schmidt, G.A., Jungclaus, J.H., Ammann, C.M., Bard, E., Braconnot, P., Crowley, T.J., et al. (2011). Climate forcing reconstructions for use in PMIP simulations of the last millennium (v1.0). Geoscientific Model Development, 4, 33-45.

25. Senatore A., Mendicino G., Smiatek G., Kunstmann H. (2011) Regional climate change projections and hydrological impact analysis for a Mediterranean basin in Southern Italy. Journal of Hydrology, 399, 70–92.

26. Seubert, S., Fern´andez-Montes, S., Philipp, A., Hertig, E., Jacobeit, J., Vogt, G., et al. (2014). Mediterranean climate extremes in synoptic downscaling assessment, doi: 10.1007/s00704-013-0993-y

27. Somot, S., Sevault, F., Déqué, M., Crépon, M. (2008). 21st century climate change scenario for the Mediterranean using a coupled atmosphere–ocean regional climate model. Global Planet Change, 63, 112–126.

28. van der Linden, P., Mitchell, J.F.B. (eds.), (2009). ENSEMBLES: Climate Change and its Impacts: Summary of research and results from the

ENSEMBLES project. Met Office Hadley Centre, FitzRoy Road, Exeter EX1 3PB, UK.

29. van Vuuren, D.P., Edmonds, J., Kainuma, M., Riahi, K., Thomson, A., Hibbard, K., et al. (2011). The representative concentration pathways: An overview, doi: 10.1007/s10584-011-0148-z

30. van Vliet, M.T.H., Blenkinsop, S., Burton, A., Harpham, C., Broers, H.P., Fowler, H.J. (2012). A multi-model ensemble of downscaled spatial climate change scenarios for the Dommel catchment, Western Europe, doi: 10.1007/s10584-011-0131-8.

Annex 1: Seasonal global average GCM parameters and their change for RCP8.5

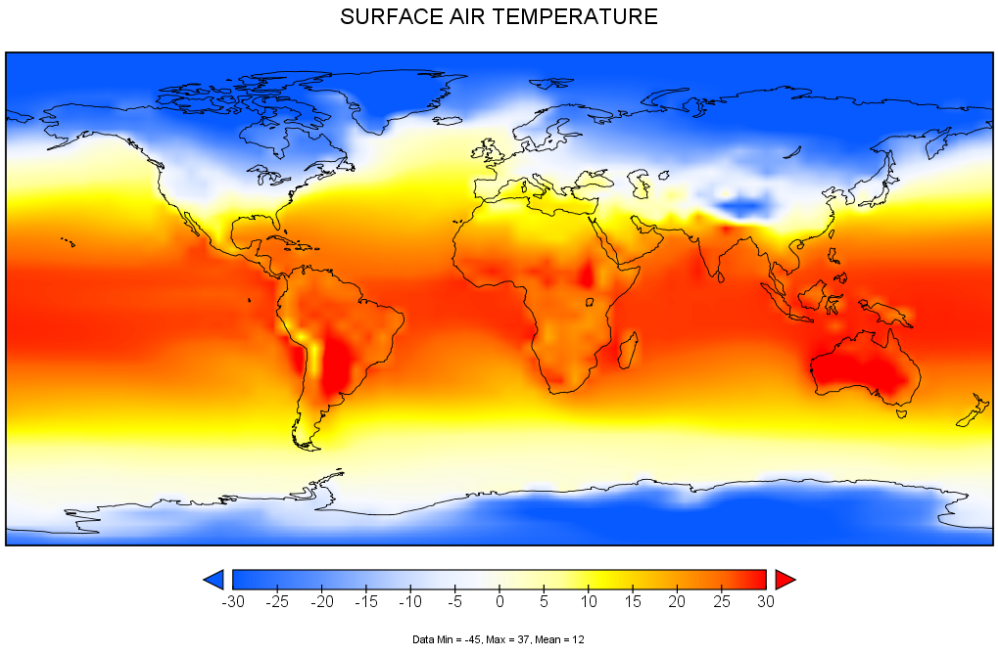

a

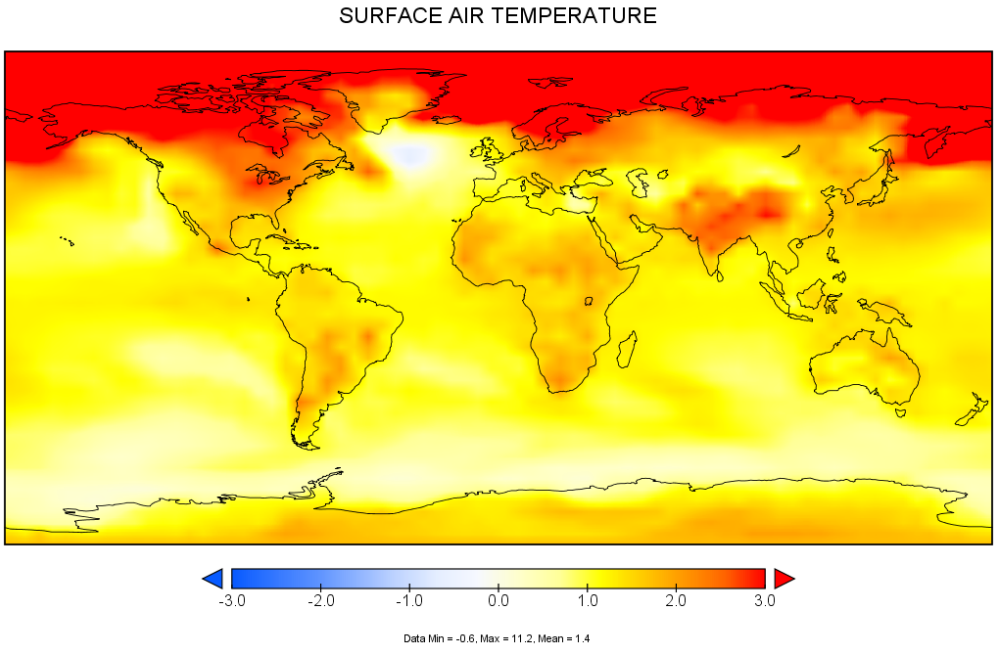

b

(a). Winter (JFD) average surface air temperature for the 1981-2010 historical simulations, (b). JFD average surface air temperature differences (°C) for 2031–2060 minus 1981–2010 of the corresponding historical simulation for RCP8.5

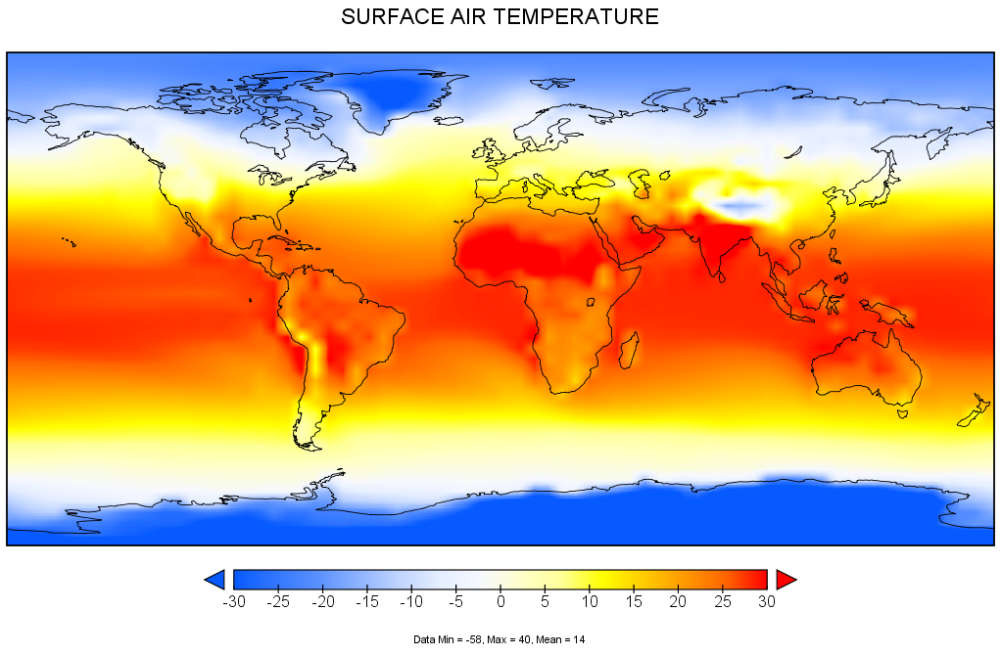

a

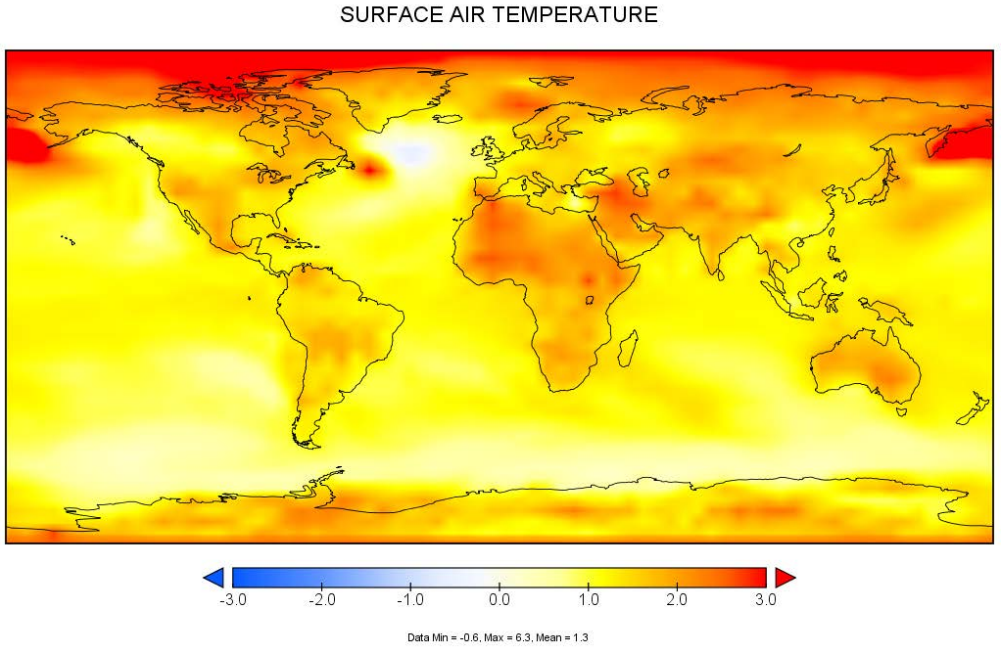

b

(a). Spring (MAM) average surface air temperature for the 1981-2010 historical simulations, (b). MAM average surface air temperature differences (°C) for 2031–2060 minus 1981–2010 of the corresponding historical simulation for RCP8.5

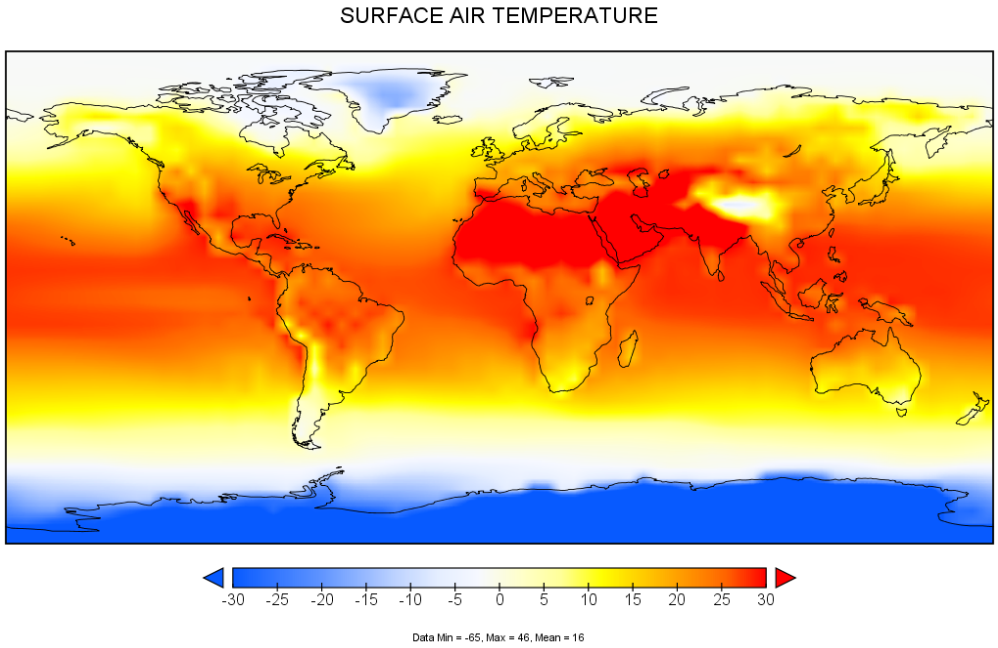

a

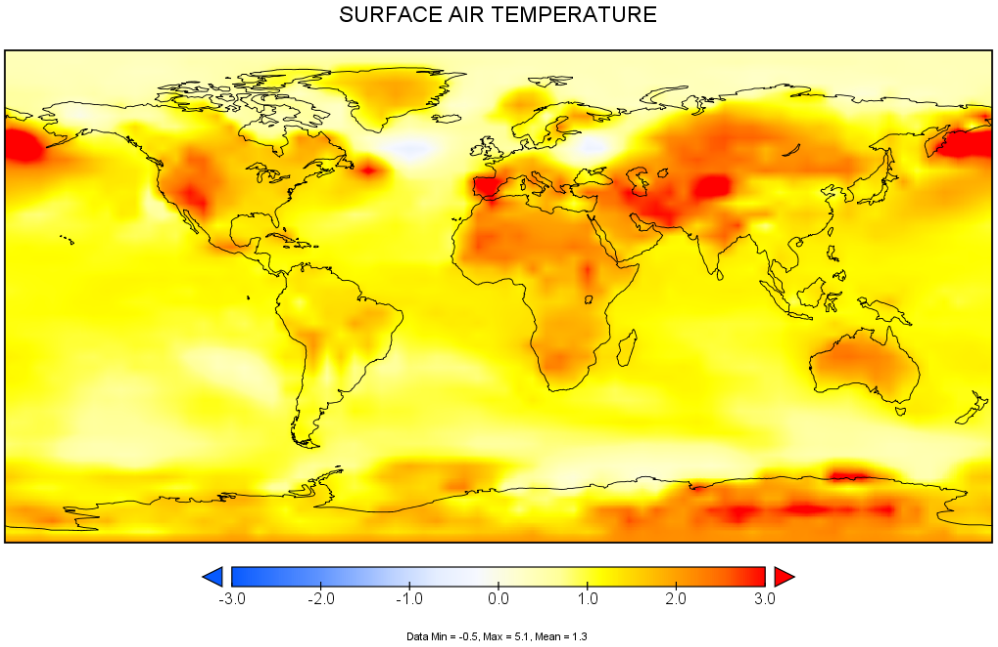

b

(a). Summer (JJA) average surface air temperature for the 1981-2010 historical simulations, (b). JJA average surface air temperature differences (°C) for 2031–2060 minus 1981–2010 of the corresponding historical simulation for RCP8.5

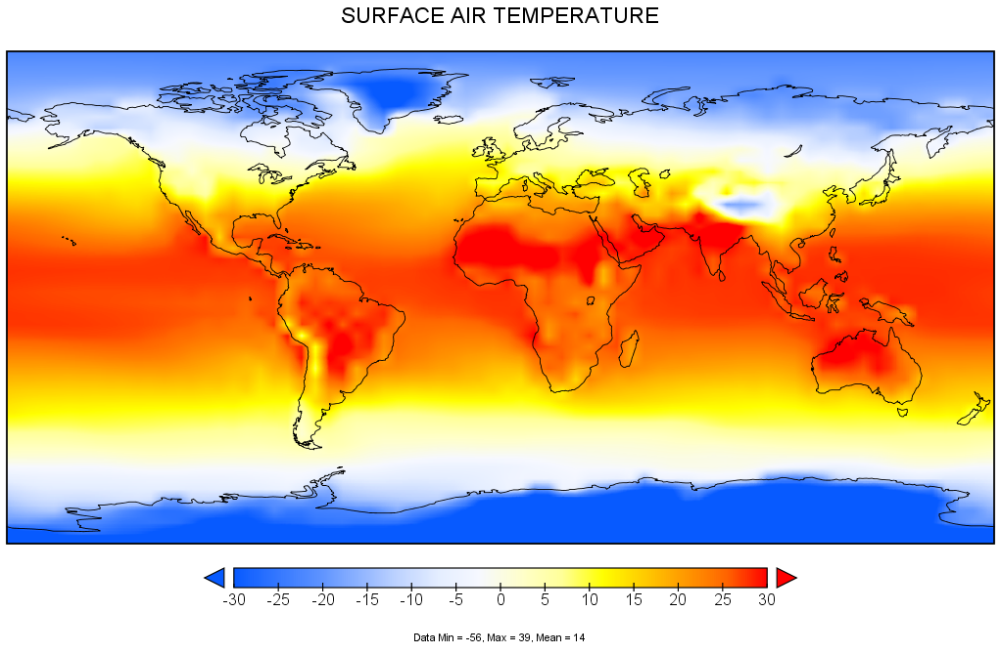

a

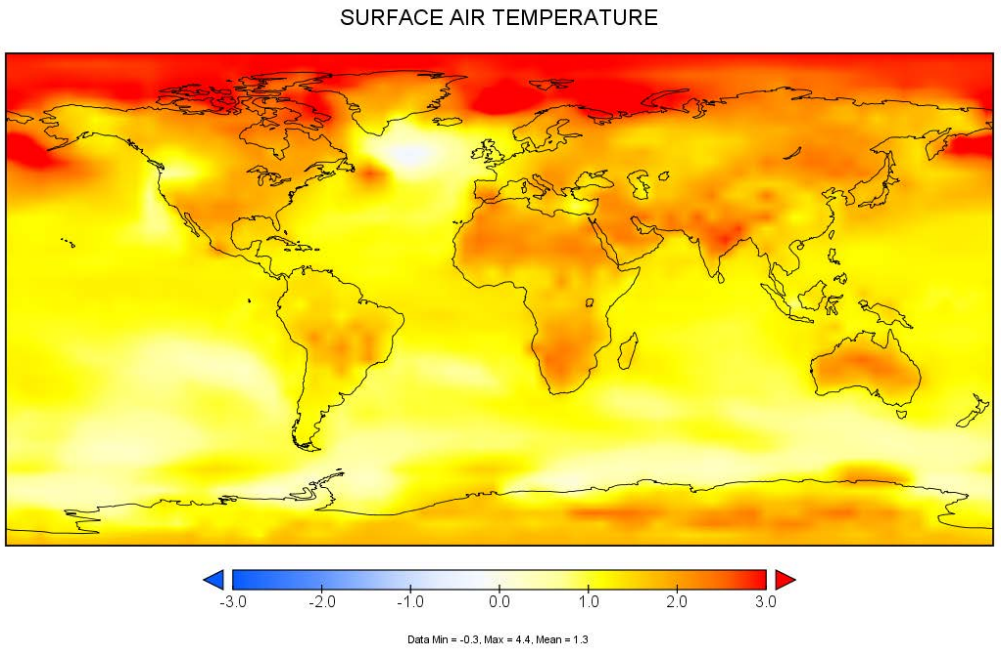

b

(a). Autumn (SON) average surface air temperature for the 1981-2010 historical simulations, (b). SON average surface air temperature differences (°C) for 2031–2060 minus 1981–2010 of the corresponding historical simulation for RCP8.5

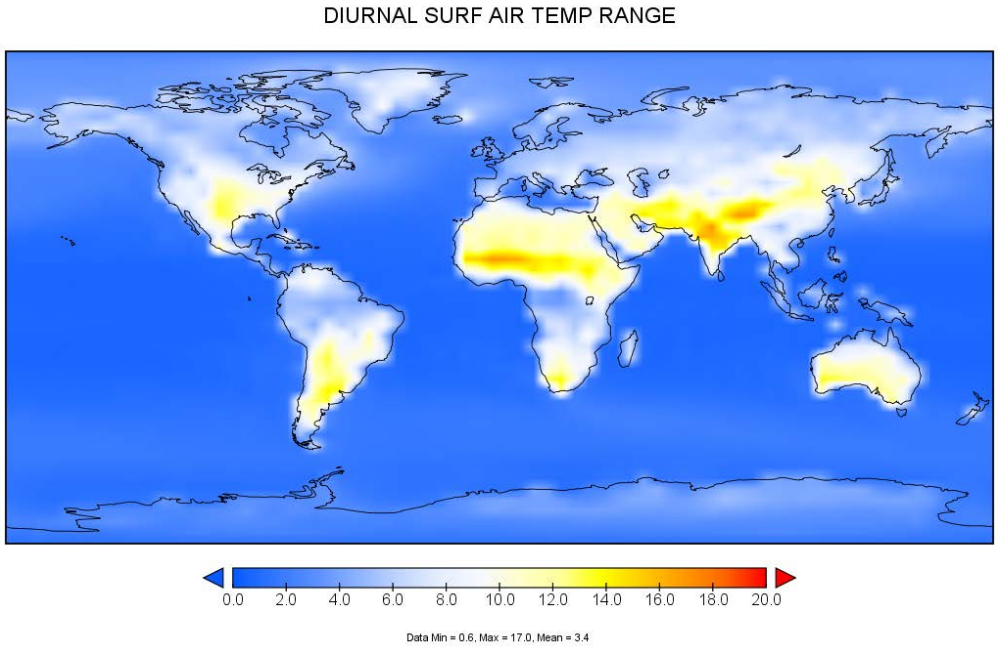

a

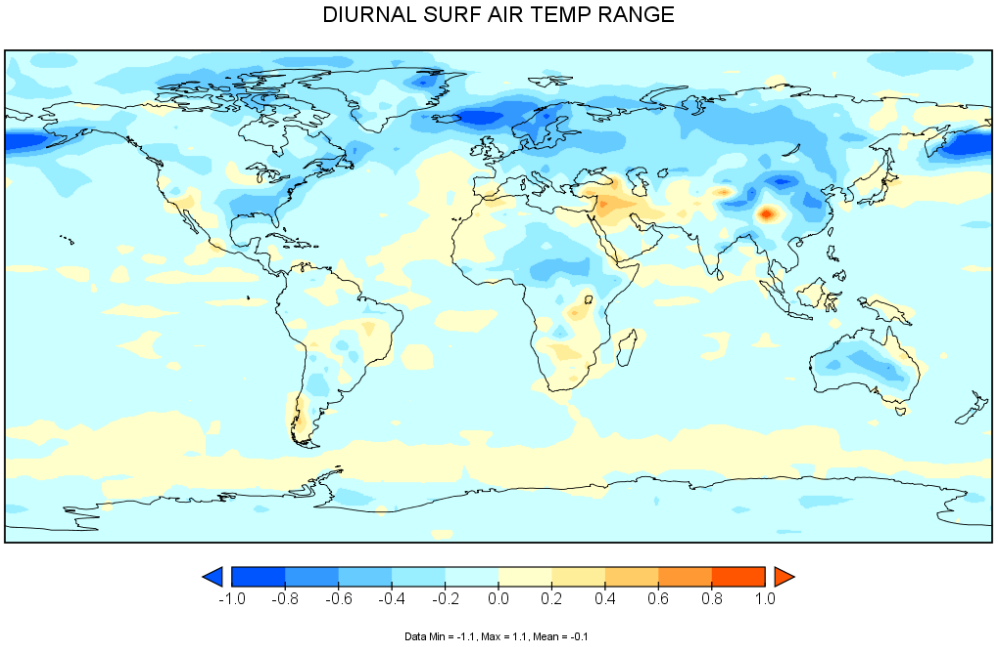

b

(a). Winter (JFD) average diurnal surface air temperature range (°C) for the 1981-2010 historical simulations, (b). JFD diurnal surface air temperature range differences (°C) for 2031–2060 minus 1981–2010 of the corresponding historical simulation for RCP8.5

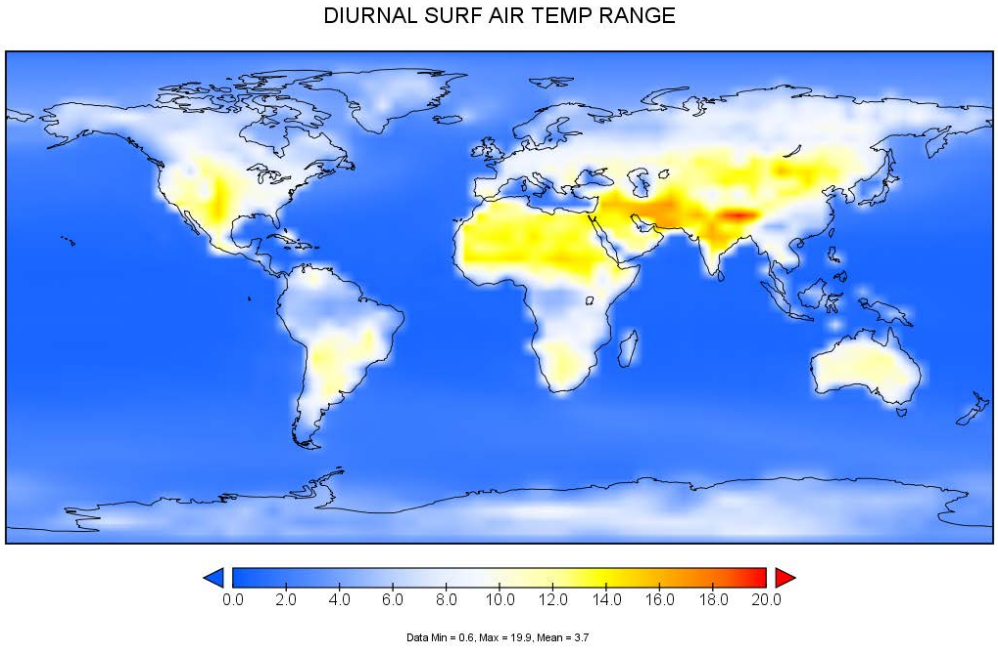

a

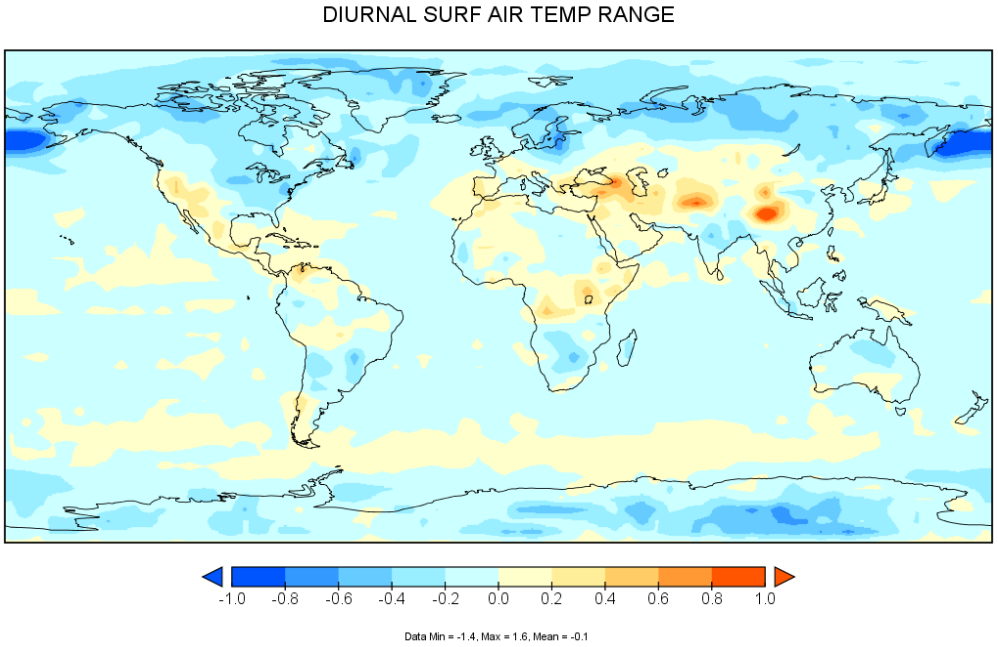

b

(a). Spring (MAM) average diurnal surface air temperature range (°C) for the 1981-2010 historical simulations, (b). MAM diurnal surface air temperature range differences (°C) for 2031–2060 minus 1981–2010 of the corresponding historical simulation for RCP8.5

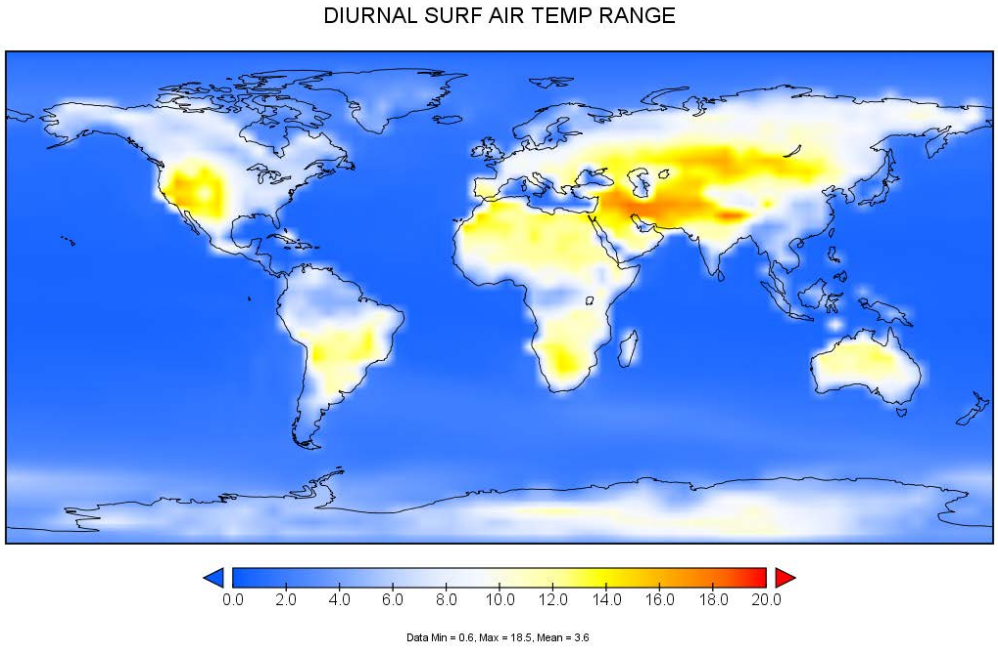

a

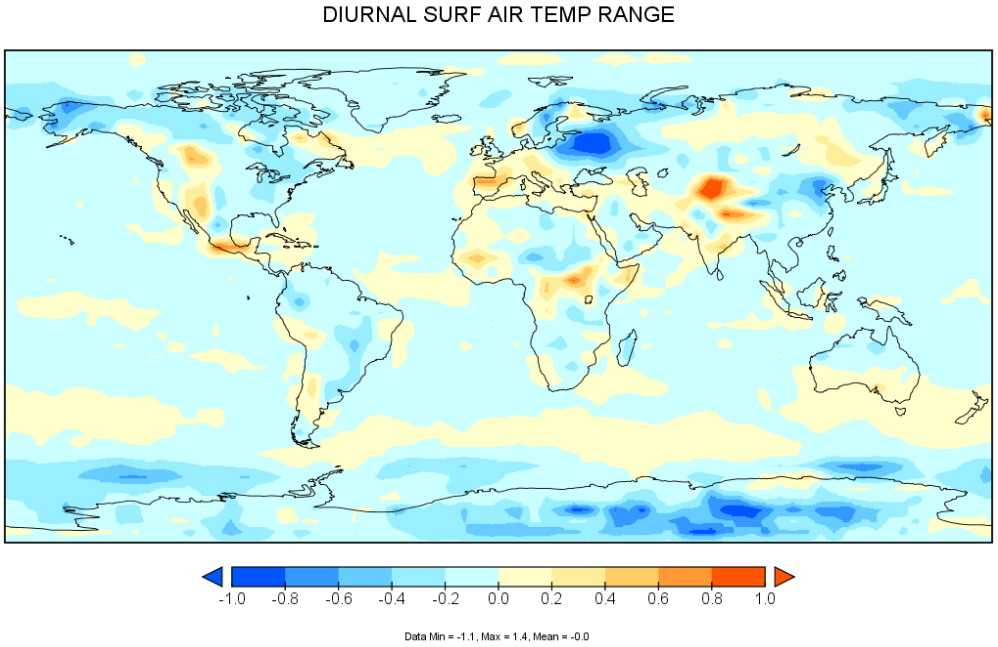

b

(a). Summer (JJA) average diurnal surface air temperature range (°C) for the 1981-2010 historical simulations, (b). JJA diurnal surface air temperature range differences (°C) for 2031–2060 minus 1981–2010 of the corresponding historical simulation for RCP8.5

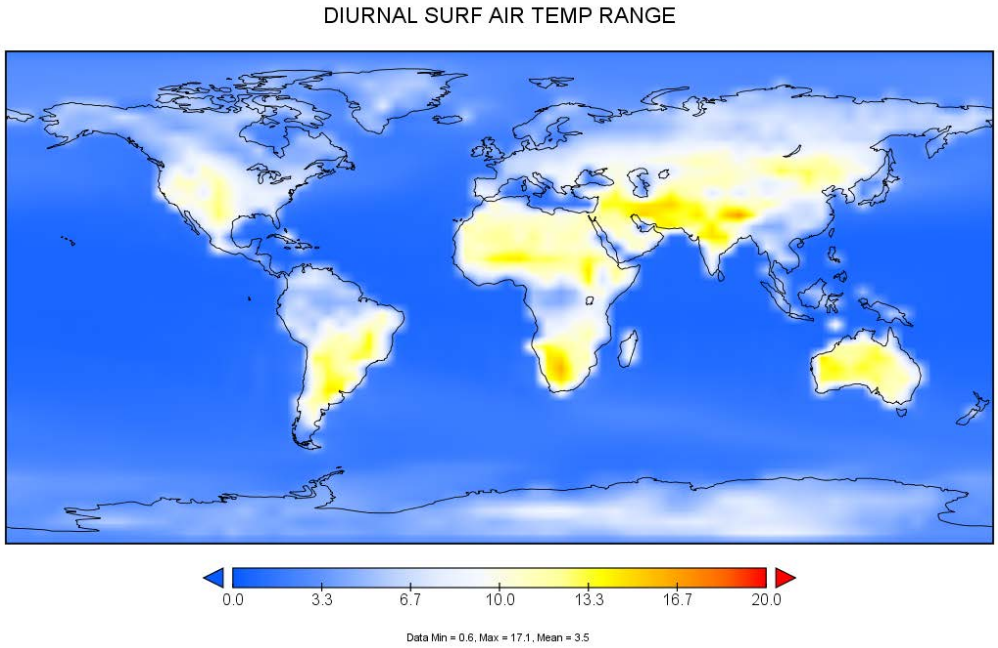

a

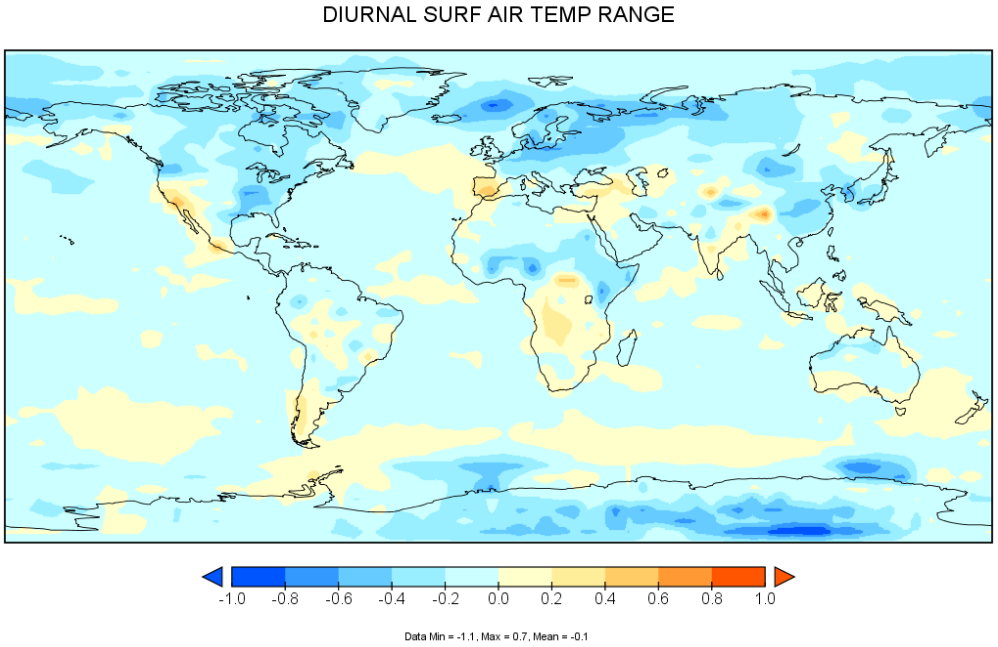

b

(a). Autumn (SON) average diurnal surface air temperature range (°C) for the 1981-2010 historical simulations, (b). SON diurnal surface air temperature range differences (°C) for 2031–2060 minus 1981–2010 of the corresponding historical simulation for RCP8.5

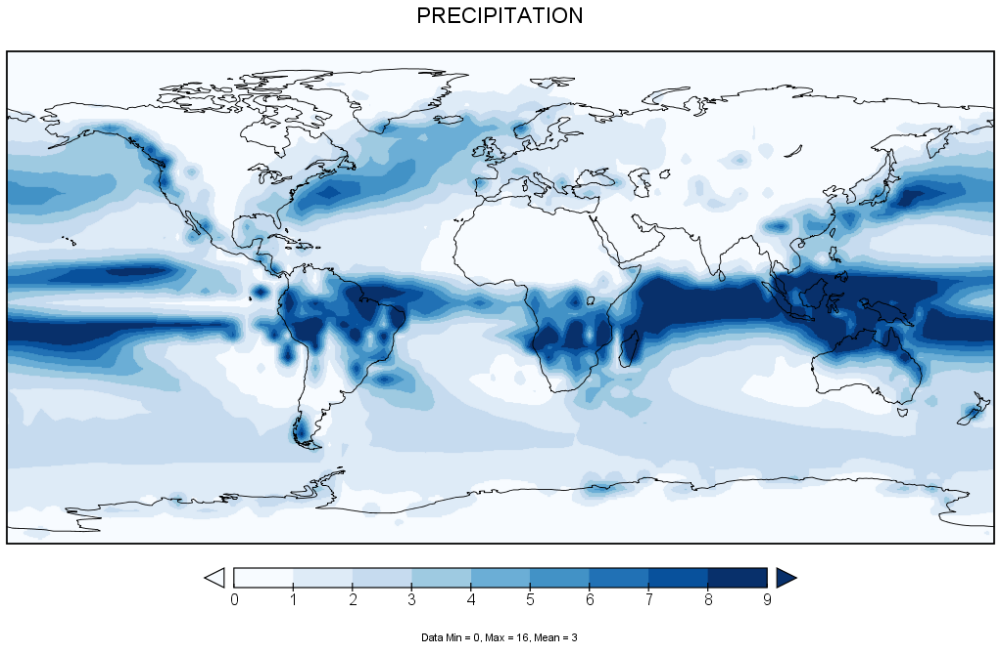

a

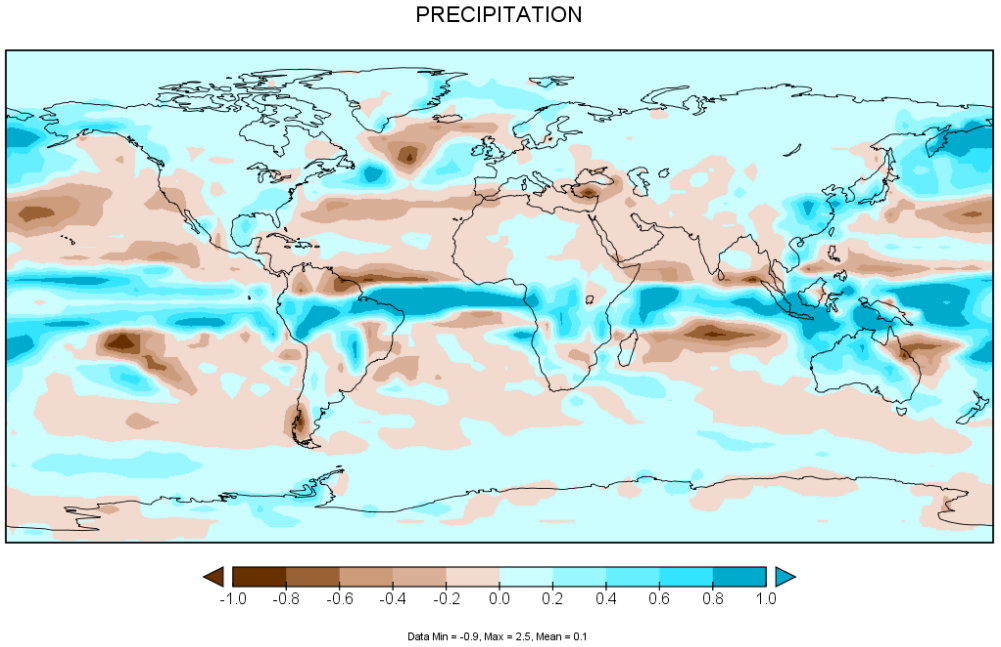

b

(a). Winter (JFD) average precipitation (mm/day) for the 1981-2010 historical simulations, (b). JFD precipitation differences (mm/day) for 2031–2060 minus 1981–2010 of the corresponding historical simulation for RCP8.5

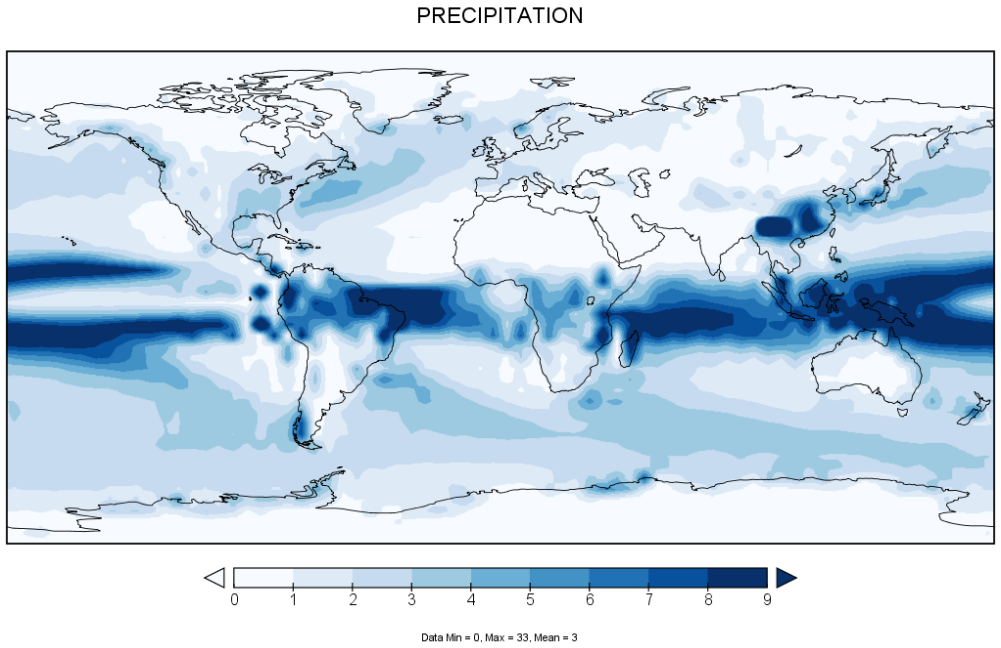

a

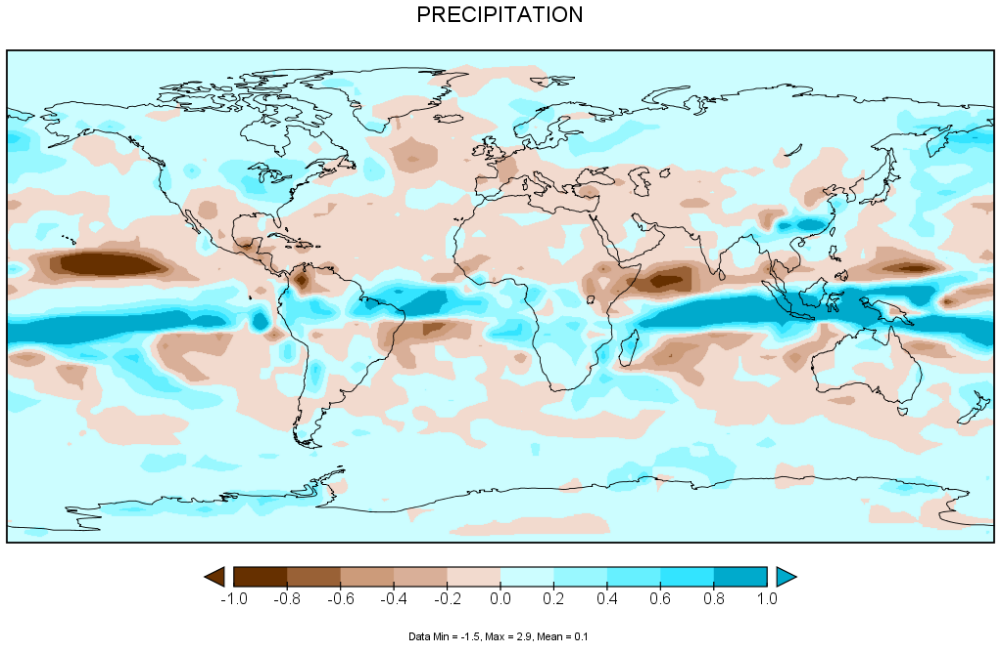

b

(a). Spring (MAM) average precipitation (mm/day) for the 1981-2010 historical simulations, (b). MAM precipitation differences (mm/day) for 2031–2060 minus 1981–2010 of the corresponding historical simulation for RCP8.5

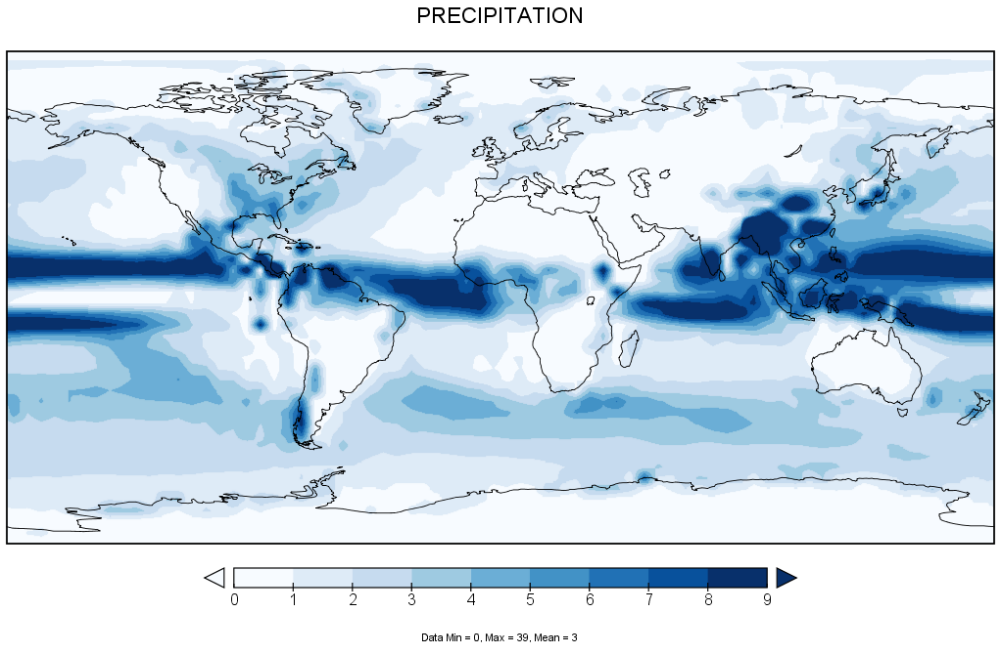

a

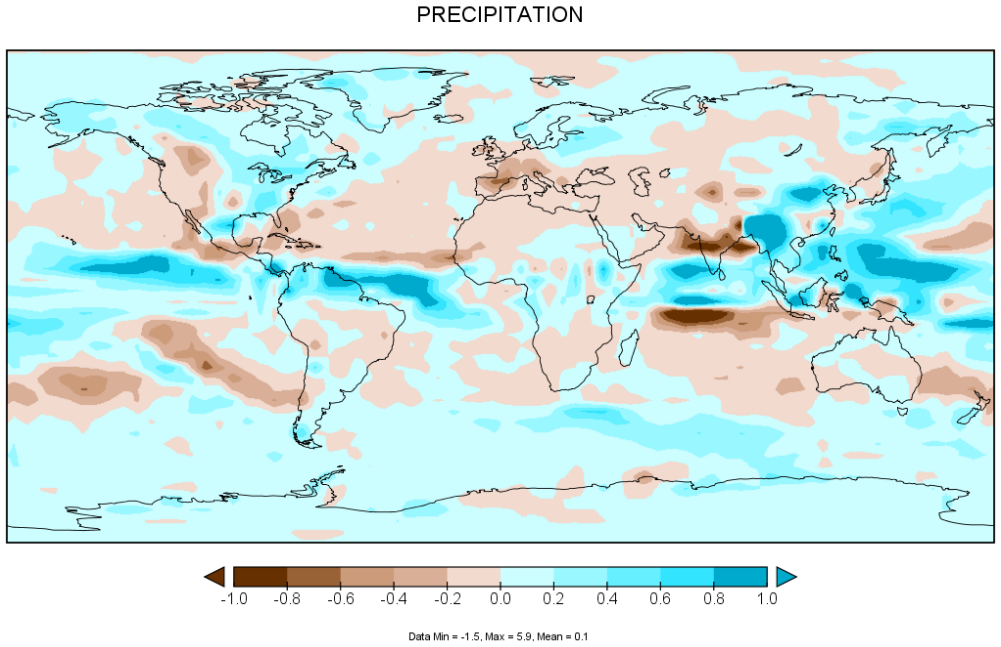

b

(a). Summer (JJA) average precipitation (mm/day) for the 1981-2010 historical simulations, (b). JJA precipitation differences (mm/day) for 2031–2060 minus 1981–2010 of the corresponding historical simulation for RCP8.5

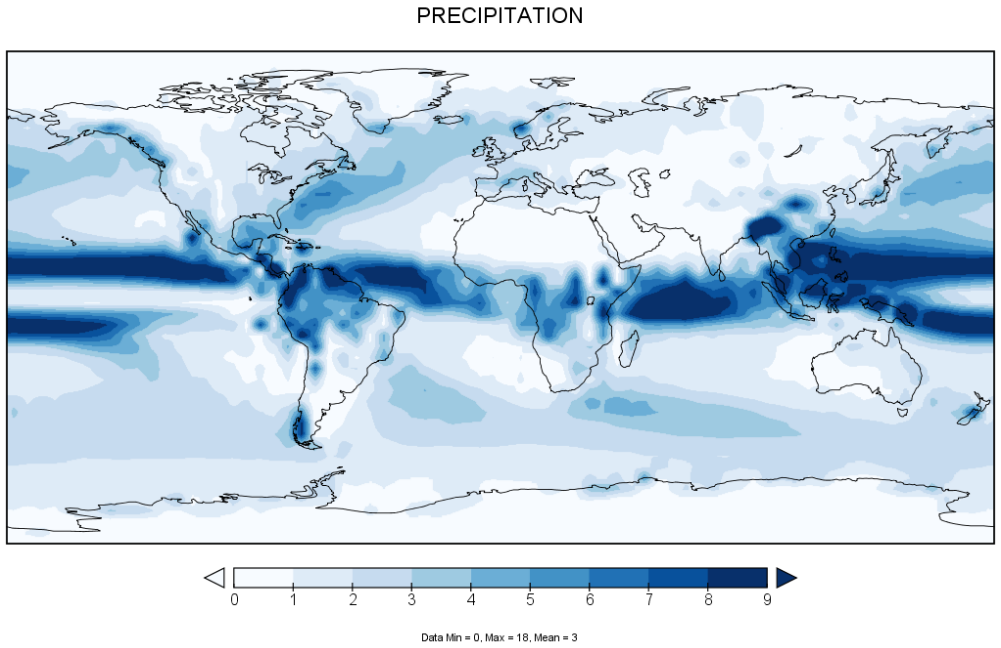

a

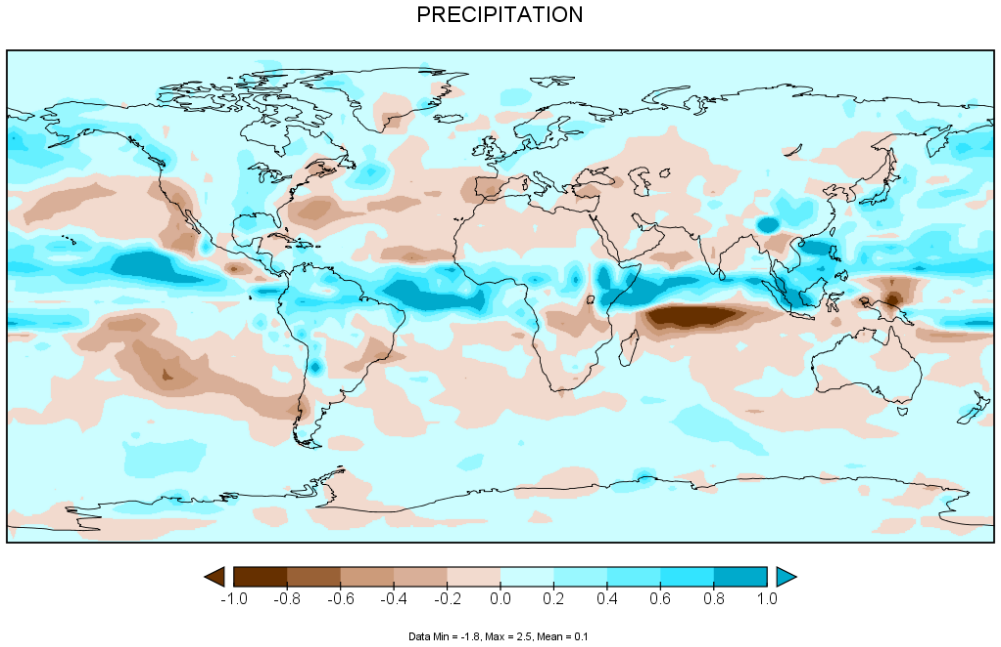

b

(a). Autumn (SON) average precipitation (mm/day) for the 1981-2010 historical simulations, (b). SON precipitation differences (mm/day) for 2031–2060 minus 1981–2010 of the corresponding historical simulation for RCP8.5

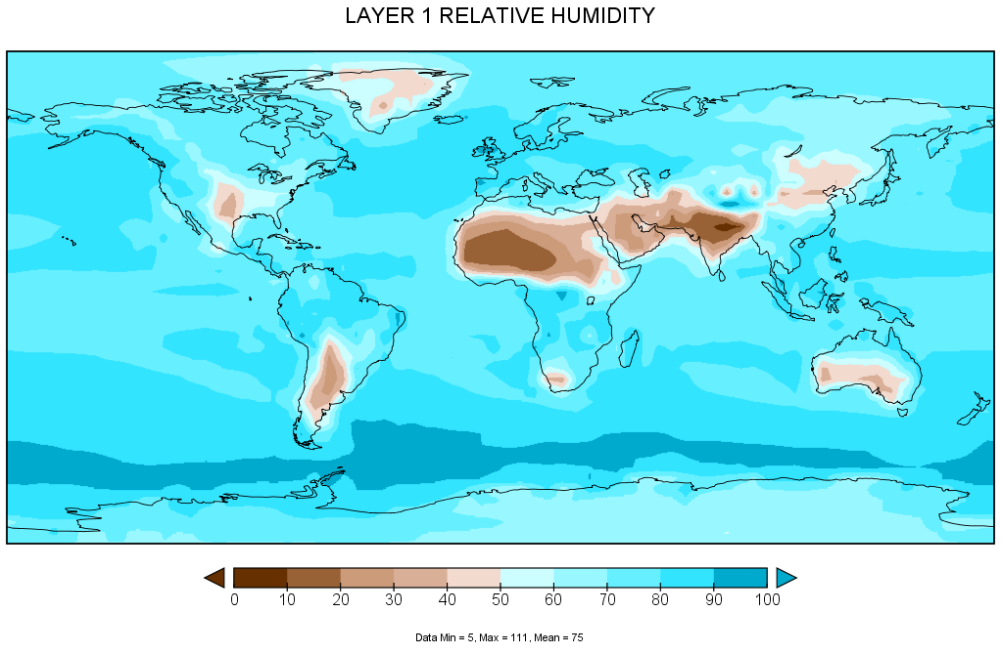

a

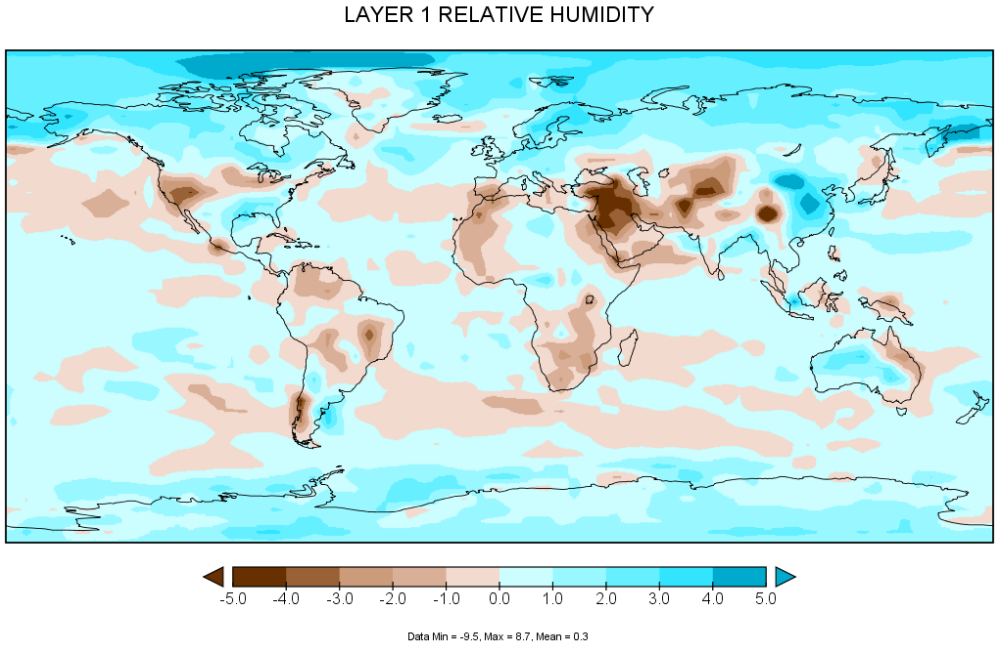

b

(a). Winter (JFD) average relative humidity (%) for the 1981-2010 historical simulations (b). JFD relative humidity differences (%) for 2031–2060 minus 1981–2010 of the corresponding historical simulation for RCP8.5

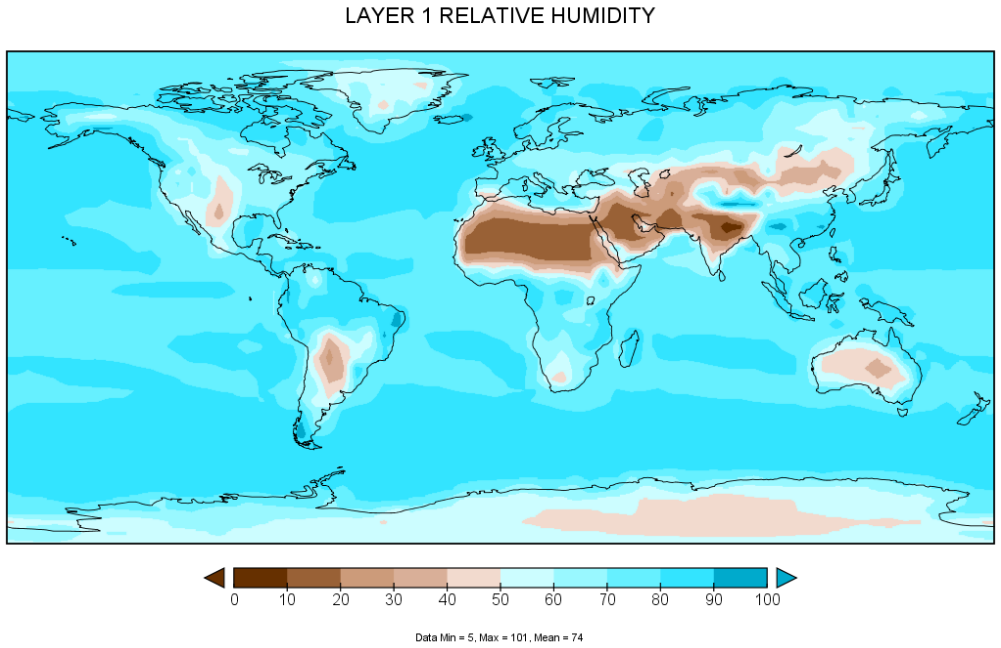

a

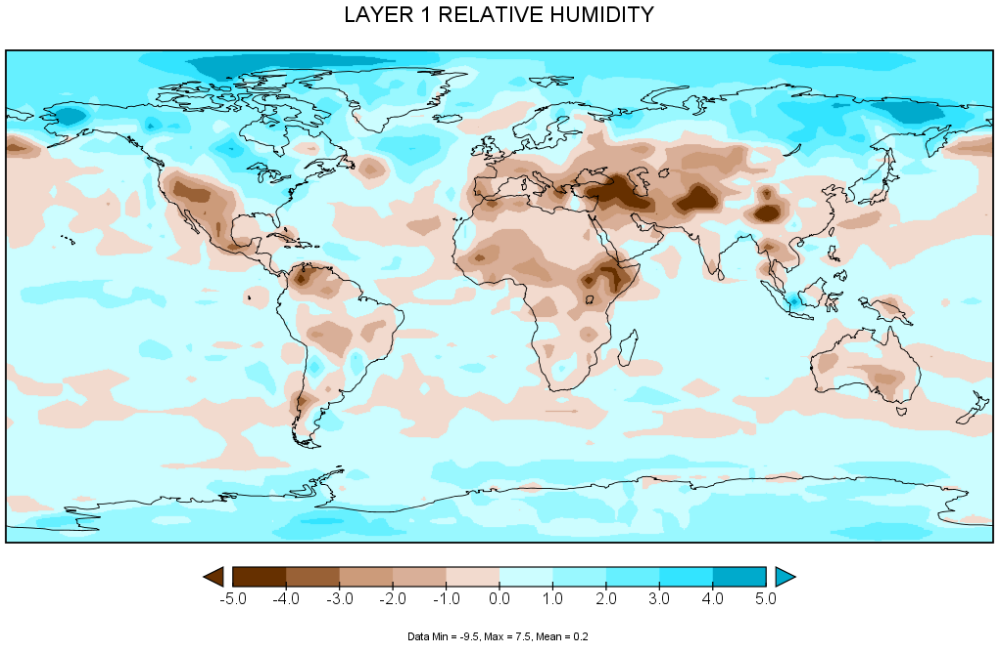

b

(a). Spring (MAM) average relative humidity (%) for the 1981-2010 historical simulations (b). MAM relative humidity differences (%) for 2031–2060 minus 1981–2010 of the corresponding historical simulation for RCP8.5

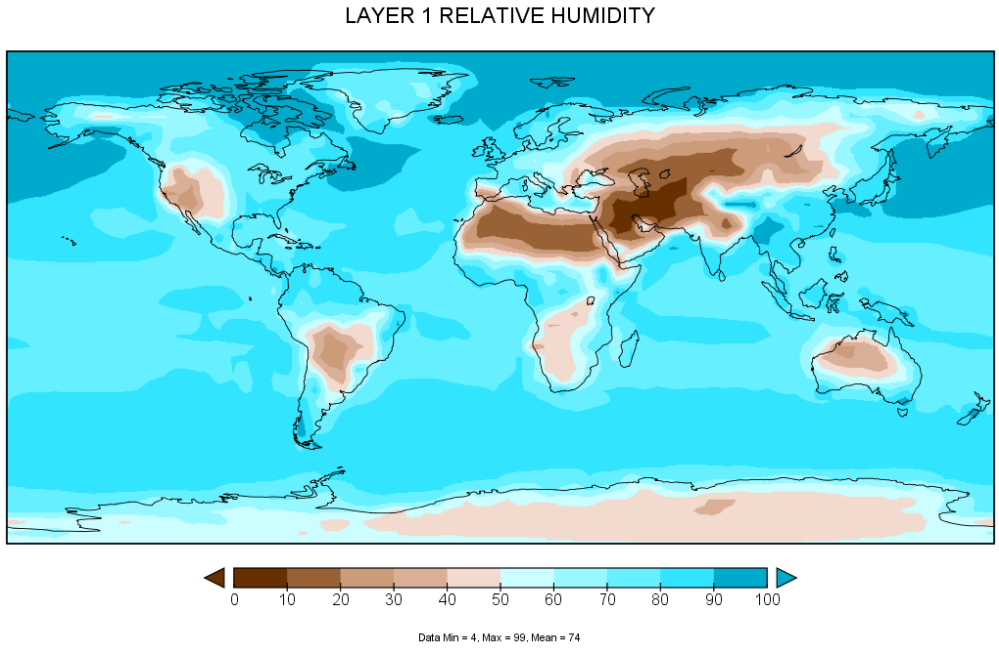

a

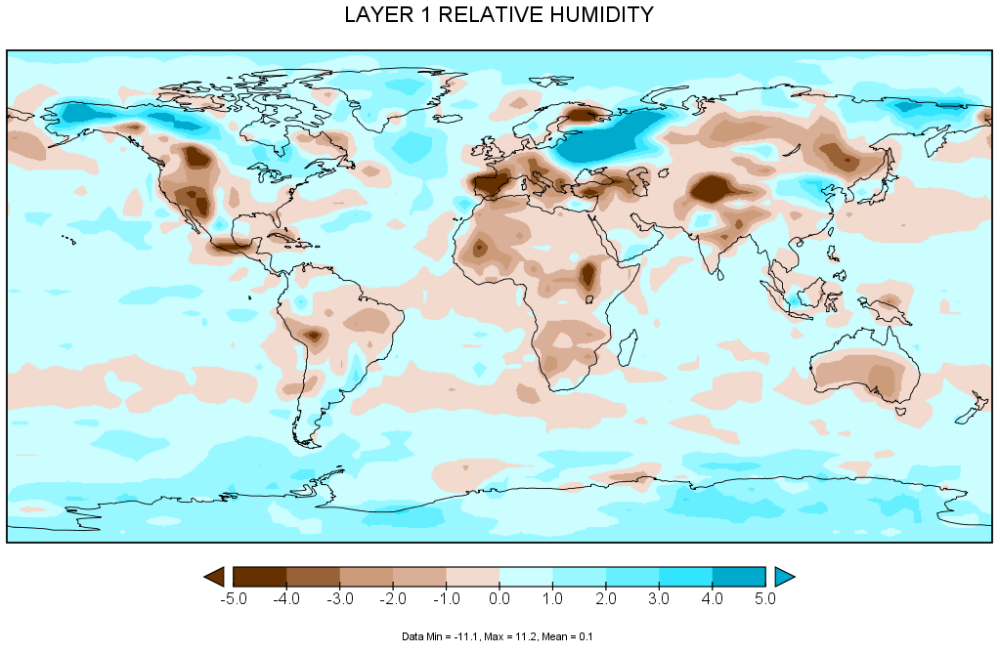

b

(a). Summer (JJA) average relative humidity (%) for the 1981-2010 historical simulations (b). JJA relative humidity differences (%) for 2031–2060 minus 1981–2010 of the corresponding historical simulation for RCP8.5

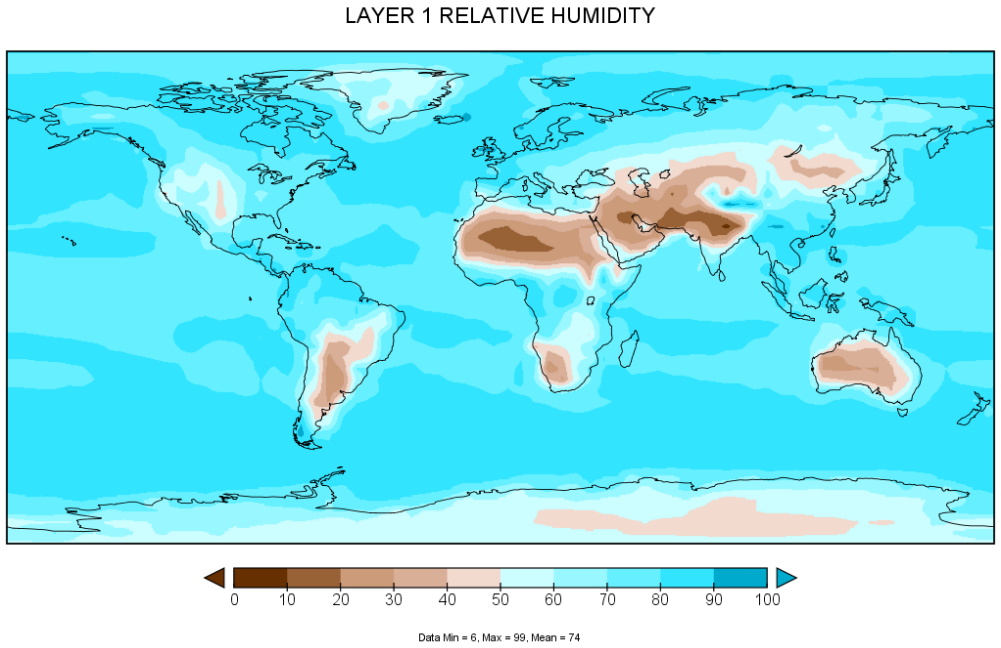

a

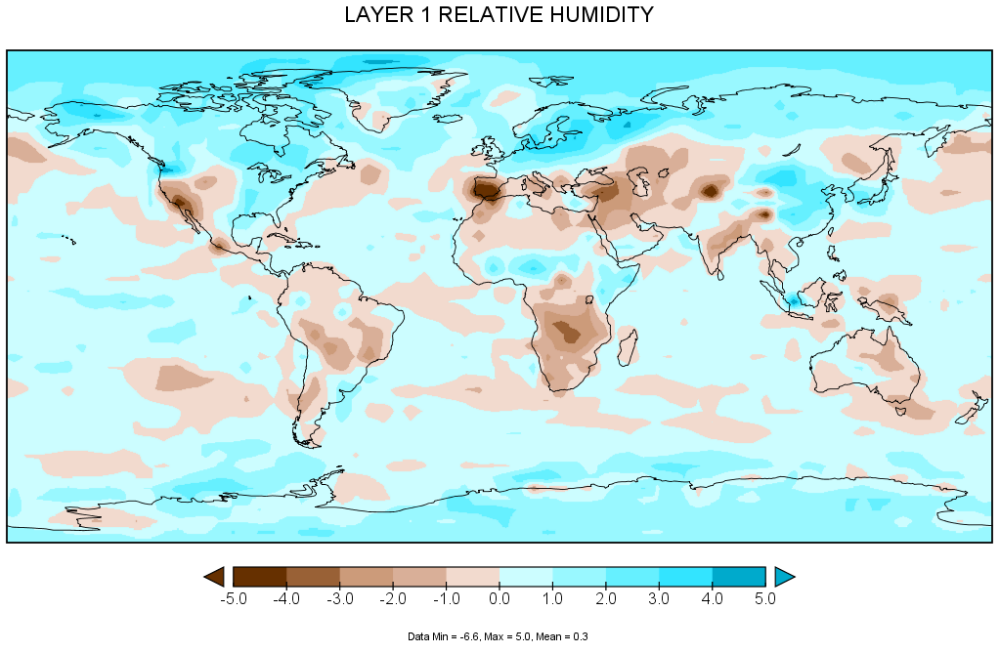

b

(a). Autumn (SON) average relative humidity (%) for the 1981-2010 historical simulations (b). SON relative humidity differences (%) for 2031–2060 minus 1981–2010 of the corresponding historical simulation for RCP8.5

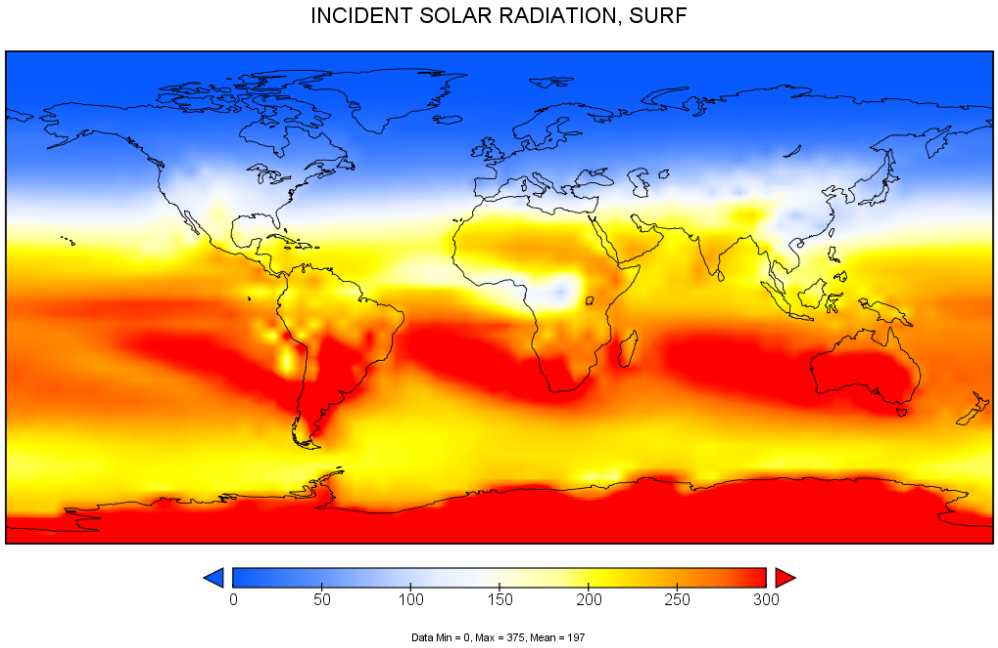

a

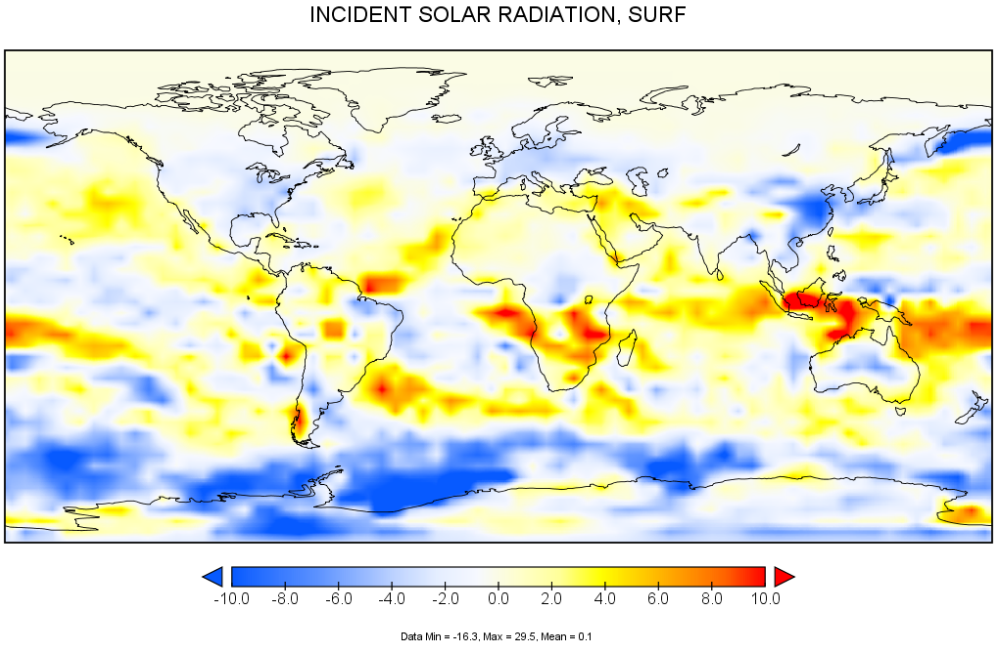

b

(a). Winter (JFD) average incident solar radiation at the surface (W/m^2) for the 1981-2010 historical simulations (b). JFD incident solar radiation differences (W/m^2) for 2031–2060 minus 1981–2010 of the corresponding historical simulation for RCP8.5

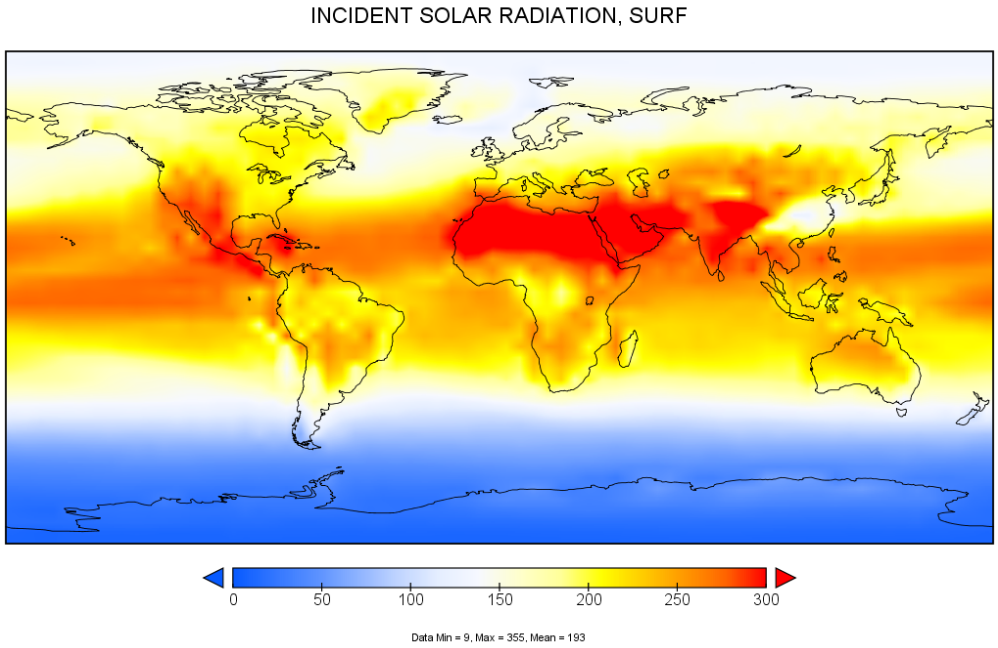

a

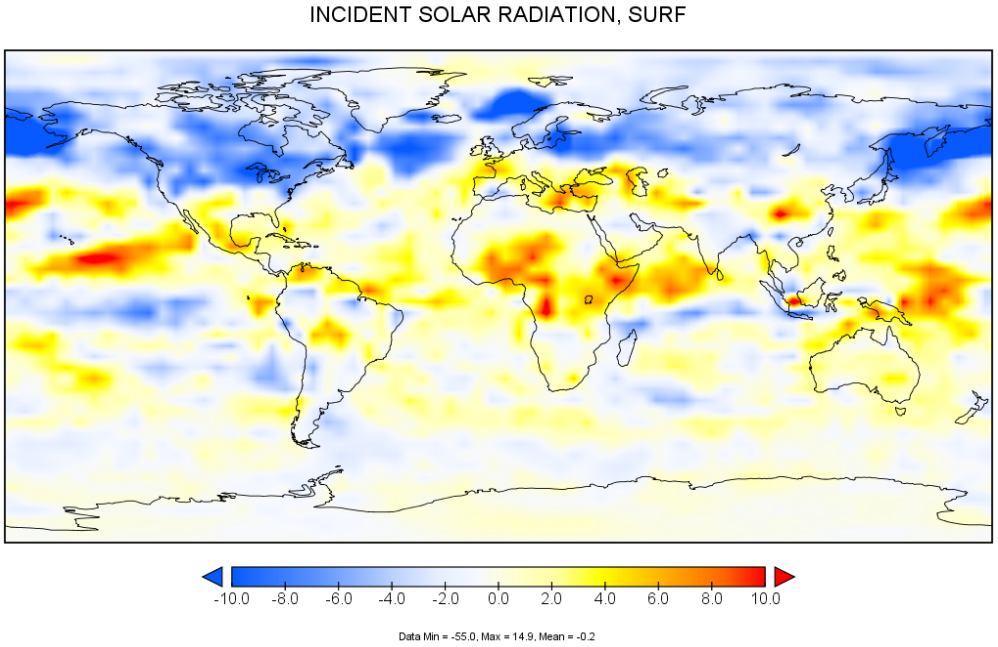

b

(a). Spring (MAM) average incident solar radiation at the surface (W/m^2) for the 1981-2010 historical simulations (b). MAM incident solar radiation differences (W/m^2) for 2031–2060 minus 1981–2010 of the corresponding historical simulation for RCP8.5

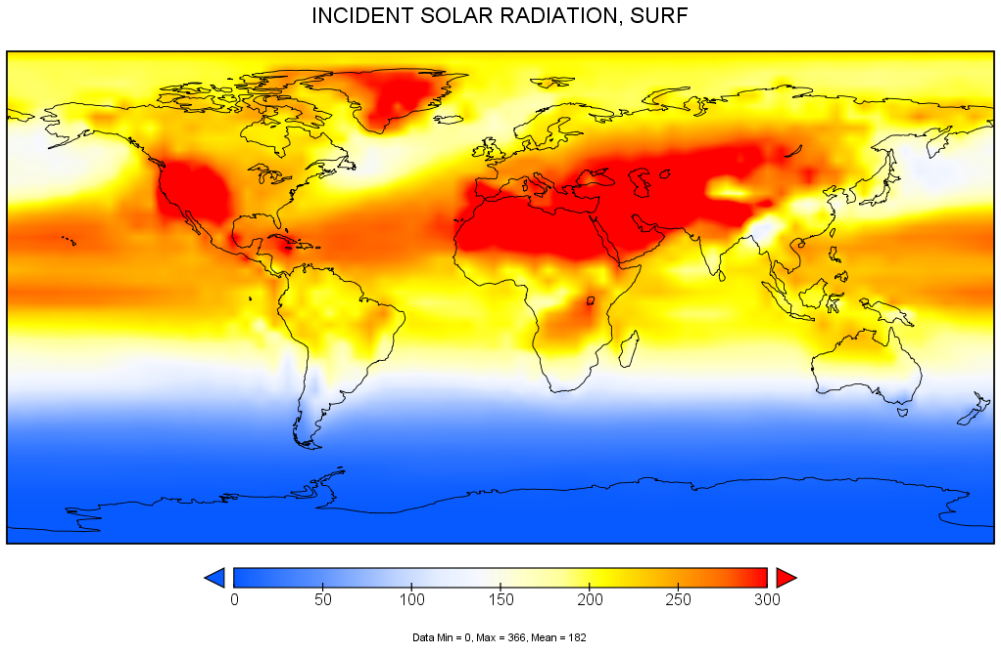

a

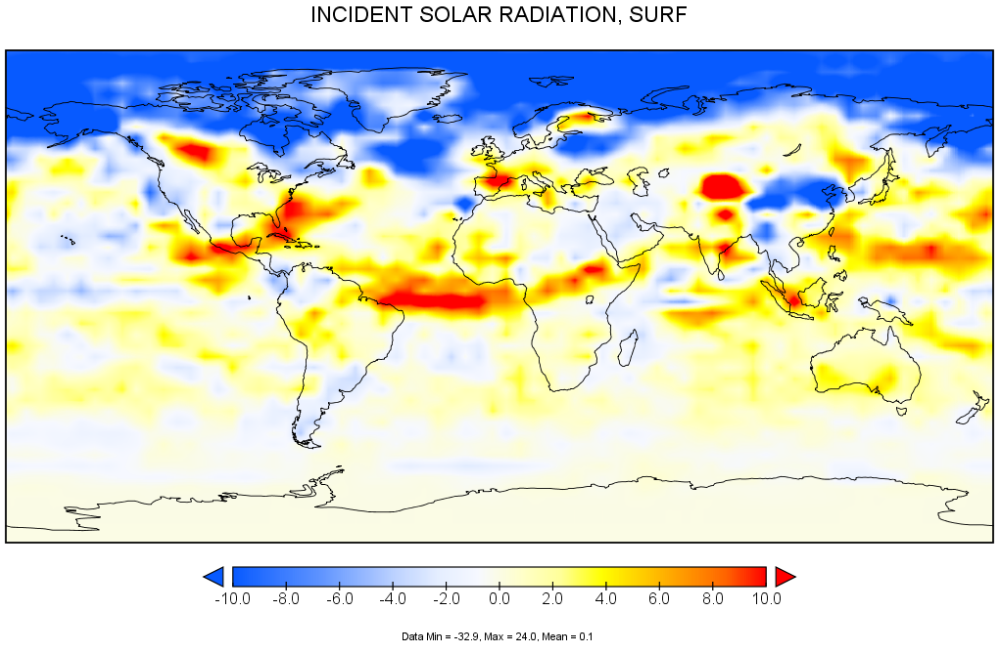

b

(a). Summer (JJA) average incident solar radiation at the surface (W/m^2) for the 1981-2010 historical simulations (b). JJA incident solar radiation differences (W/m^2) for 2031–2060 minus 1981–2010 of the corresponding historical simulation for RCP8.5

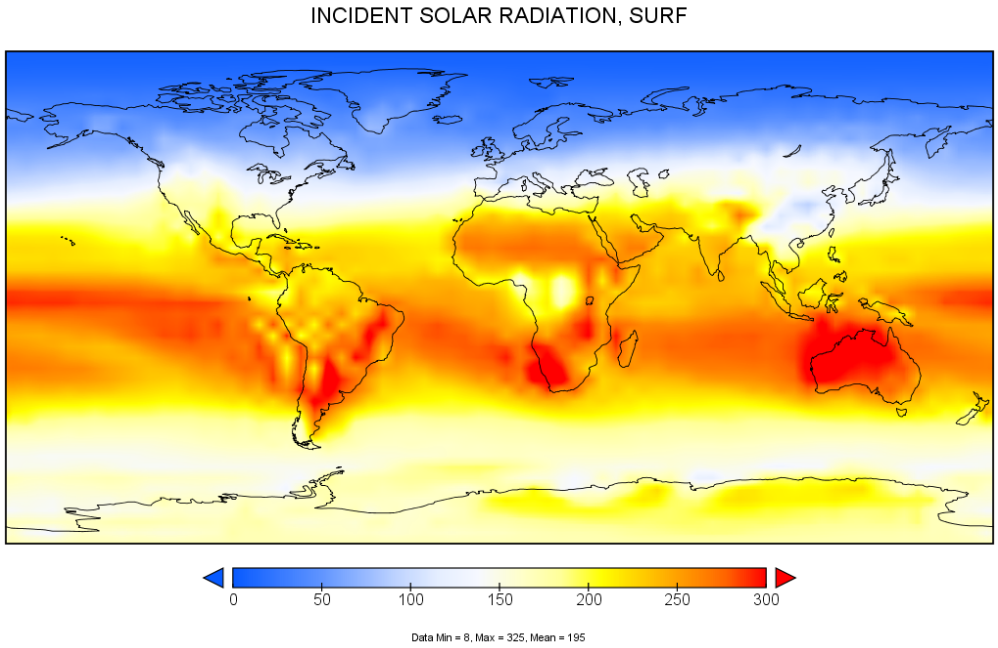

a

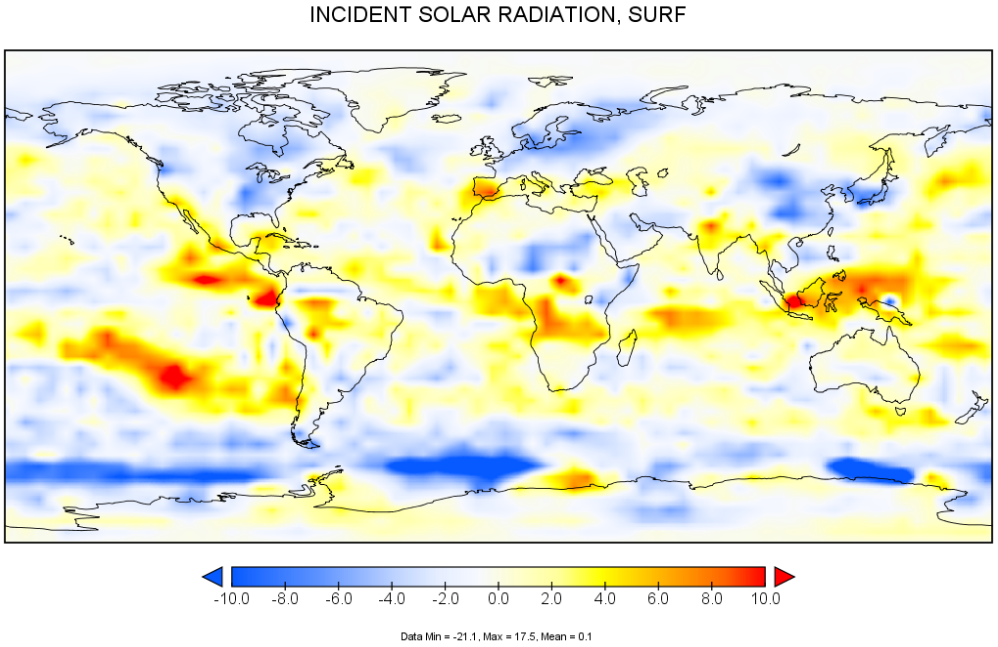

b

(a). Autumn (SON) average incident solar radiation at the surface (W/m^2) for the 1981-2010 historical simulations (b). SON incident solar radiation differences (W/m^2) for 2031–2060 minus 1981–2010 of the corresponding historical simulation for RCP8.5

Annex 2: Seasonal global average GCM parameters and their change for RCP4.5

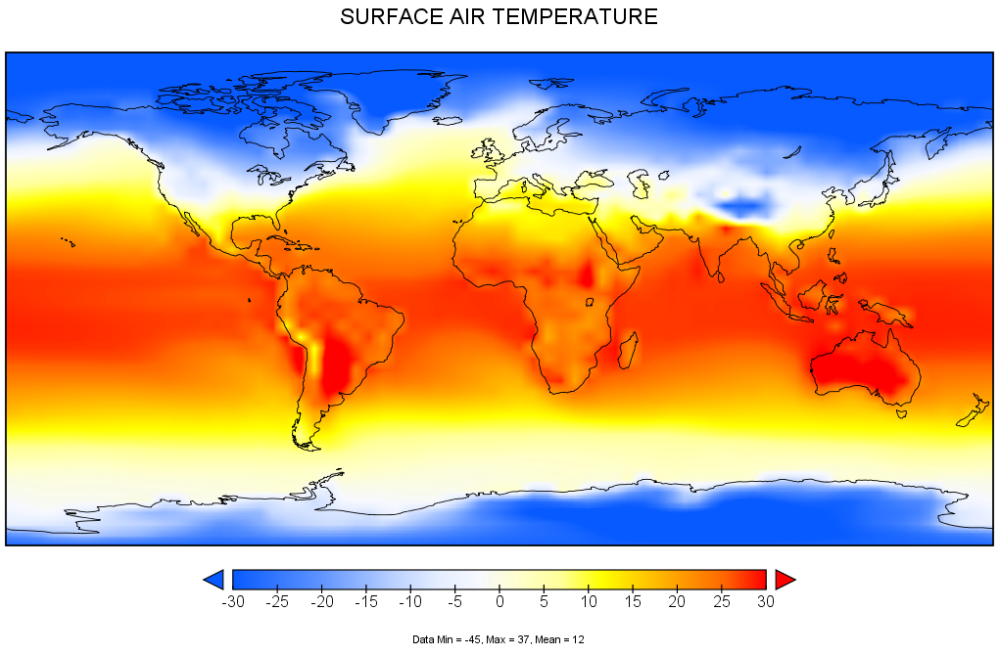

a

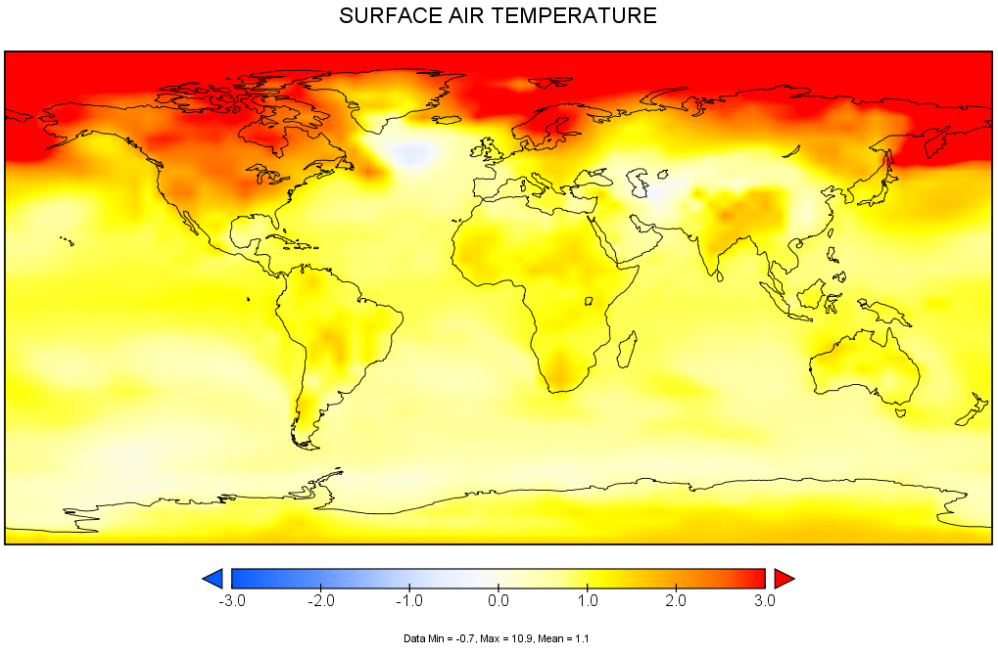

b

(a). Winter (JFD) average surface air temperature for the 1981-2010 historical simulations, (b). JFD average surface air temperature differences (°C) for 2031–2060 minus 1981–2010 of the corresponding historical simulation for RCP4.5

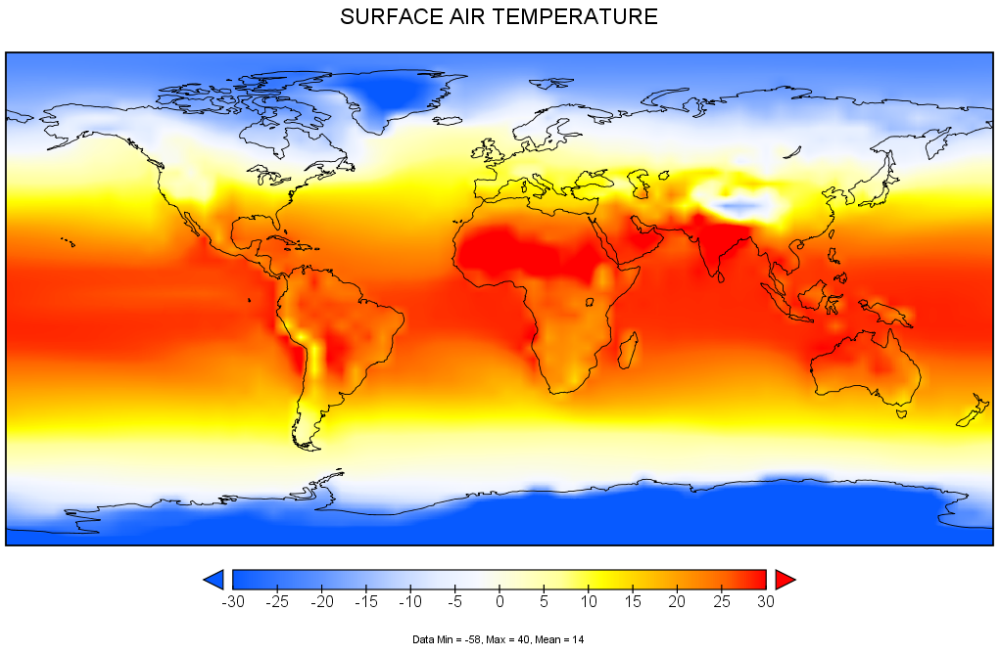

a

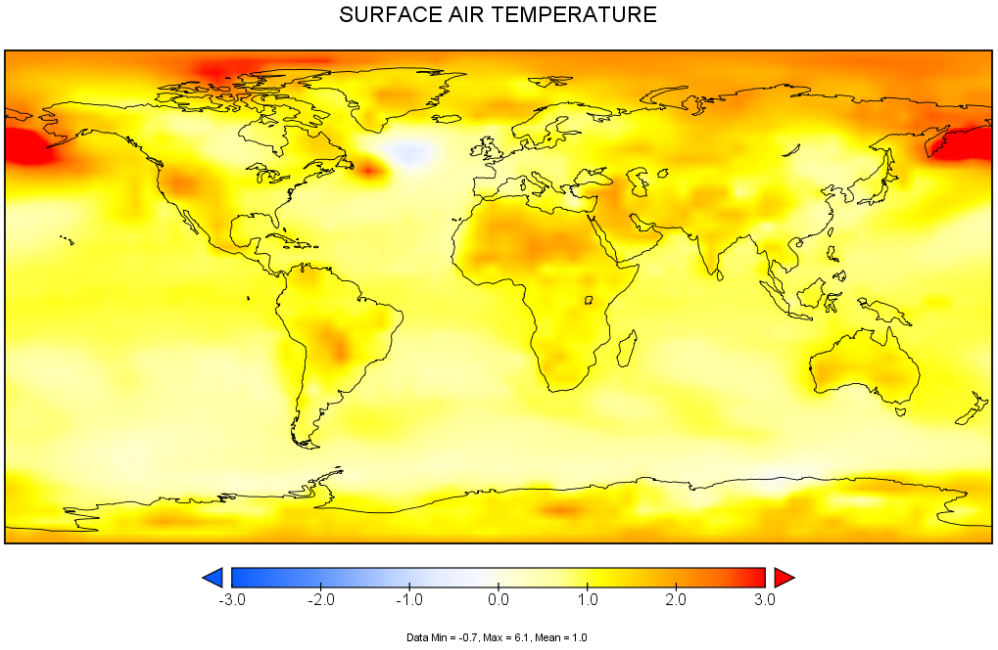

b

(a). Spring (MAM) average surface air temperature for the 1981-2010 historical simulations, (b). MAM average surface air temperature differences (°C) for 2031–2060 minus 1981–2010 of the corresponding historical simulation for RCP4.5

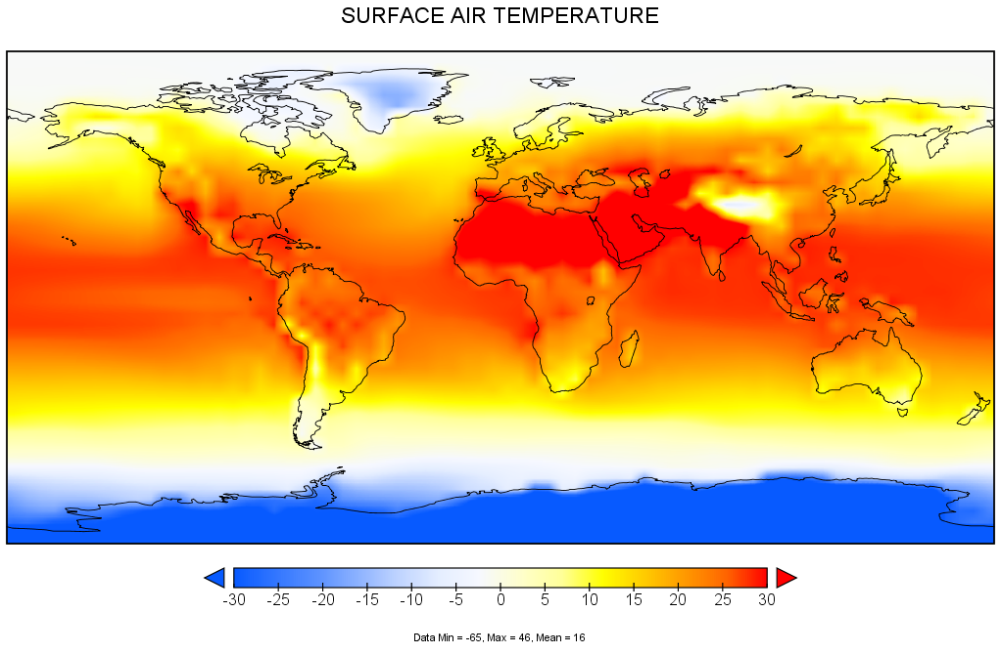

a

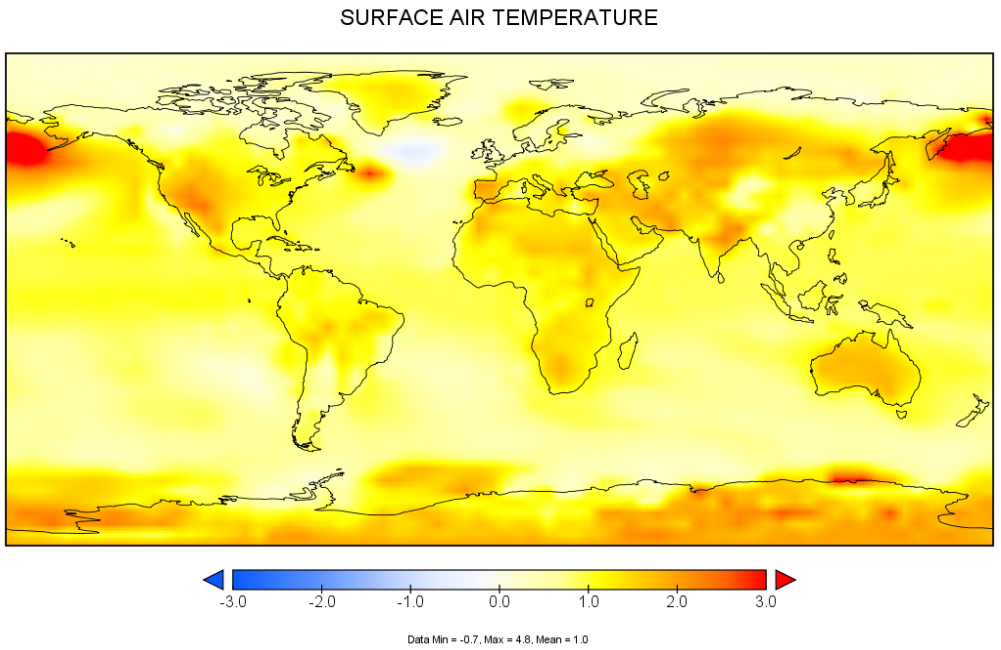

b

(a). Summer (JJA) average surface air temperature for the 1981-2010 historical simulations, (b). JJA average surface air temperature differences (°C) for 2031–2060 minus 1981–2010 of the corresponding historical simulation for RCP4.5

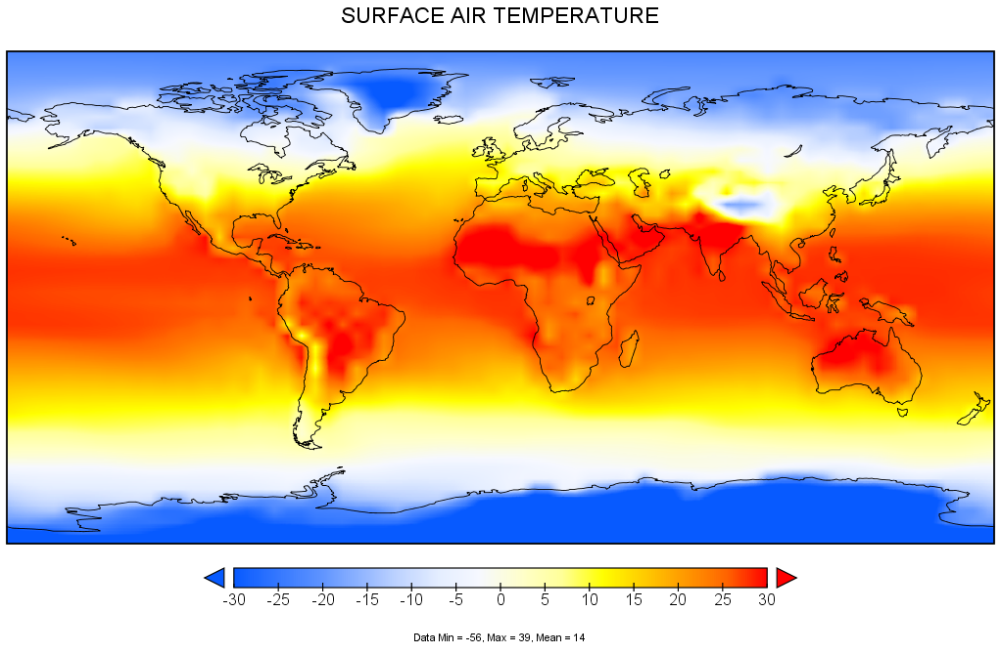

a

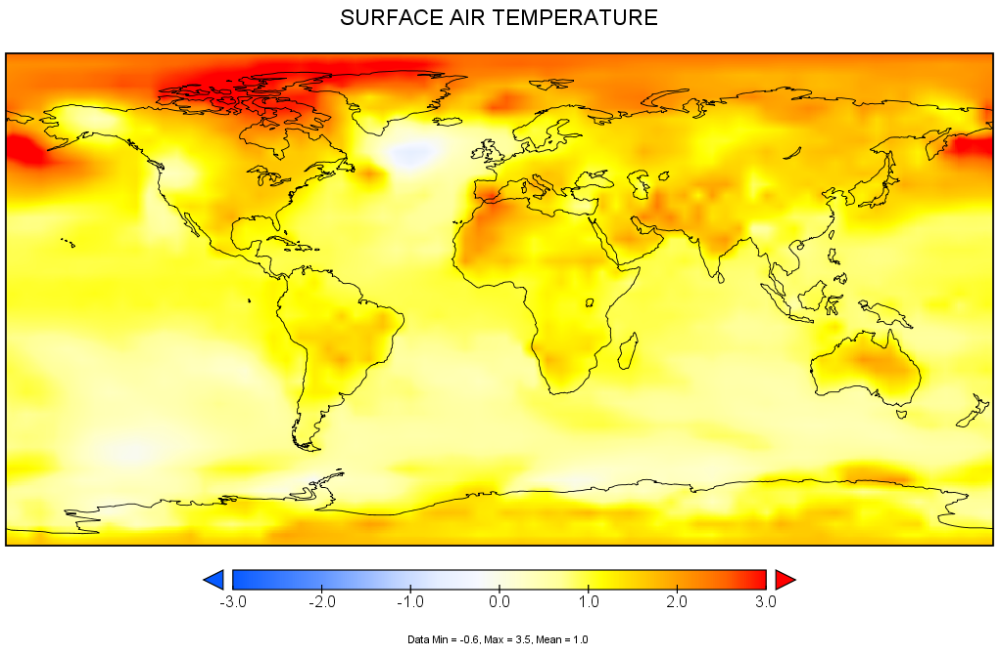

b

(a). Autumn (SON) average surface air temperature for the 1981-2010 historical simulations, (b). SON average surface air temperature differences (°C) for 2031–2060 minus 1981–2010 of the corresponding historical simulation for RCP4.5

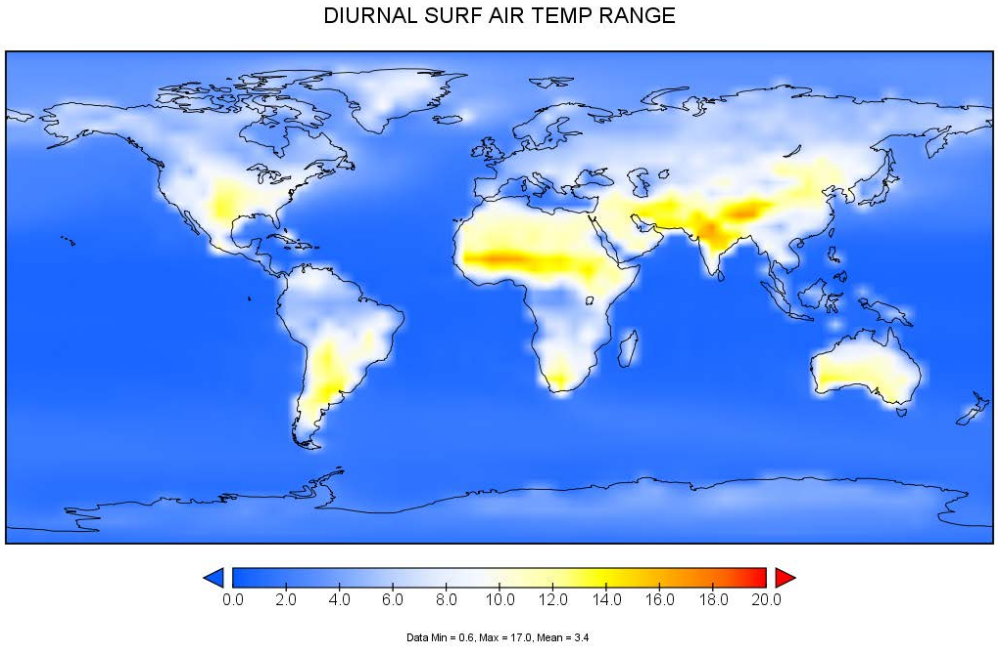

a

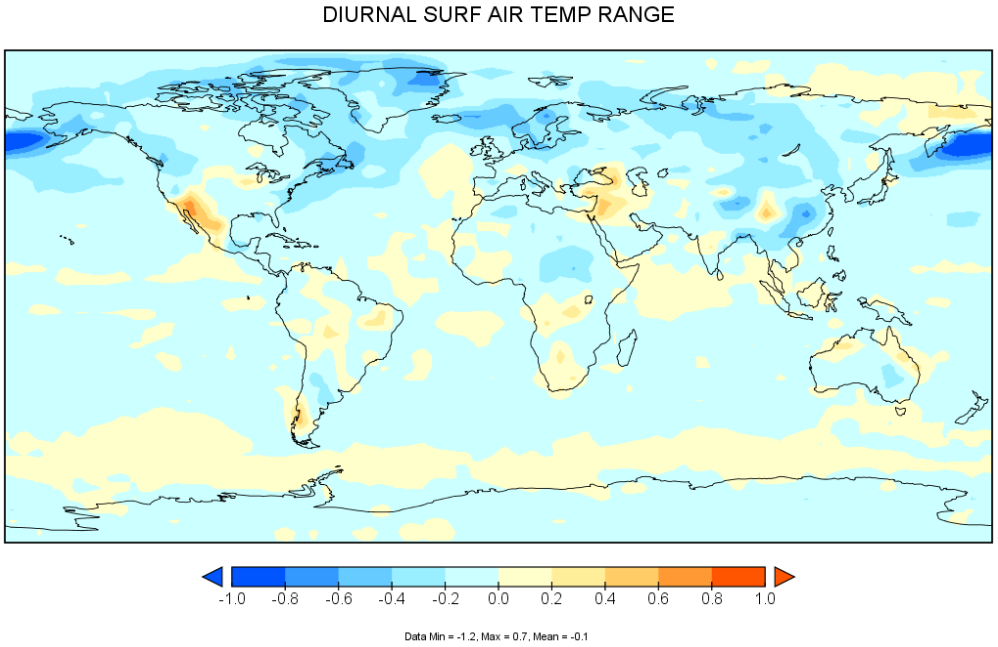

b

(a). Winter (JFD) average diurnal surface air temperature range (°C) for the 1981-2010 historical simulations, (b). JFD diurnal surface air temperature range differences (°C) for 2031–2060 minus 1981–2010 of the corresponding historical simulation for RCP4.5

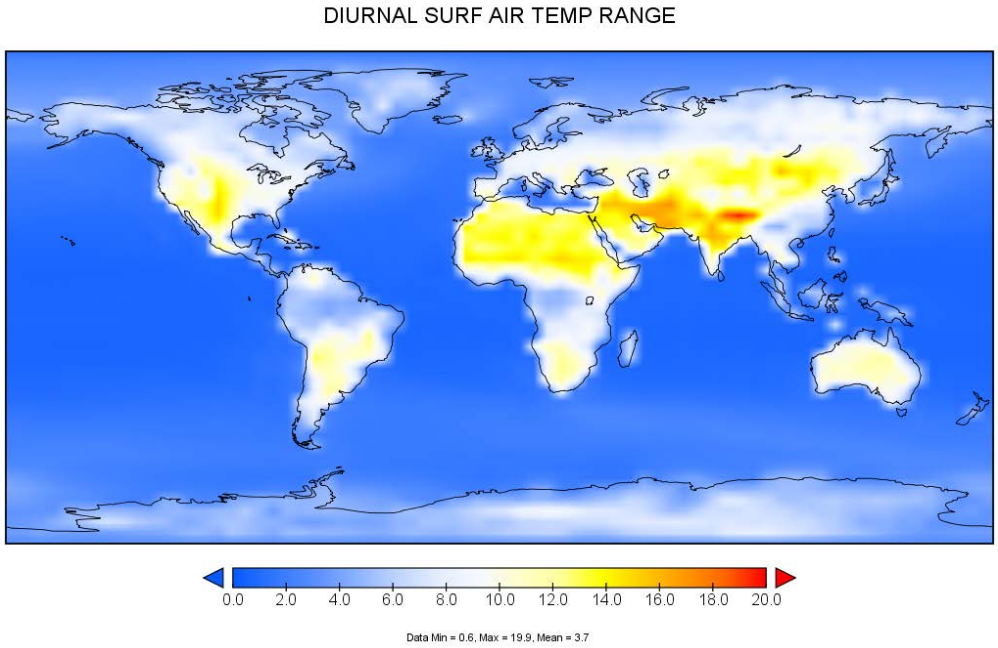

a

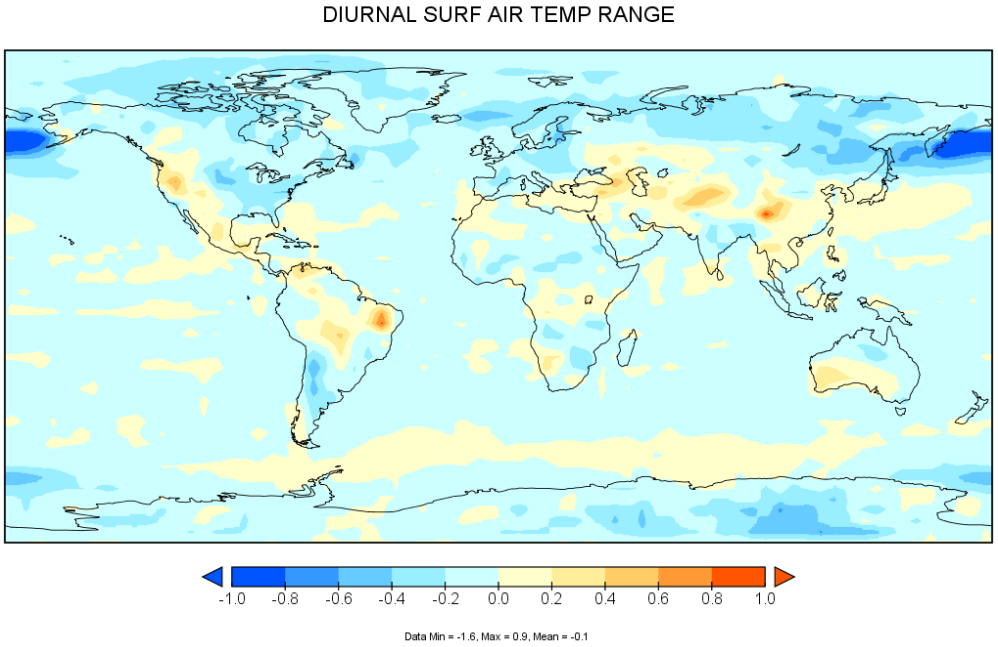

b

(a). Spring (MAM) average diurnal surface air temperature range (°C) for the 1981-2010 historical simulations, (b). MAM diurnal surface air temperature range differences (°C) for 2031–2060 minus 1981–2010 of the corresponding historical simulation for RCP4.5

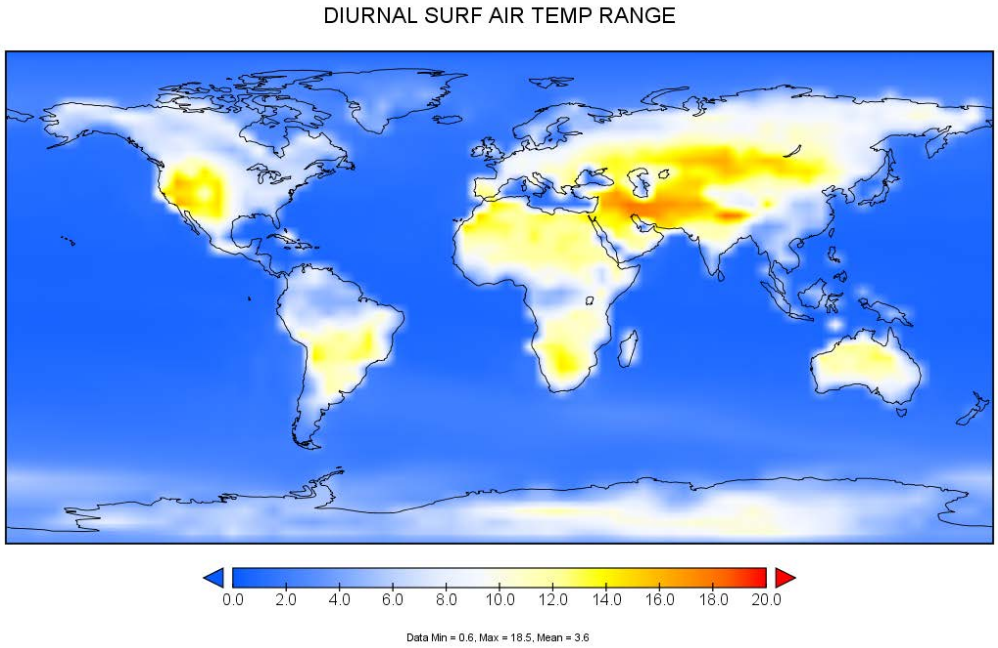

a

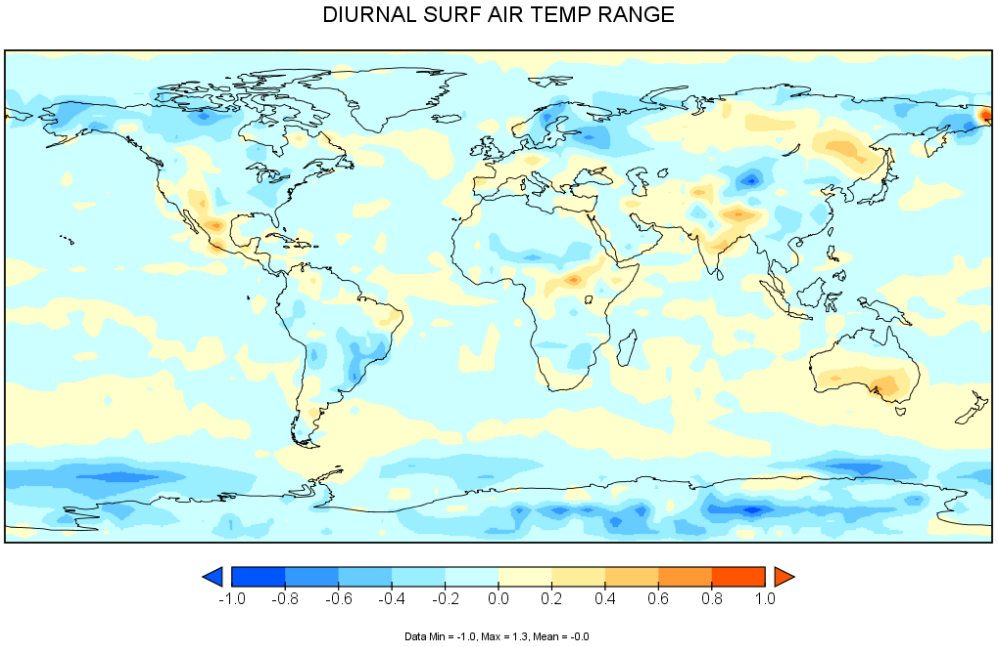

b

(a). Summer (JJA) average diurnal surface air temperature range (°C) for the 1981-2010 historical simulations, (b). JJA diurnal surface air temperature range differences (°C) for 2031–2060 minus 1981–2010 of the corresponding historical simulation for RCP4.5

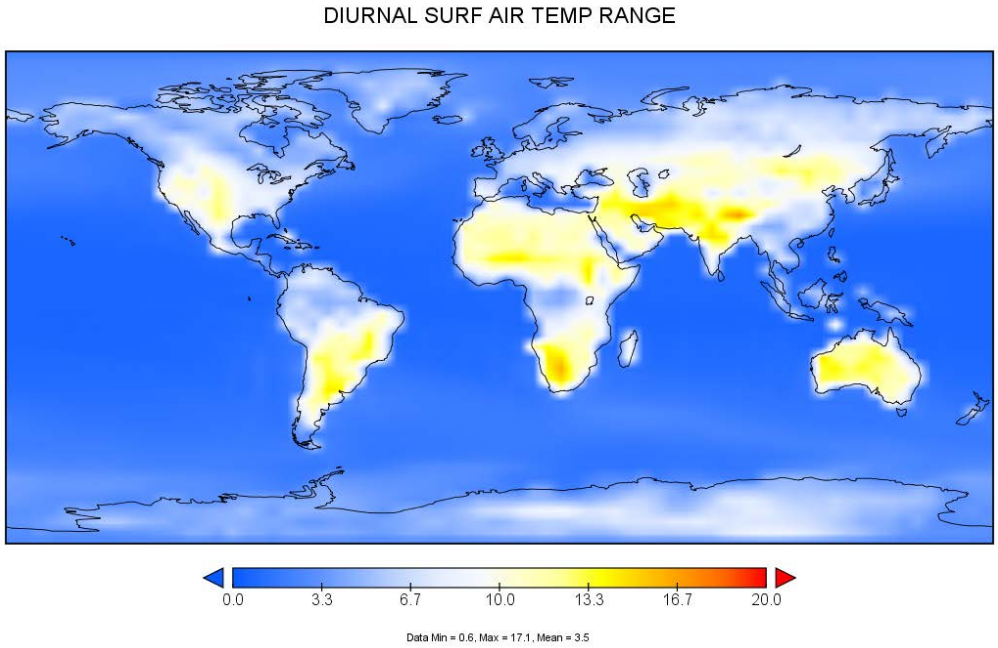

a

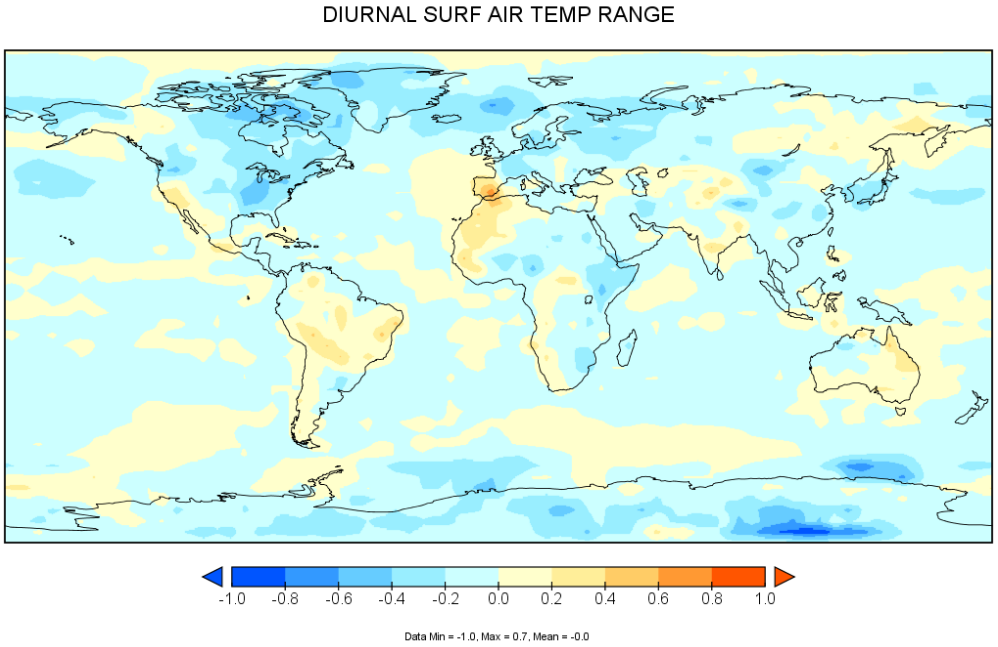

b

(a). Autumn (SON) average diurnal surface air temperature range (°C) for the 1981-2010 historical simulations, (b). SON diurnal surface air temperature range differences (°C) for 2031–2060 minus 1981–2010 of the corresponding historical simulation for RCP4.5

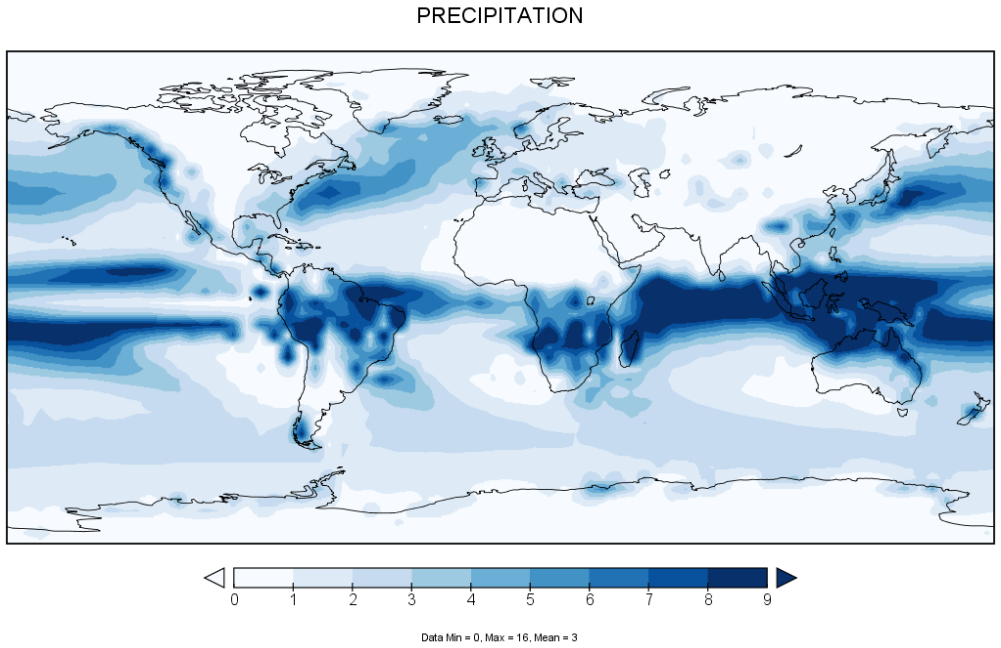

a

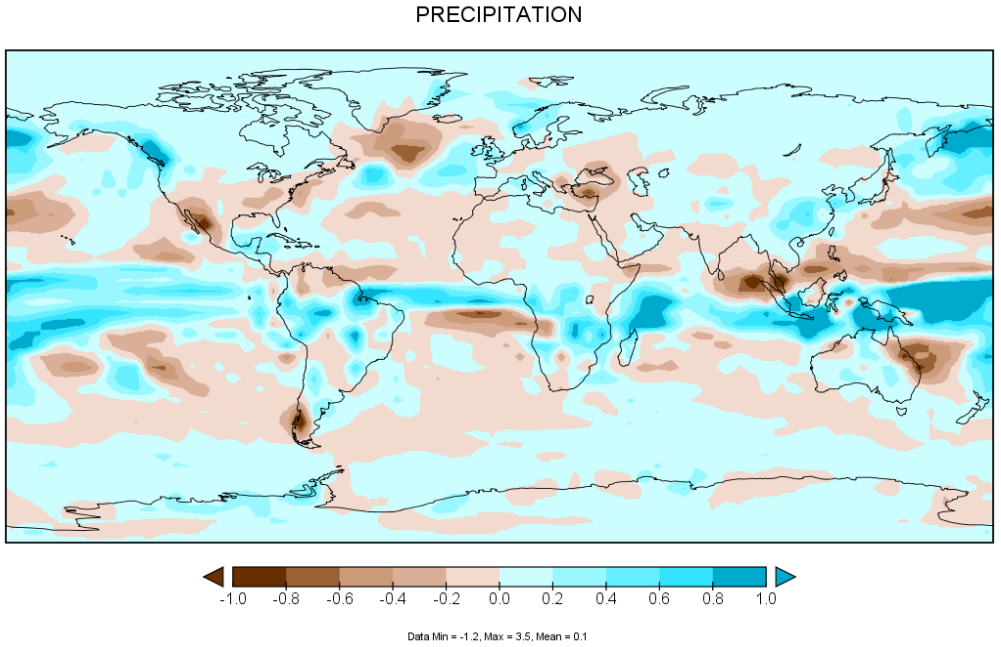

b

(a). Winter (JFD) average precipitation (mm/day) for the 1981-2010 historical simulations, (b). JFD precipitation differences (mm/day) for 2031–2060 minus 1981–2010 of the corresponding historical simulation for RCP4.5

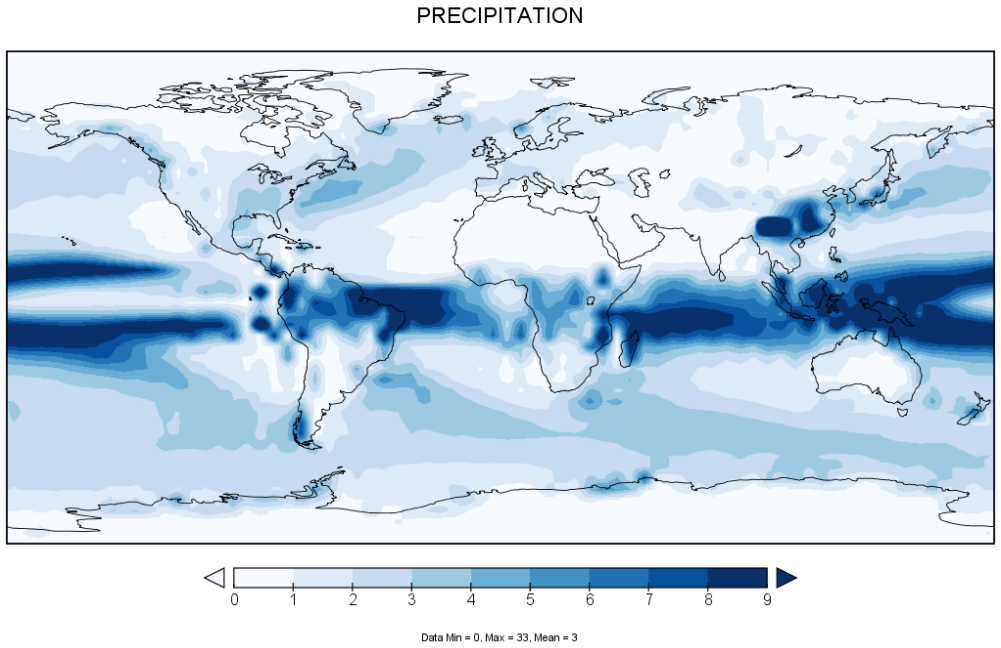

a

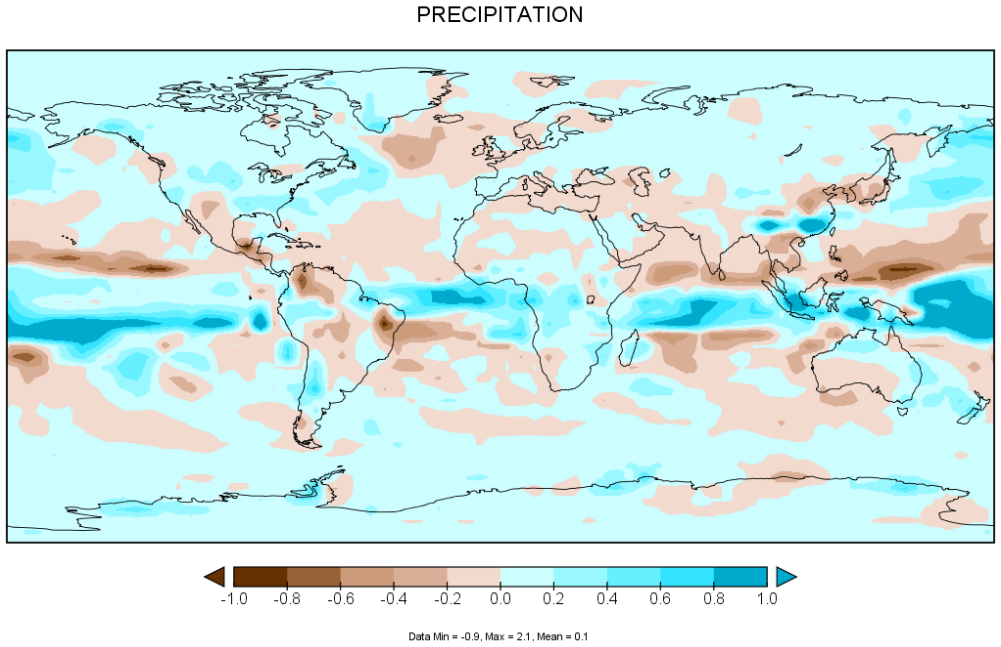

b

(a). Spring (MAM) average precipitation (mm/day) for the 1981-2010 historical simulations, (b). MAM precipitation differences (mm/day) for 2031–2060 minus 1981–2010 of the corresponding historical simulation for RCP4.5

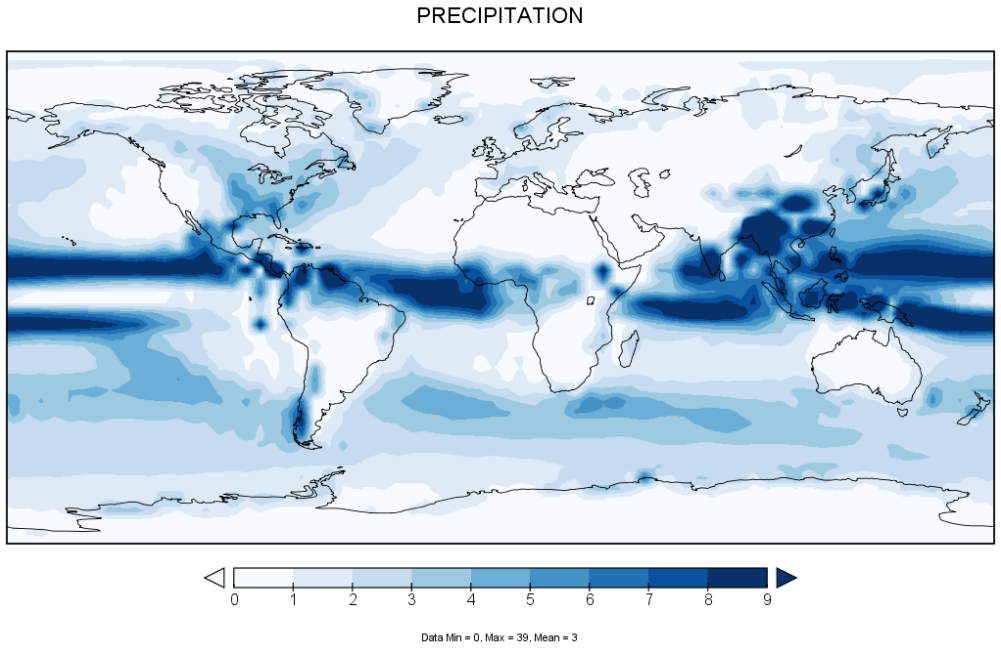

a

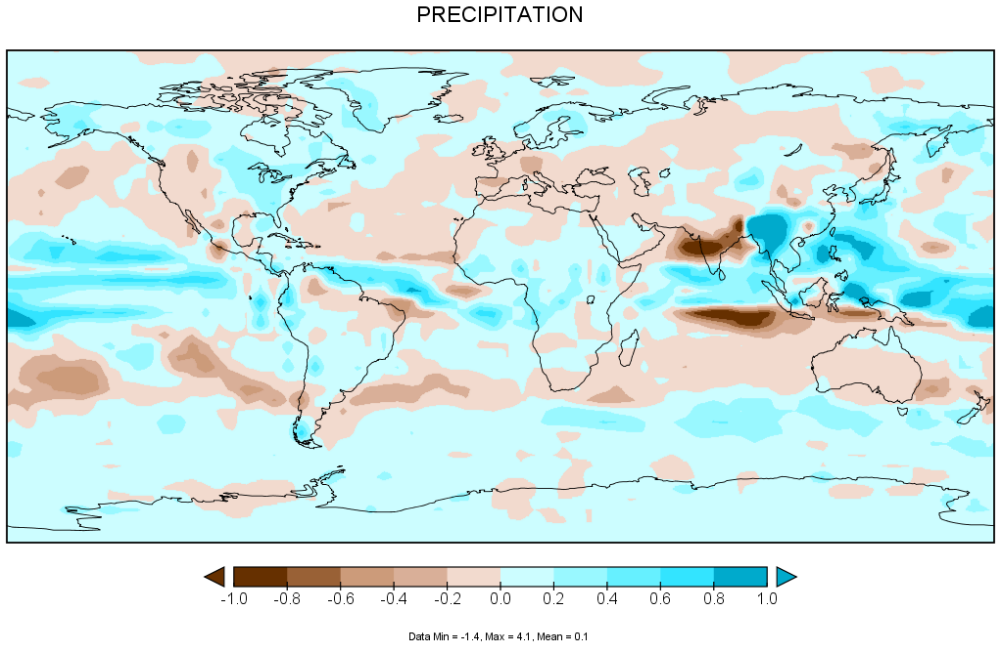

b

(a). Summer (JJA) average precipitation (mm/day) for the 1981-2010 historical simulations, (b). JJA precipitation differences (mm/day) for 2031–2060 minus 1981–2010 of the corresponding historical simulation for RCP4.5

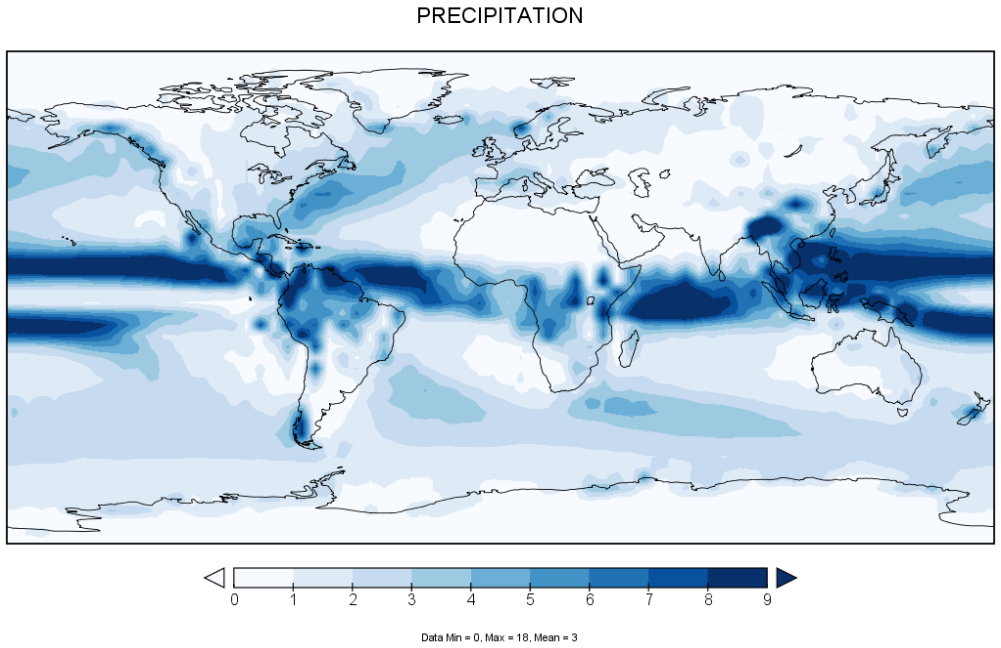

a

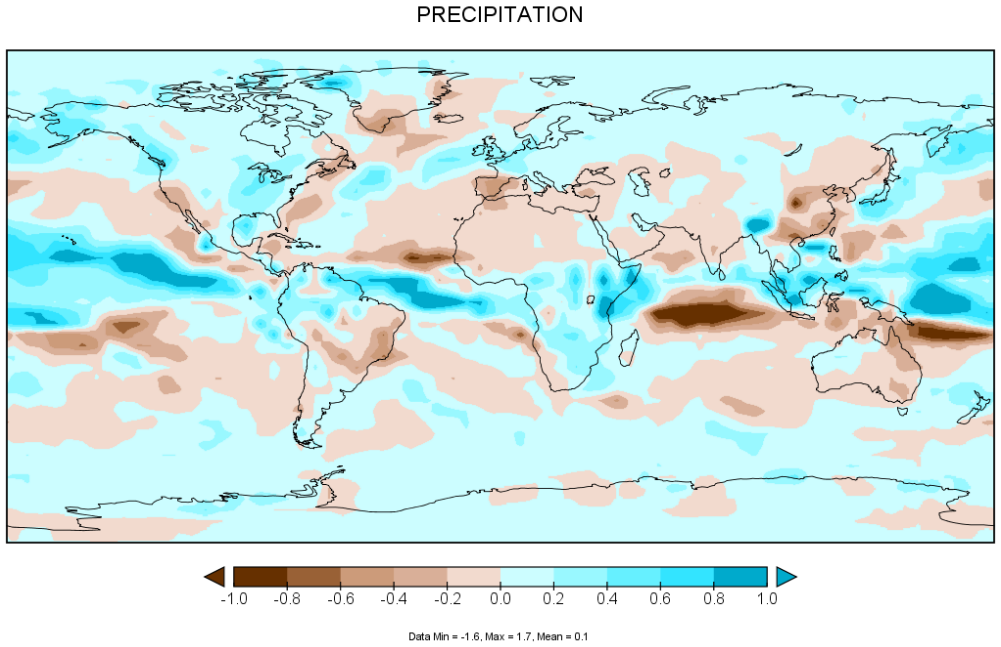

b

(a). Autumn (SON) average precipitation (mm/day) for the 1981-2010 historical simulations, (b). SON precipitation differences (mm/day) for 2031–2060 minus 1981–2010 of the corresponding historical simulation for RCP4.5

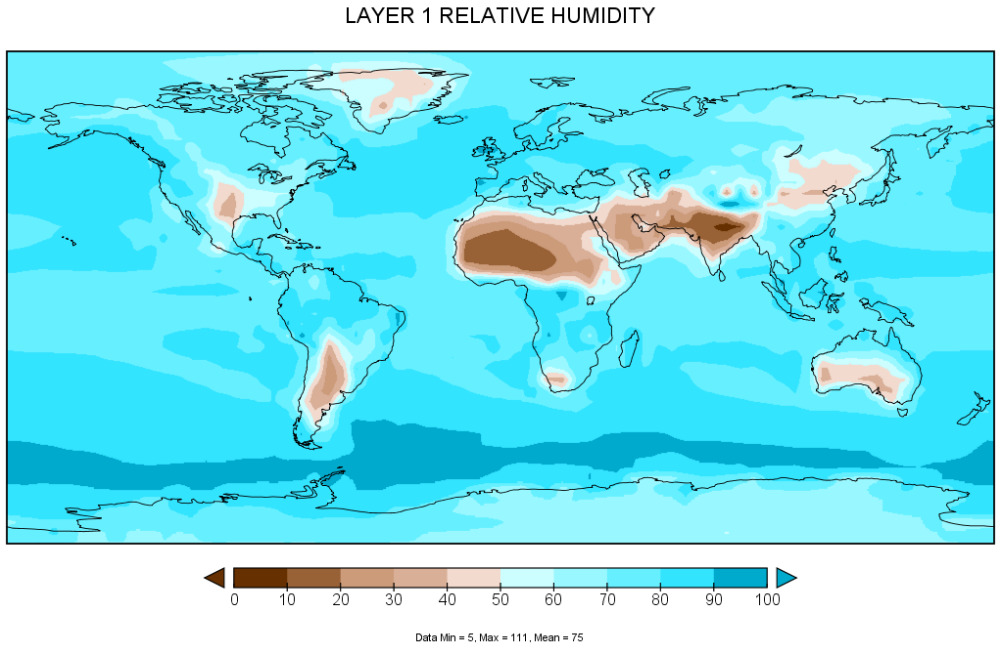

a

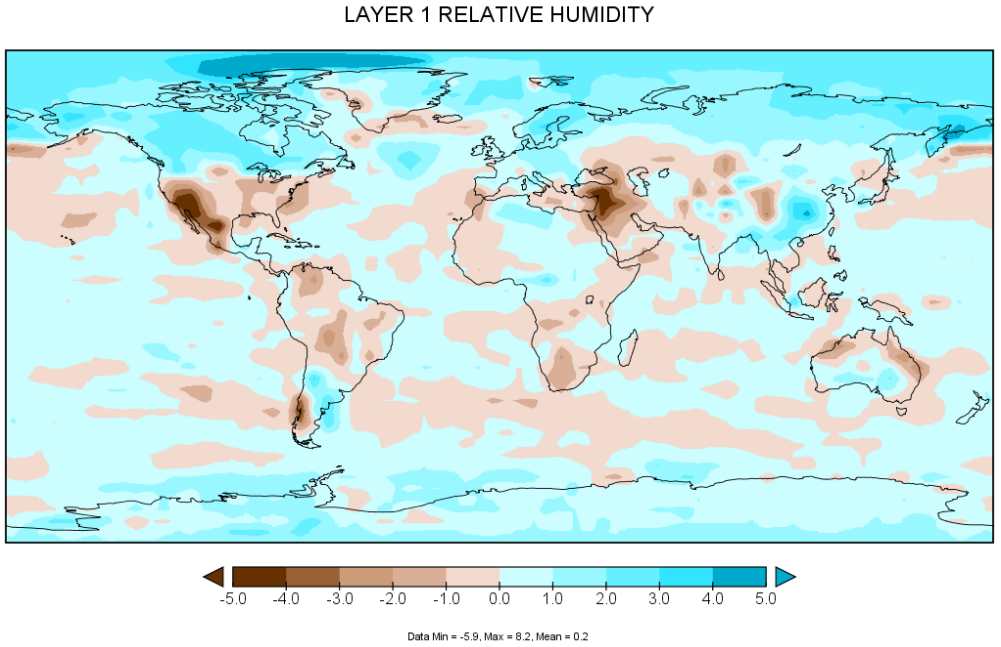

b

(a). Winter (JFD) average relative humidity (%) for the 1981-2010 historical simulations (b). JFD relative humidity differences (%) for 2031–2060 minus 1981–2010 of the corresponding historical simulation for RCP4.5

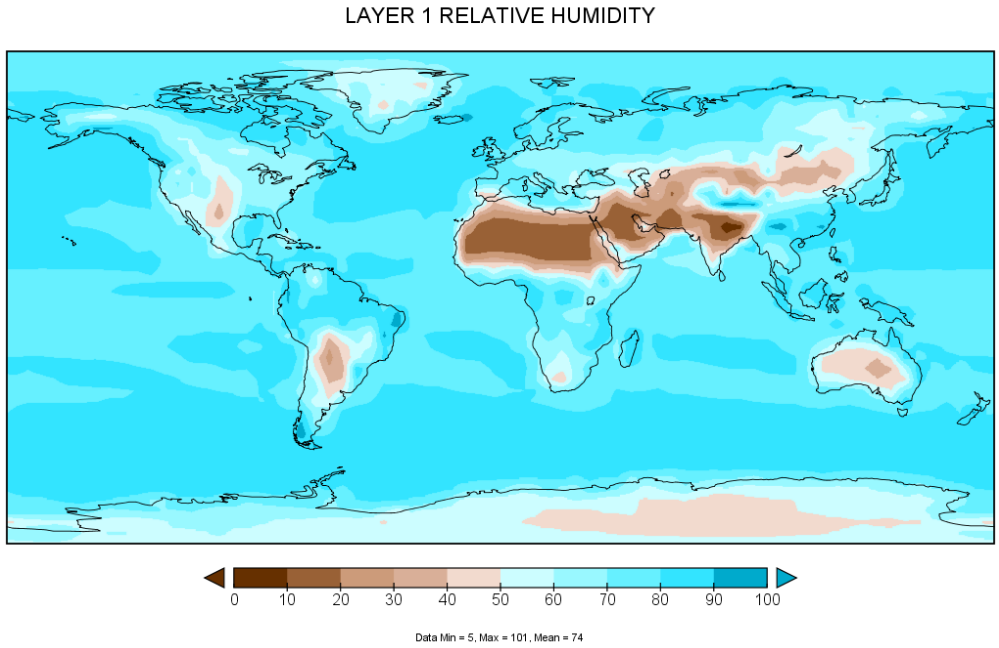

a

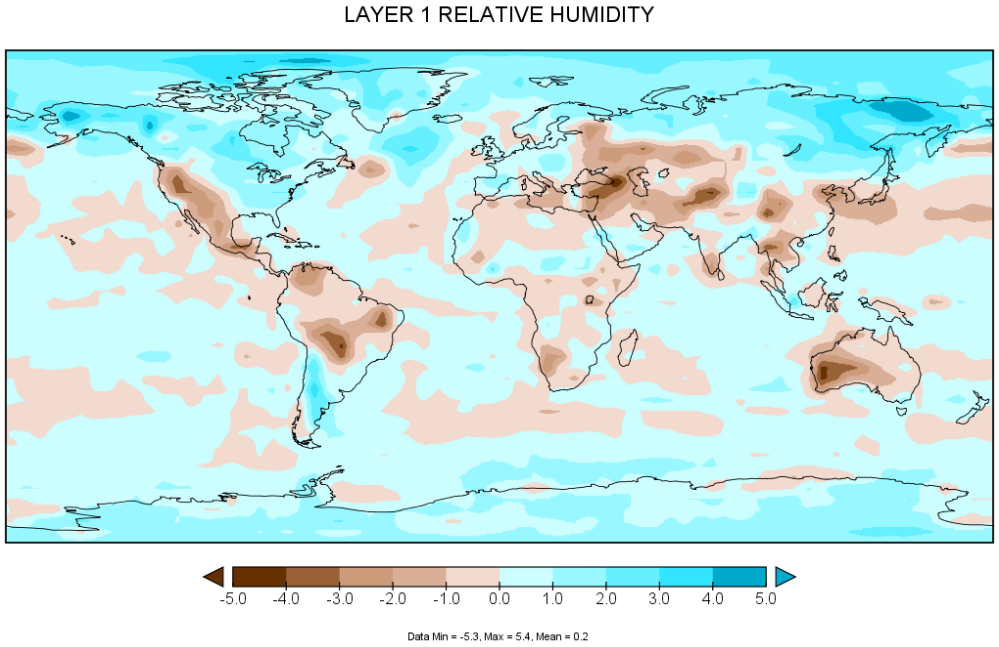

b

(a). Spring (MAM) average relative humidity (%) for the 1981-2010 historical simulations (b). MAM relative humidity differences (%) for 2031–2060 minus 1981–2010 of the corresponding historical simulation for RCP4.5

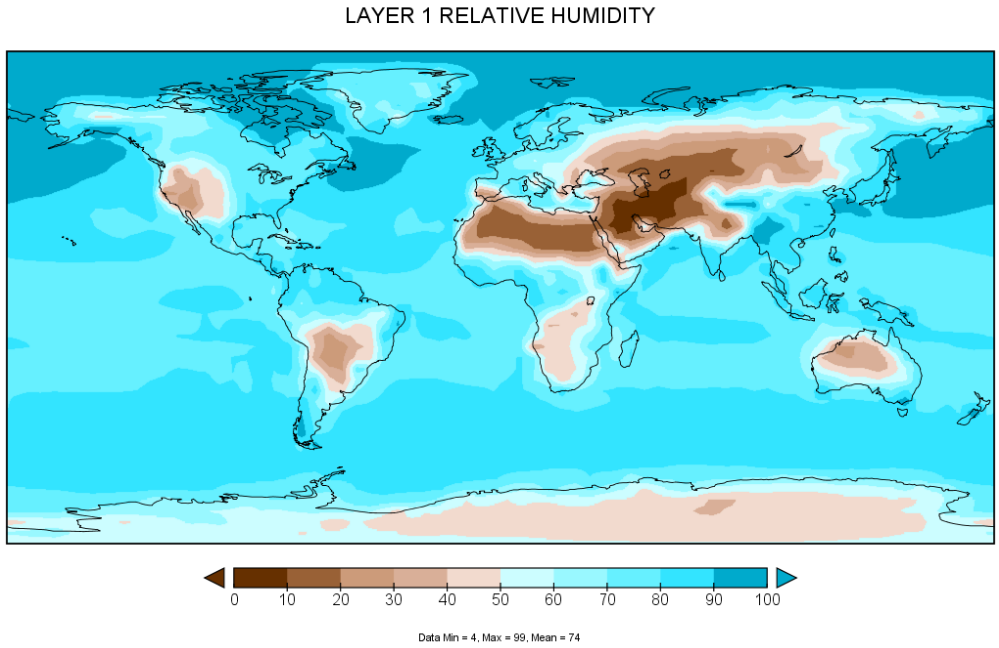

a

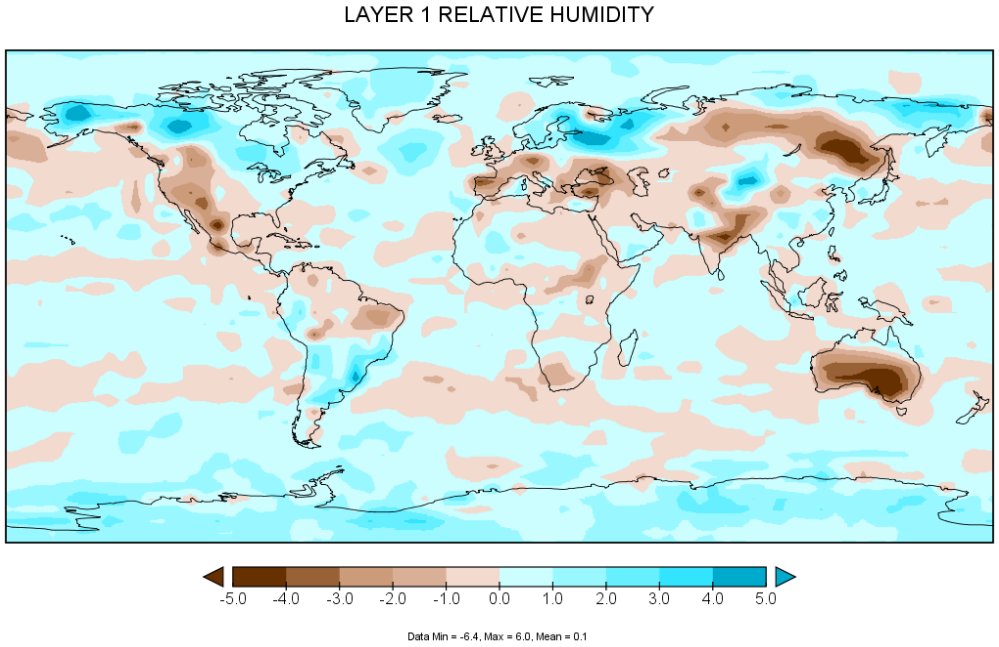

b

(a). Summer (JJA) average relative humidity (%) for the 1981-2010 historical simulations (b). JJA relative humidity differences (%) for 2031–2060 minus 1981–2010 of the corresponding historical simulation for RCP4.5

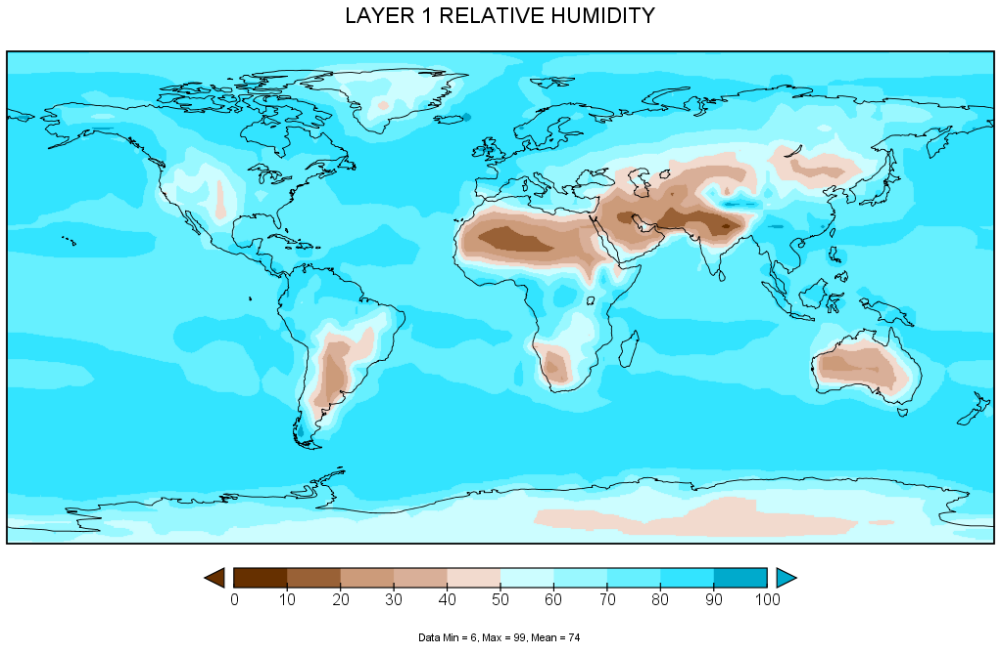

a

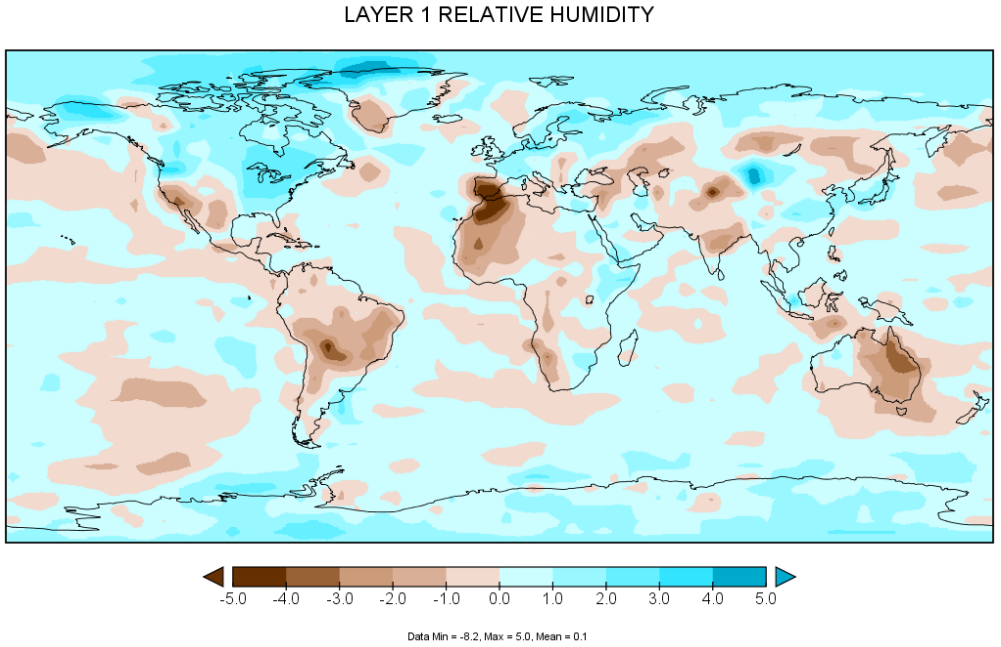

b

(a). Autumn (SON) average relative humidity (%) for the 1981-2010 historical simulations (b). SON relative humidity differences (%) for 2031–2060 minus 1981–2010 of the corresponding historical simulation for RCP4.5

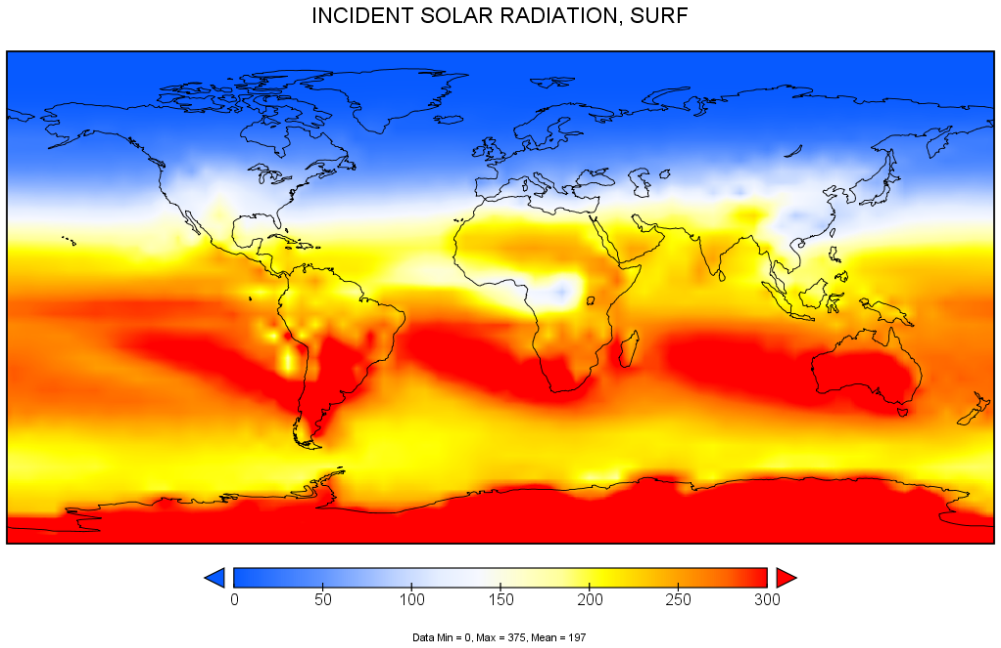

a

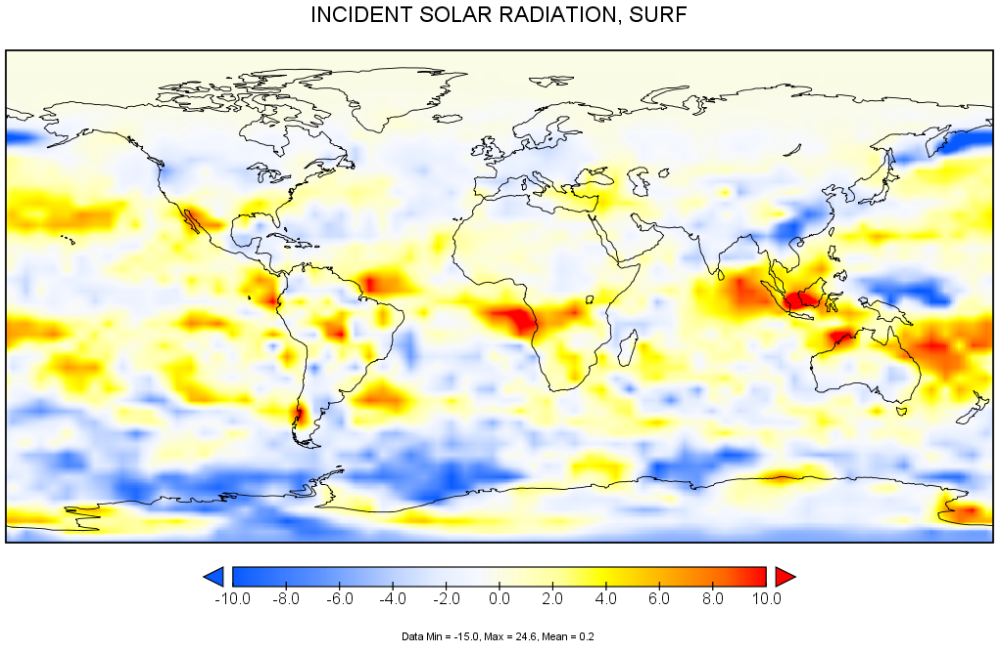

b

(a). Winter (JFD) average incident solar radiation at the surface (W/m^2) for the 1981-2010 historical simulations (b). JFD incident solar radiation differences (W/m^2) for 2031–2060 minus 1981–2010 of the corresponding historical simulation for RCP4.5

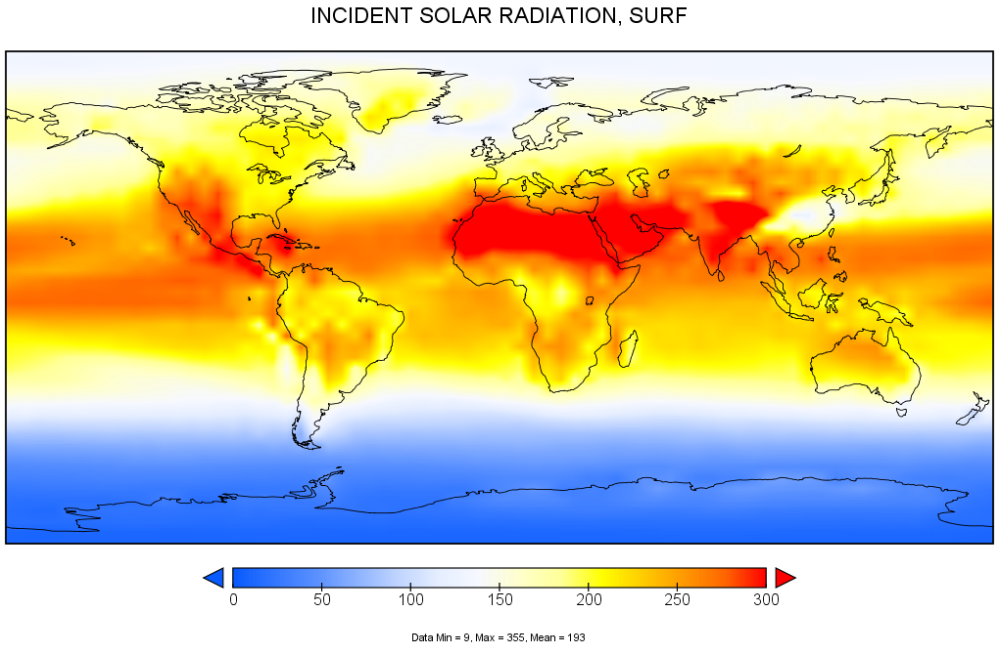

a

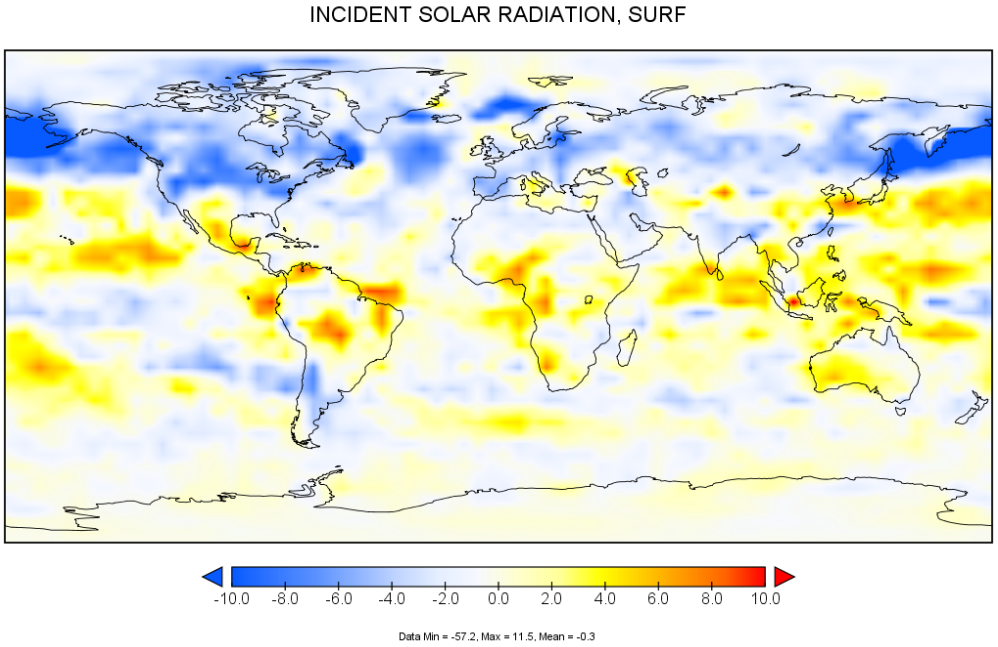

b

(a). Spring (MAM) average incident solar radiation at the surface (W/m^2) for the 1981-2010 historical simulations (b). MAM incident solar radiation differences (W/m^2) for 2031–2060 minus 1981–2010 of the corresponding historical simulation for RCP4.5

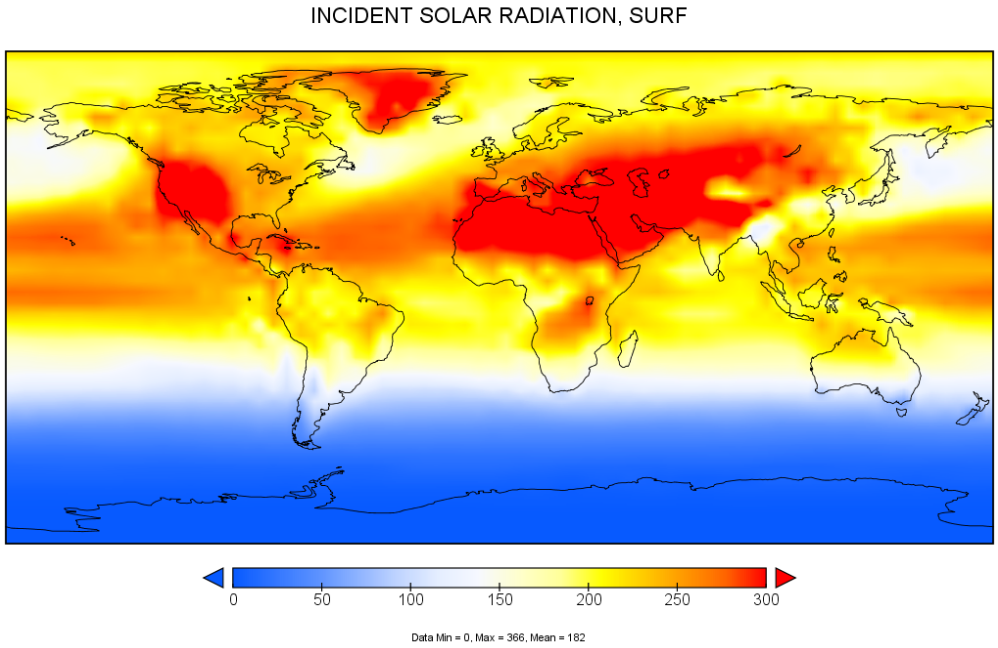

a

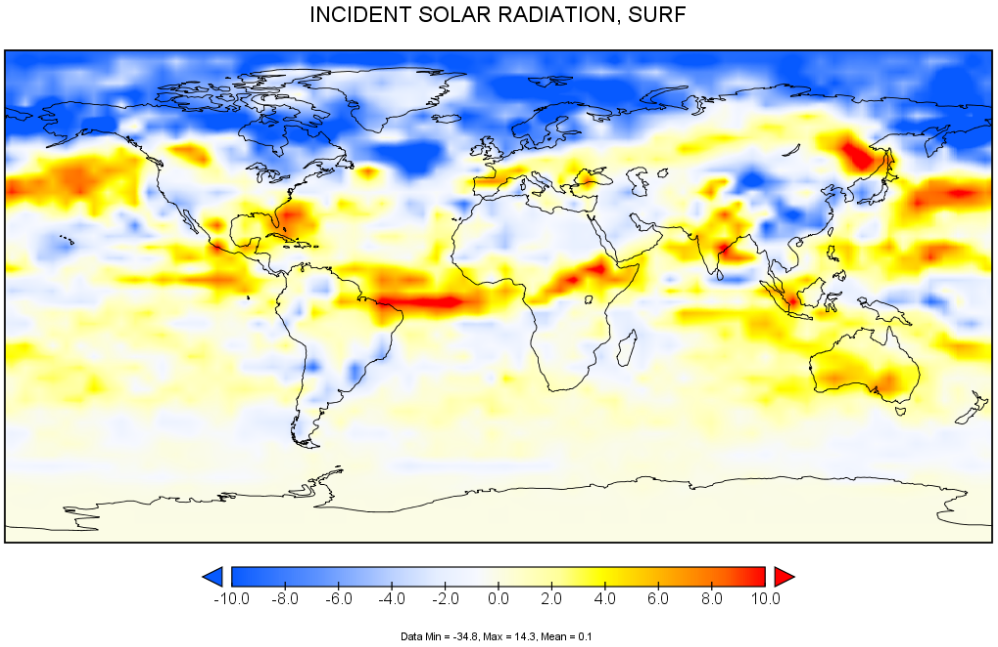

b

(a). Summer (JJA) average incident solar radiation at the surface (W/m^2) for the 1981-2010 historical simulations (b). JJA incident solar radiation differences (W/m^2) for 2031–2060 minus 1981–2010 of the corresponding historical simulation for RCP4.5

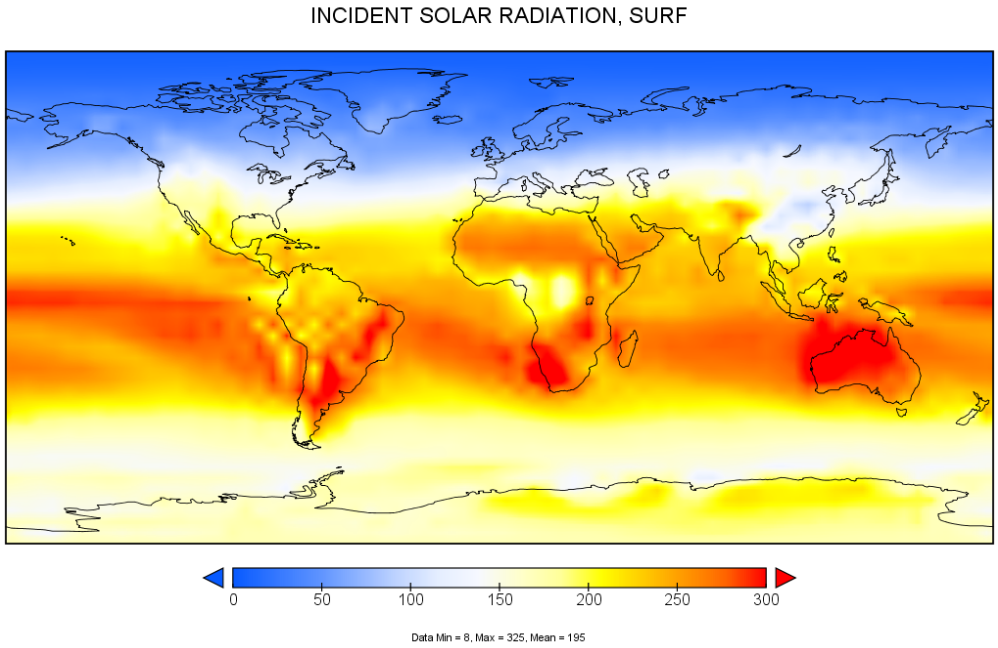

a

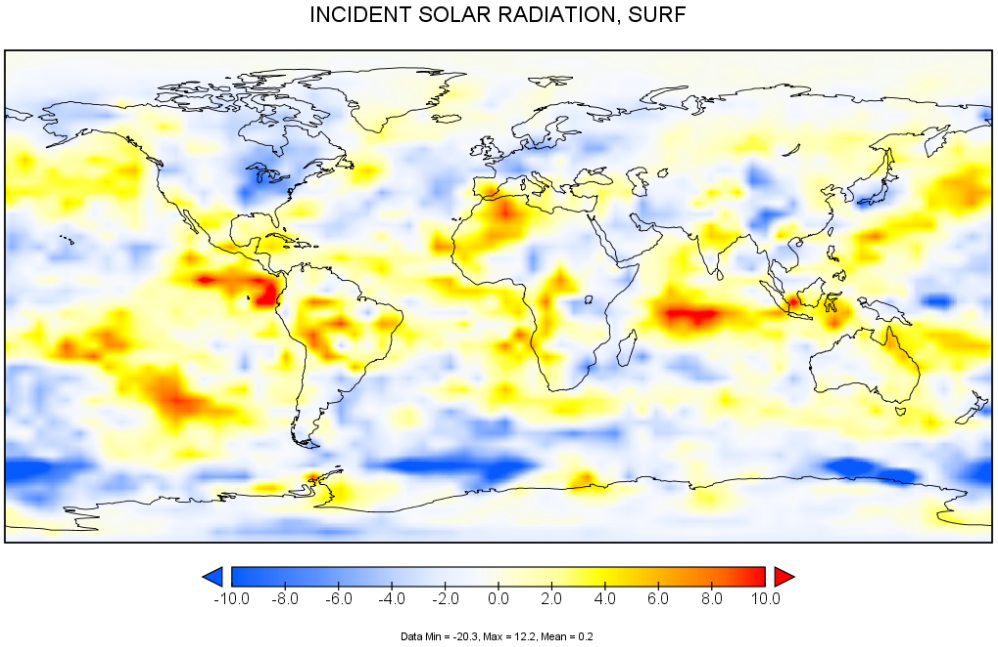

b

(a). Autumn (SON) average incident solar radiation at the surface (W/m^2) for the 1981-2010 historical simulations (b). SON incident solar radiation differences (W/m^2) for 2031–2060 minus 1981–2010 of the corresponding historical simulation for RCP4.5

Annex 3: Monthly average temperature change for RCP8.5

January

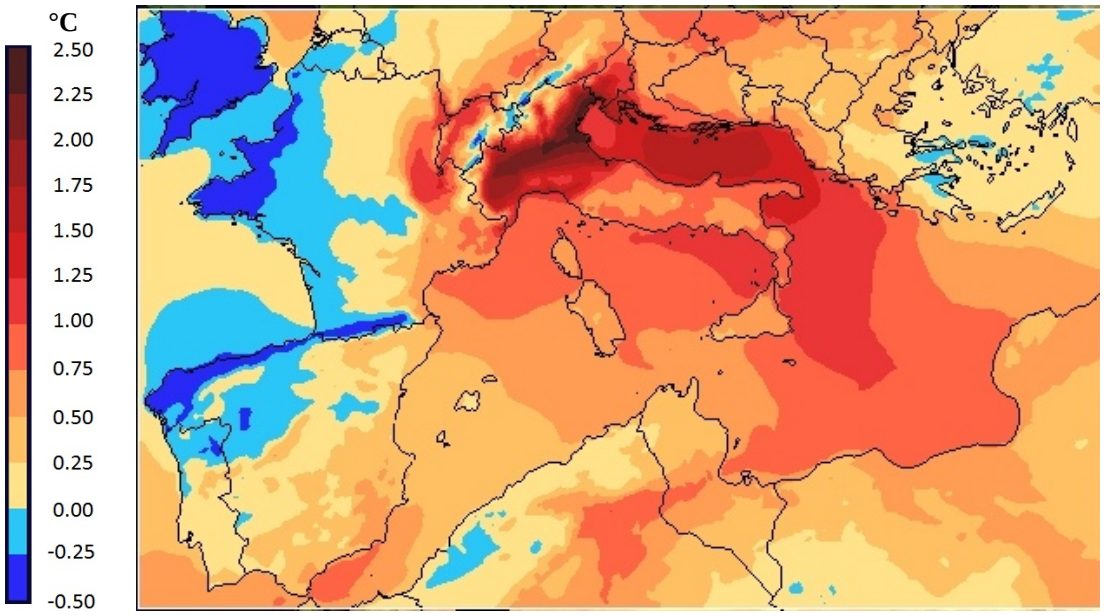

February

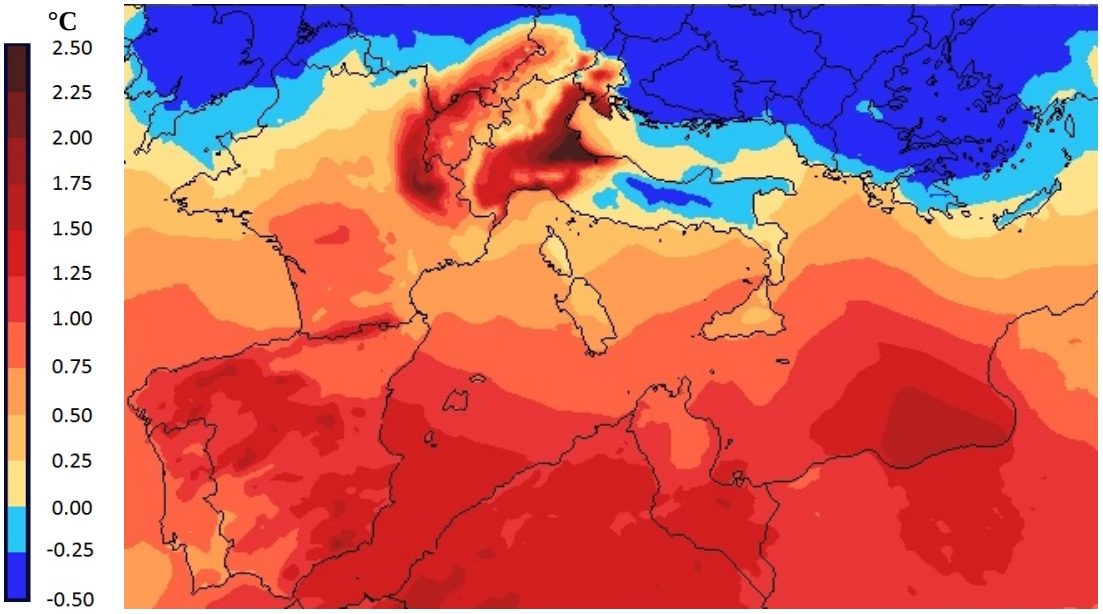

March

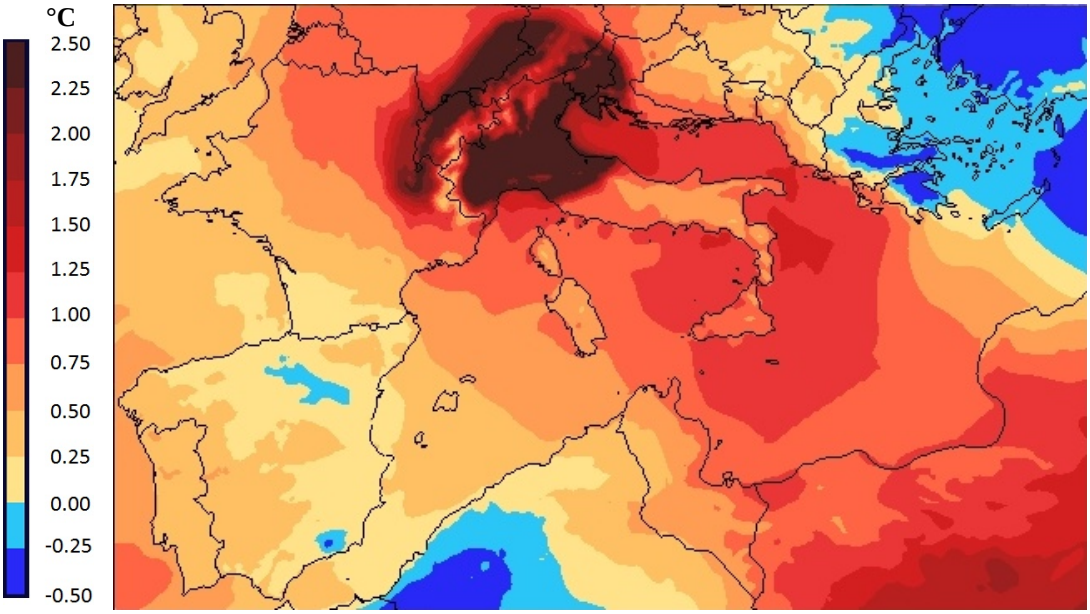
°C
2.50
2.25
2.00
1.75
1.50
1.25
1.00
0.75
0.50
0.25
0.00
-0.25
-0.50

April

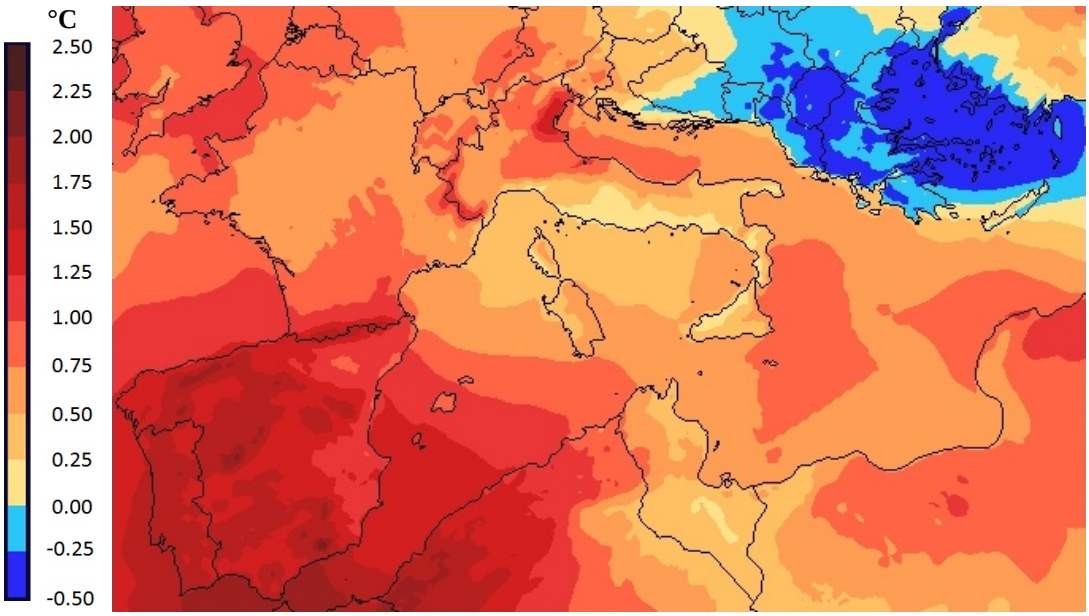
°C
2.50
2.25
2.00
1.75
1.50
1.25
1.00
0.75
0.50
0.25
0.00
-0.25
-0.50

May

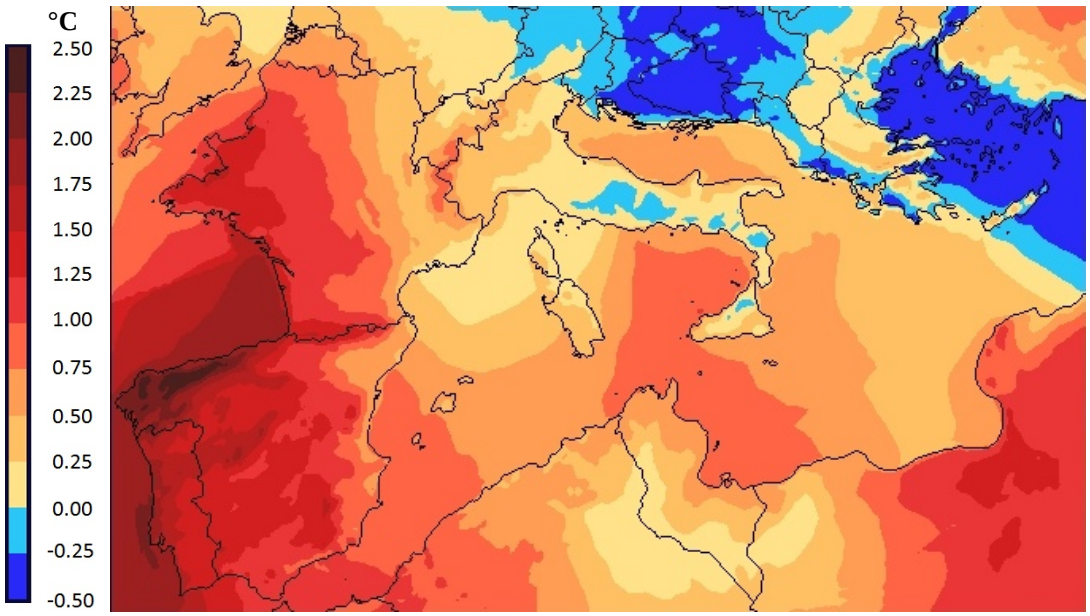
°C
2.50
2.25
2.00
1.75
1.50
1.25
1.00
0.75
0.50
0.25
0.00
-0.25
-0.50

June

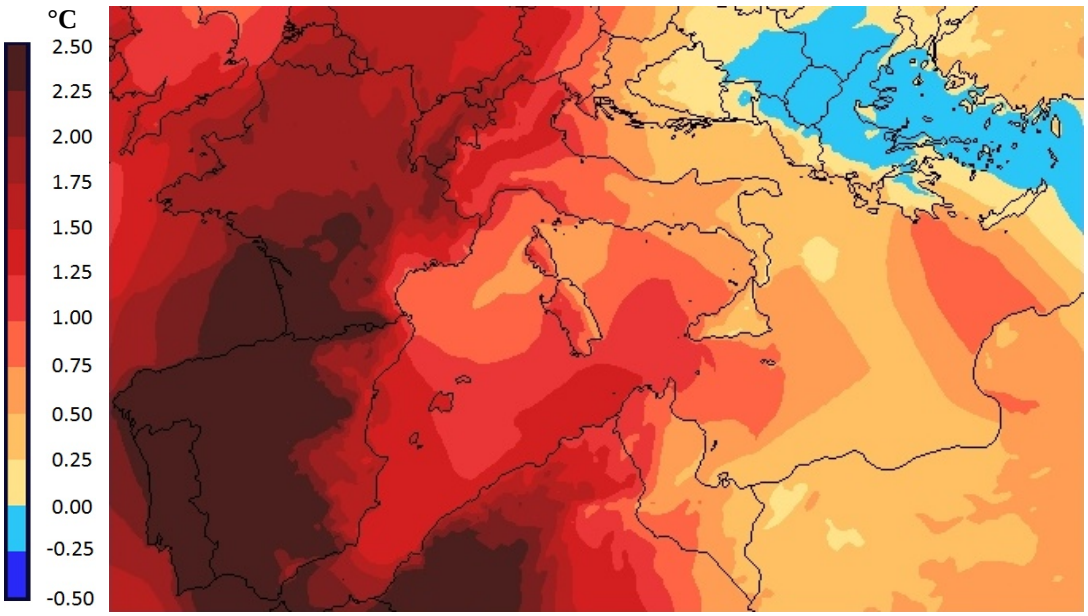
°C
2.50
2.25
2.00
1.75
1.50
1.25
1.00
0.75
0.50
0.25
0.00
-0.25
-0.50

July

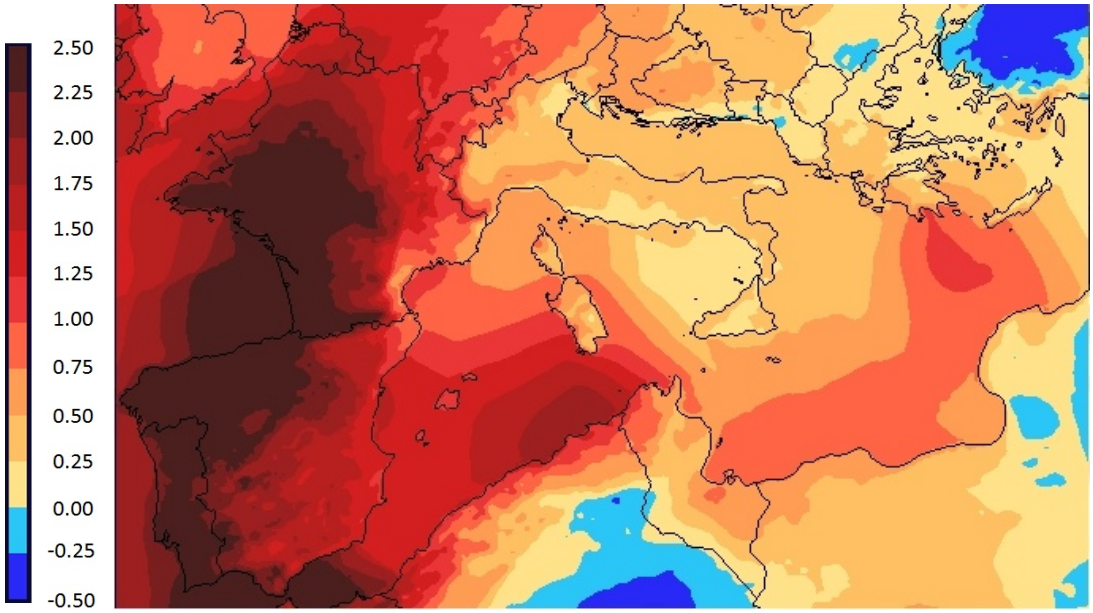
2.50
2.25
2.00
1.75
1.50
1.25
1.00
0.75
0.50
0.25
0.00
-0.25
-0.50

August

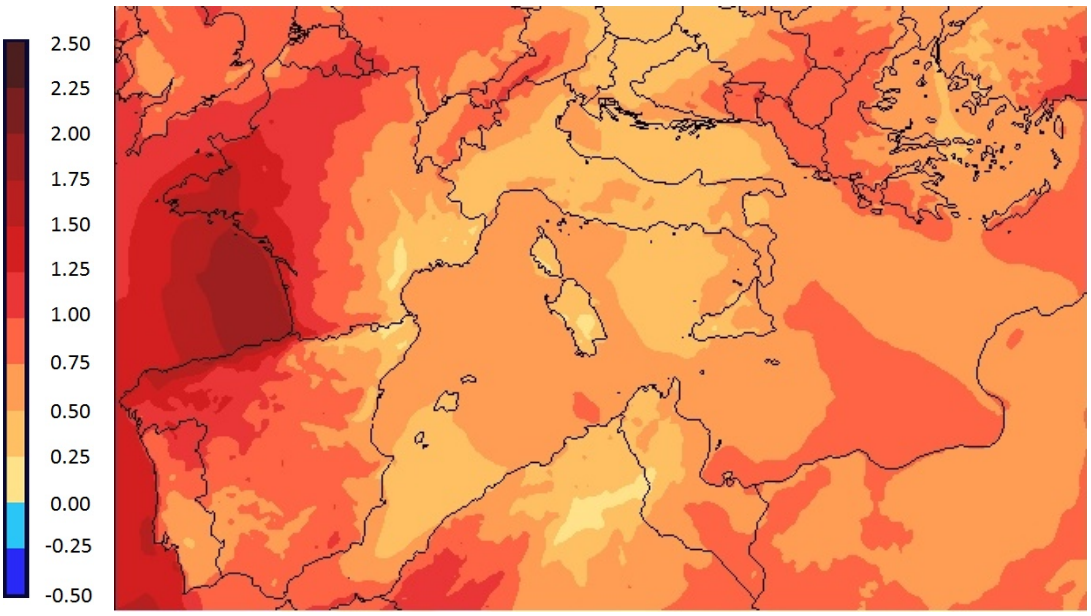
2.50
2.25
2.00
1.75
1.50
1.25
1.00
0.75
0.50
0.25
0.00
-0.25
-0.50

September

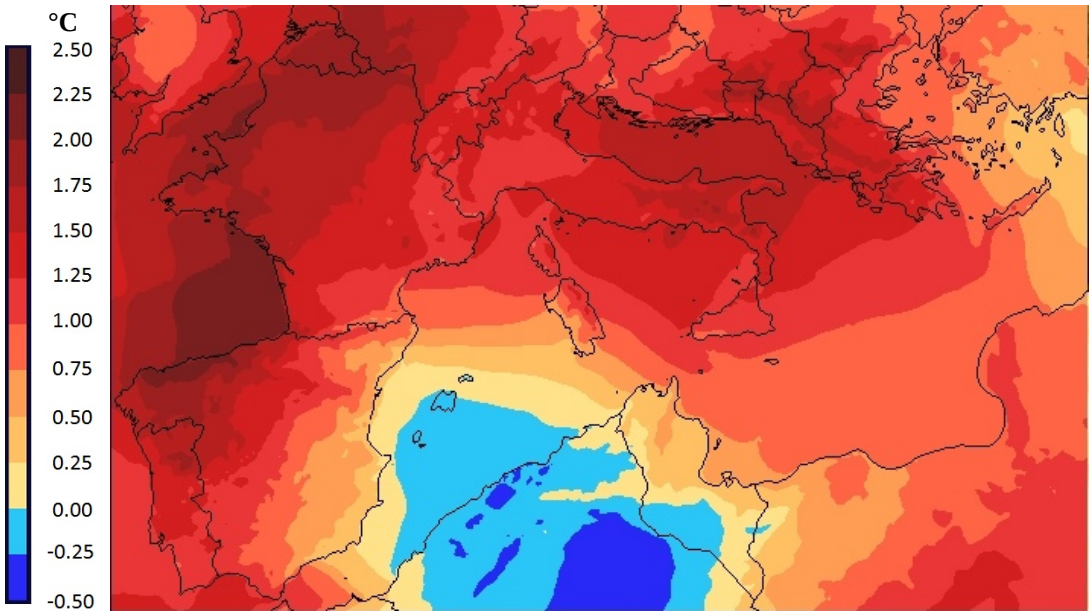

October

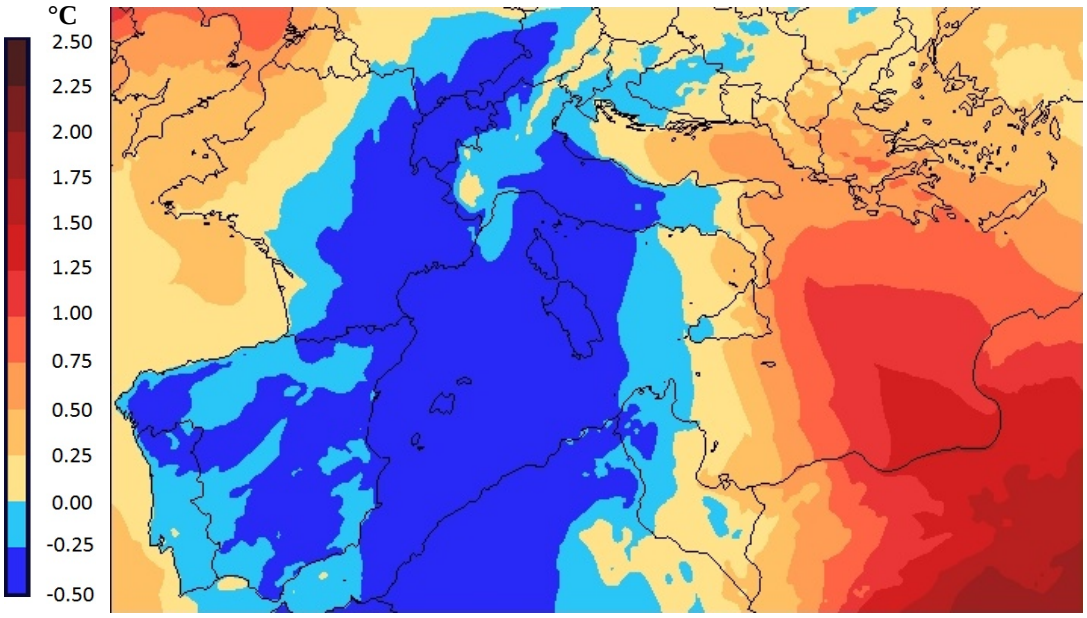

November

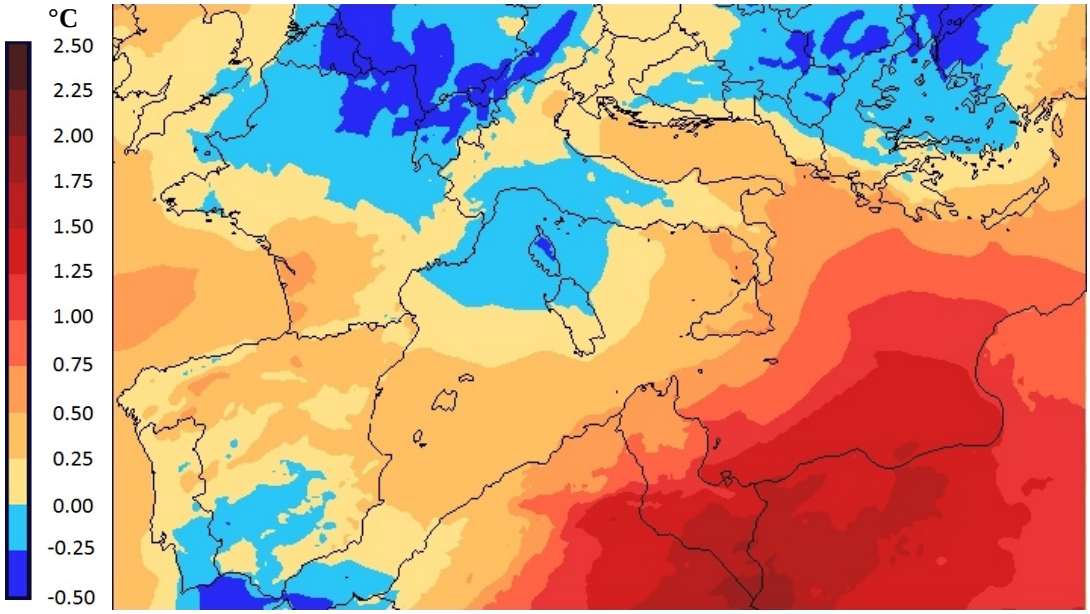

December

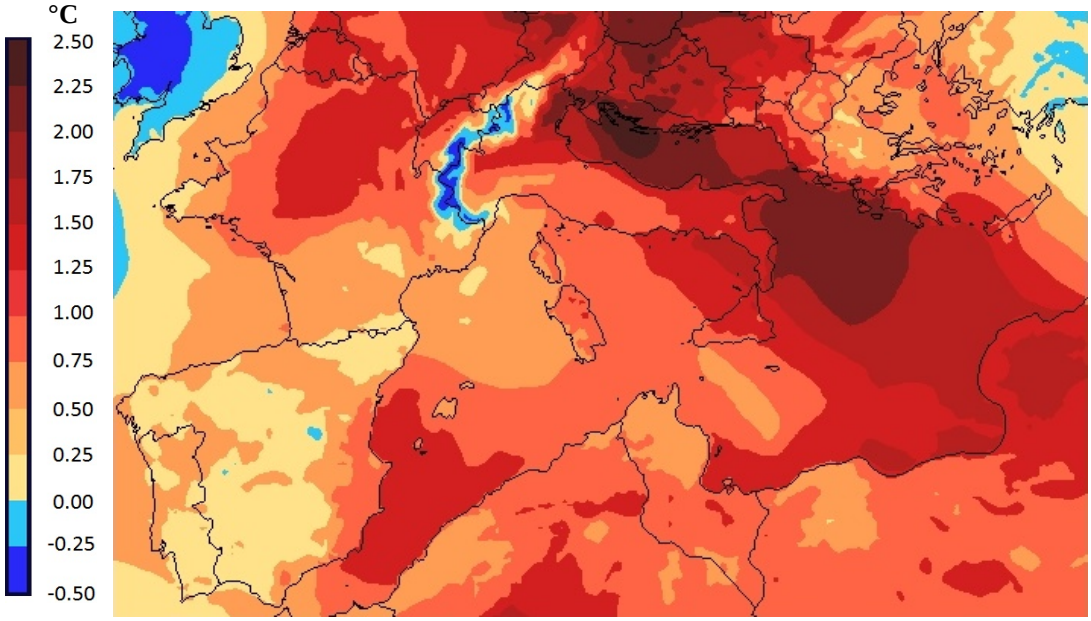

Annex 4: Monthly average precipitation change for RCP8.5

January

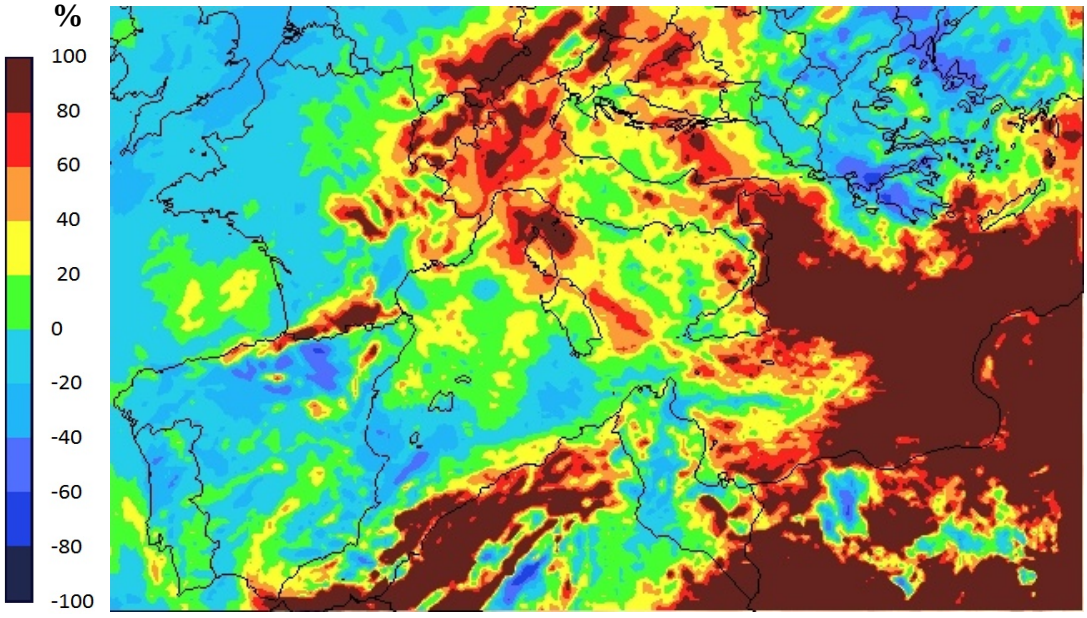

February

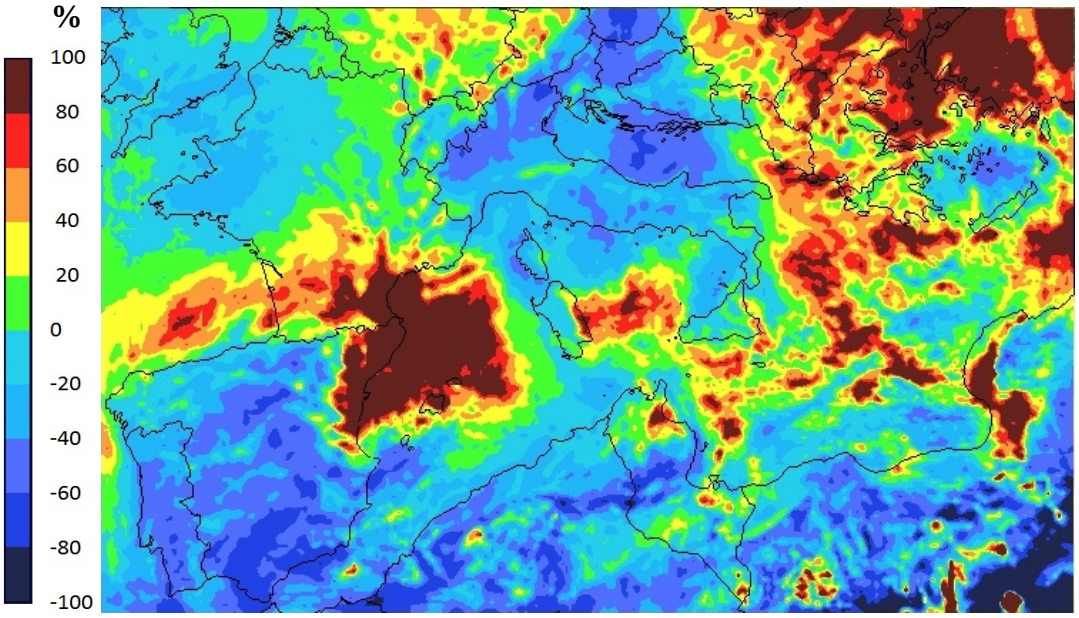

March

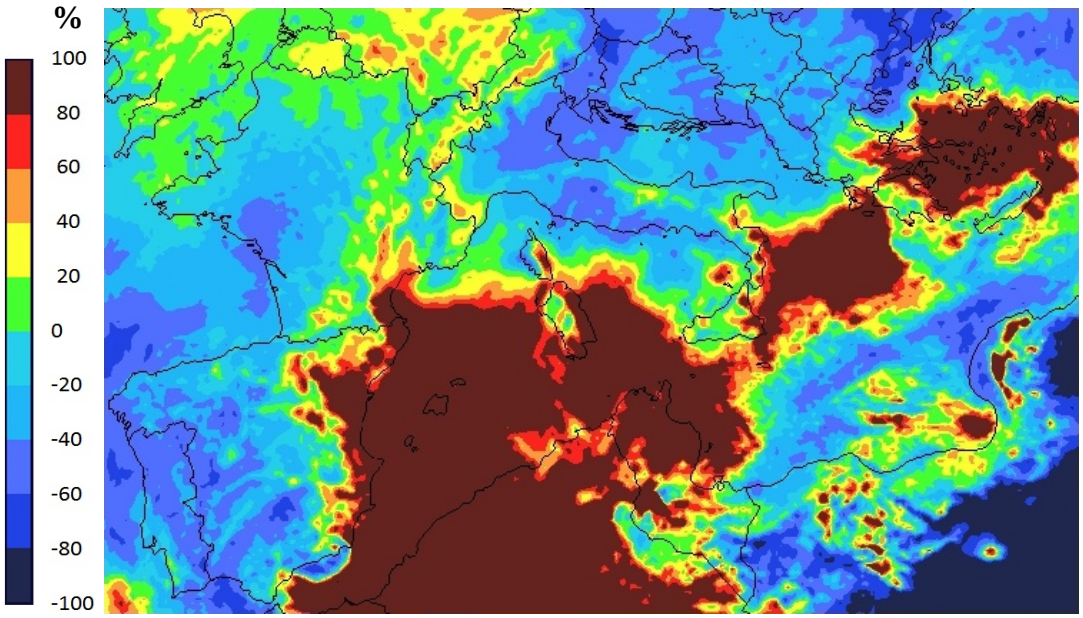

April

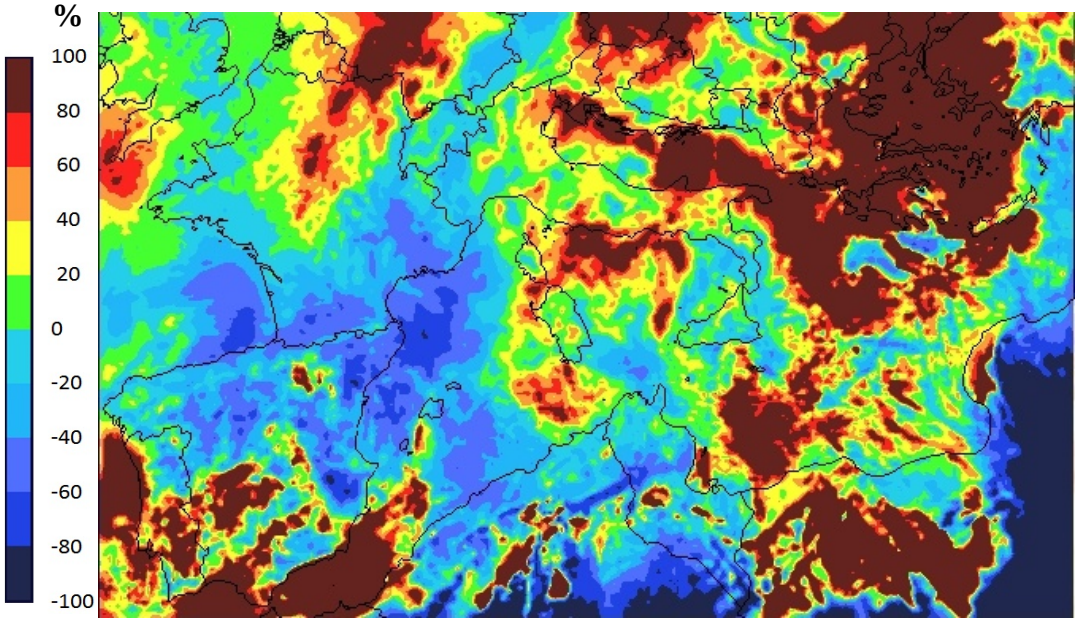

May

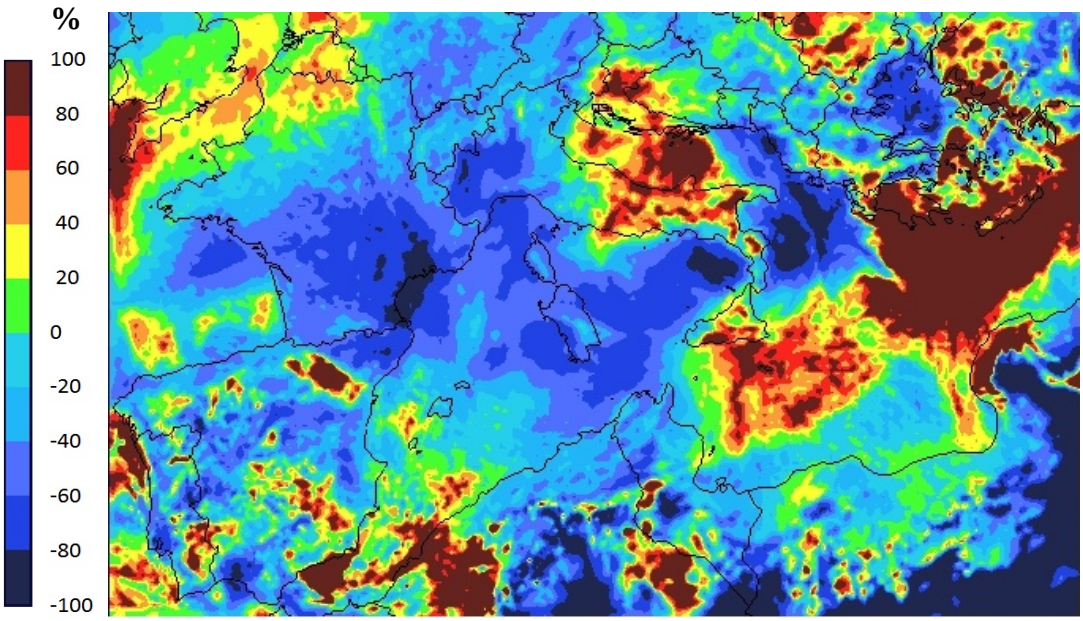

June

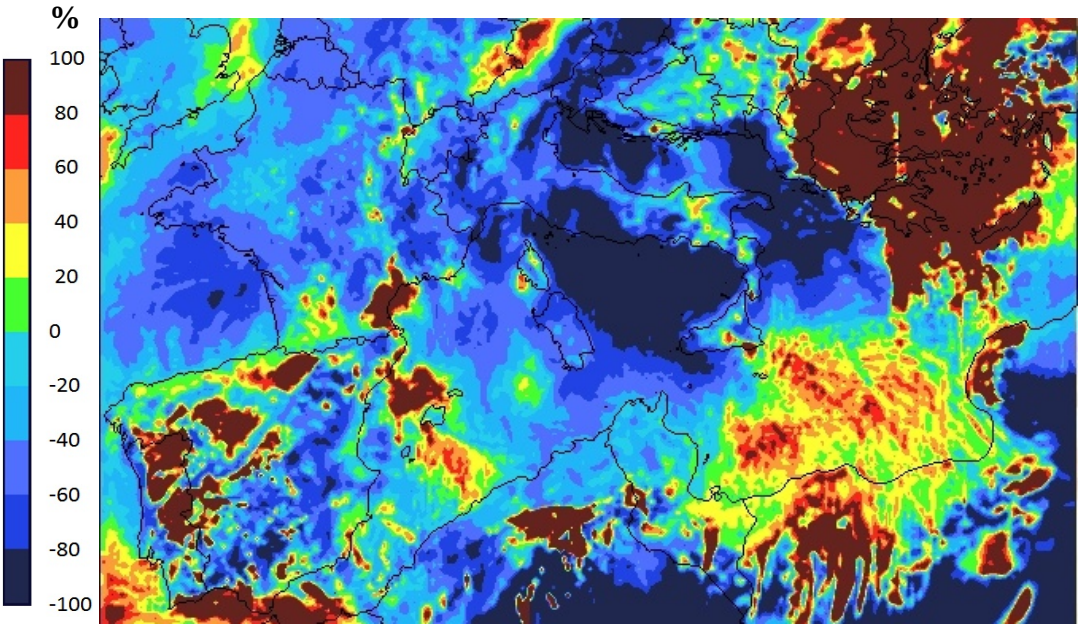

July

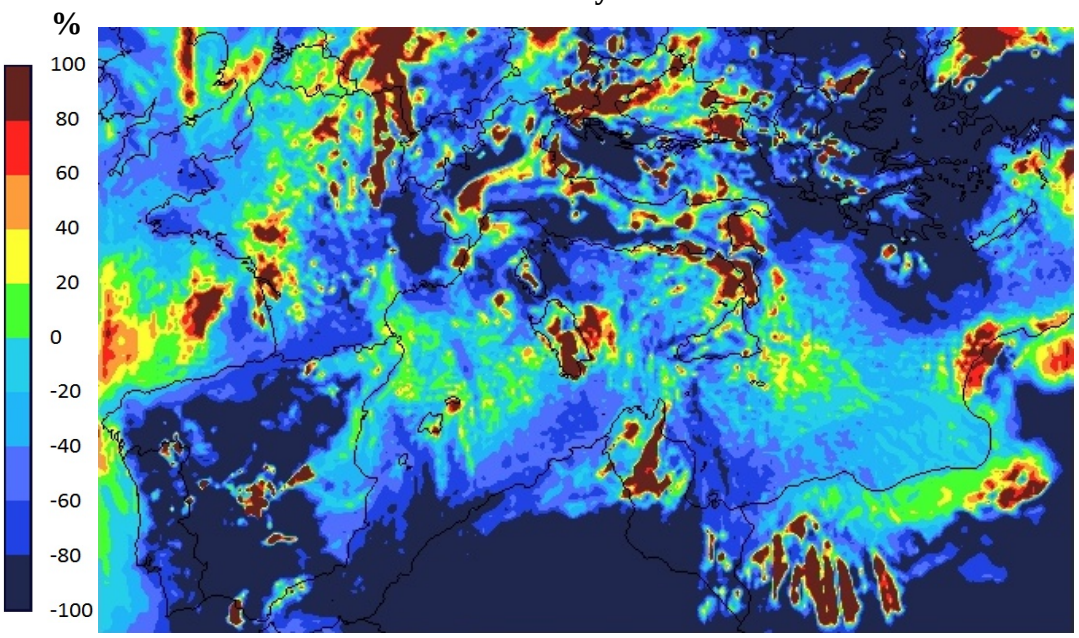

August

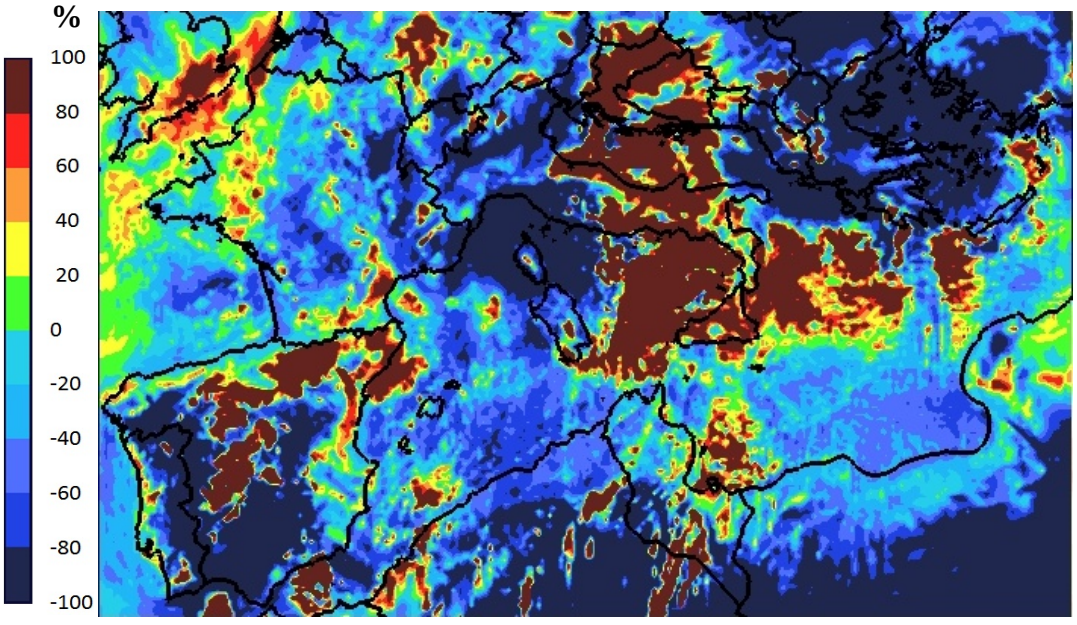

September

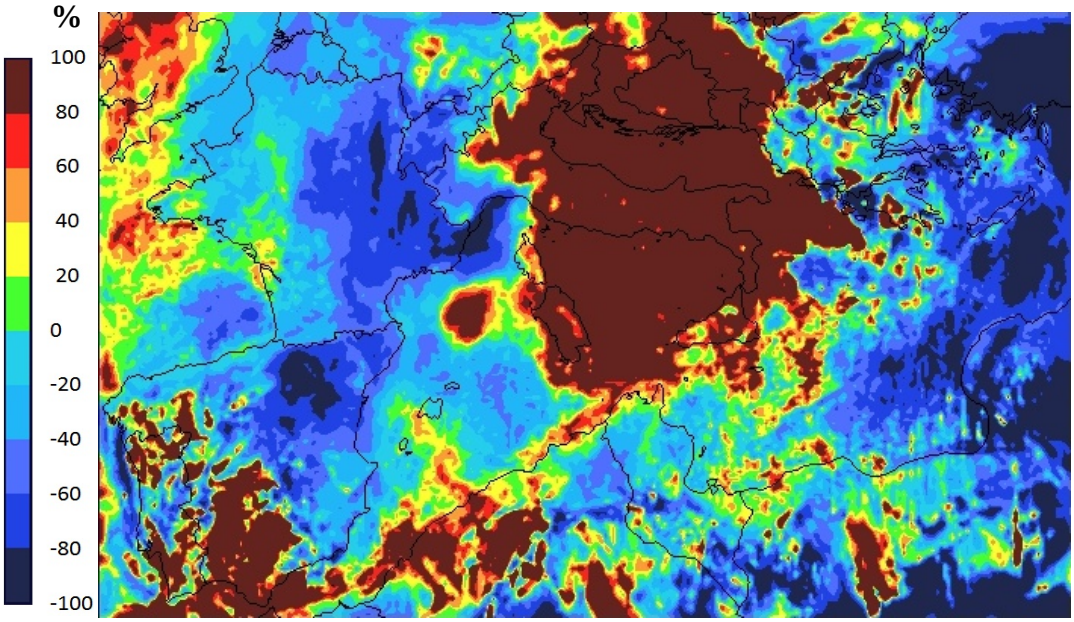

October

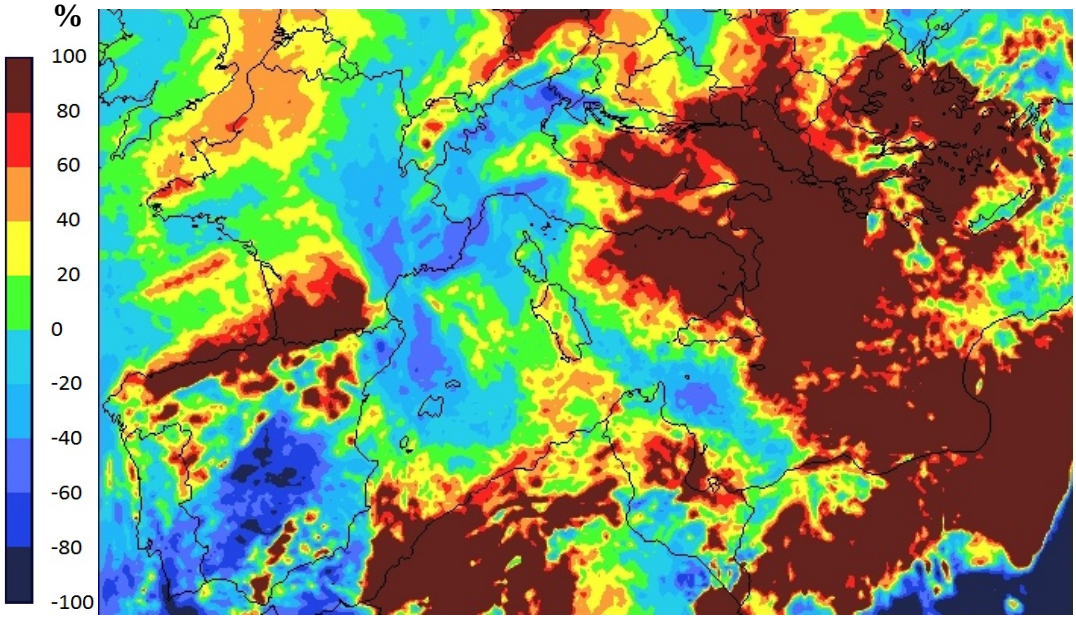

November

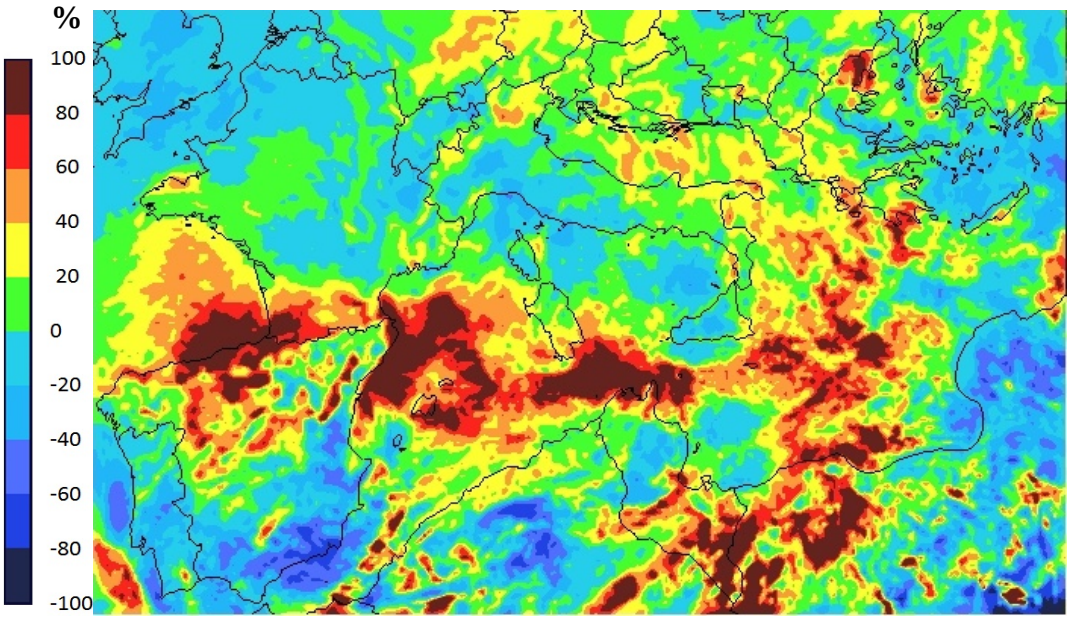

December

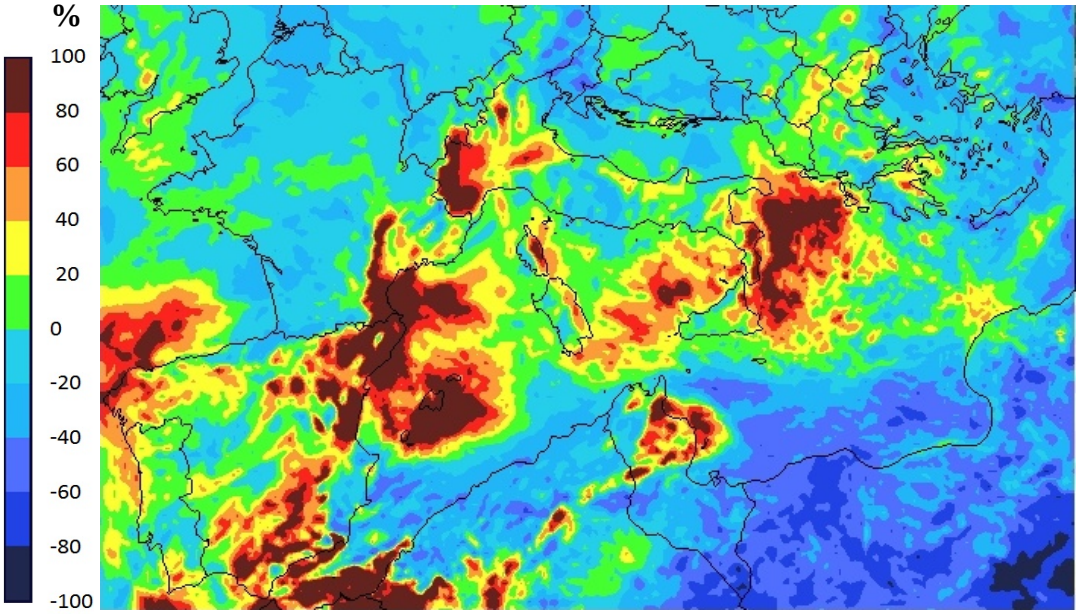

Annex 5: Monthly average temperature change for RCP4.5

January

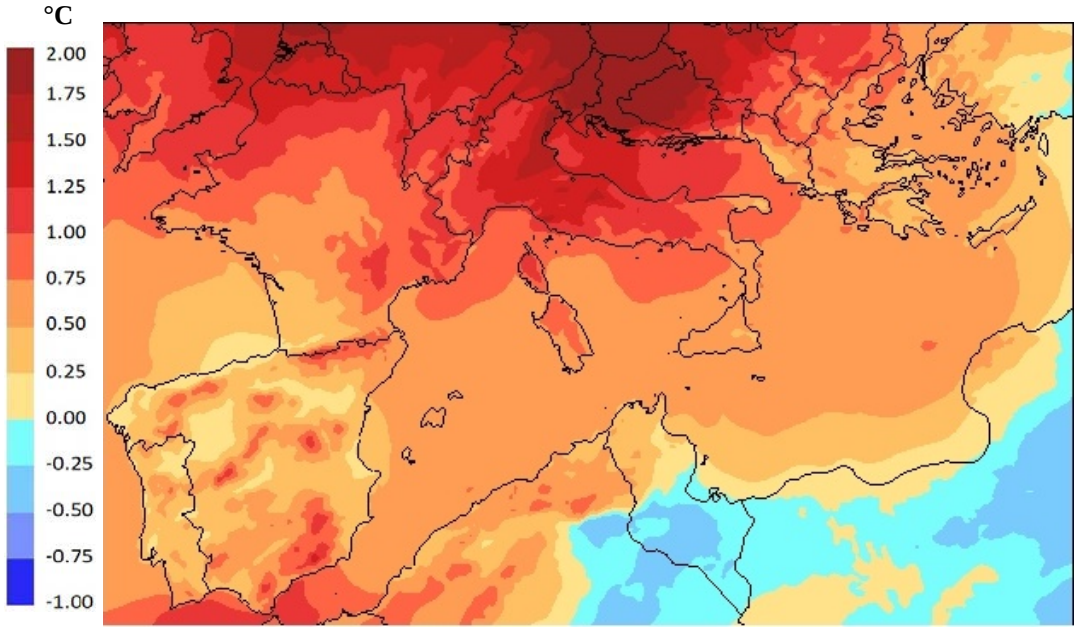

February

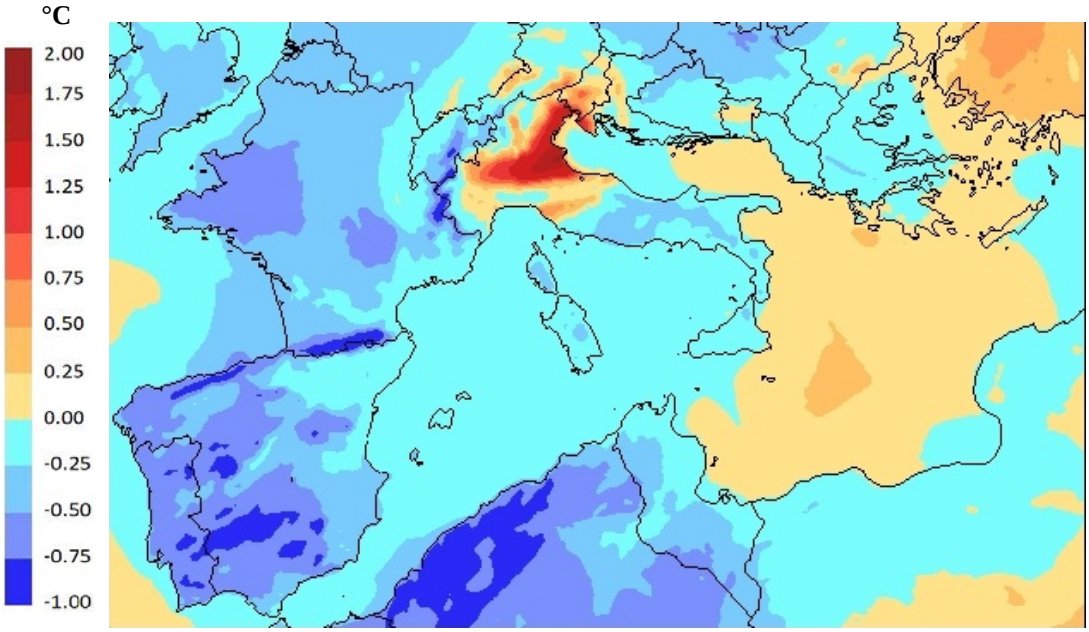

March

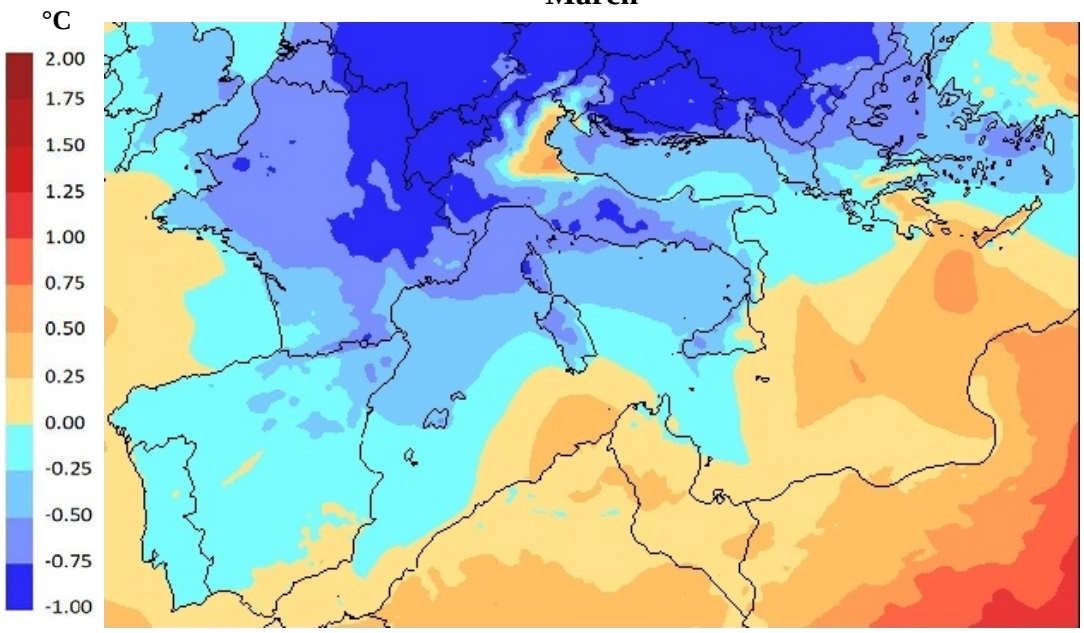
°C
2.00
1.75
1.50
1.25
1.00
0.75
0.50
0.25
0.00
-0.25
-0.50
-0.75
-1.00

April

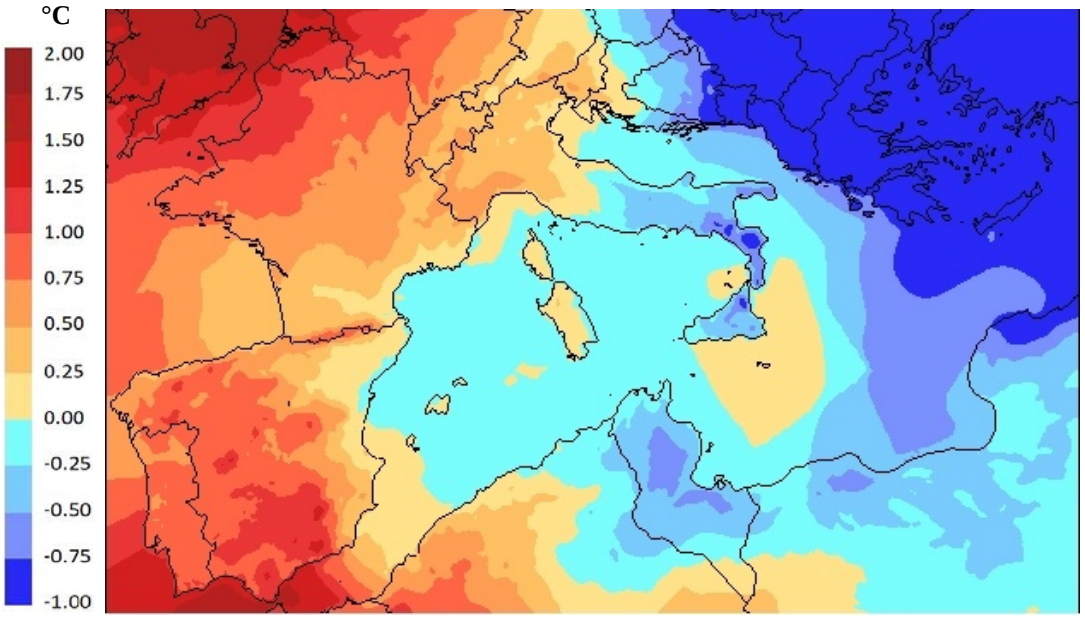
°C
2.00
1.75
1.50
1.25
1.00
0.75
0.50
0.25
0.00
-0.25
-0.50
-0.75
-1.00

May

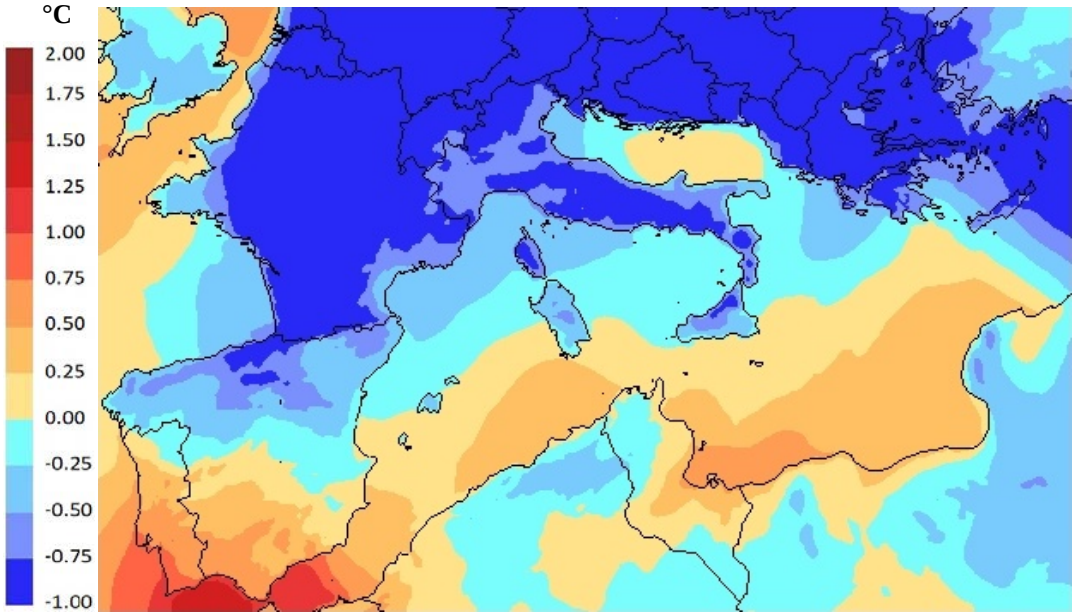
°C
2.00
1.75
1.50
1.25
1.00
0.75
0.50
0.25
0.00
-0.25
-0.50
-0.75
-1.00

June

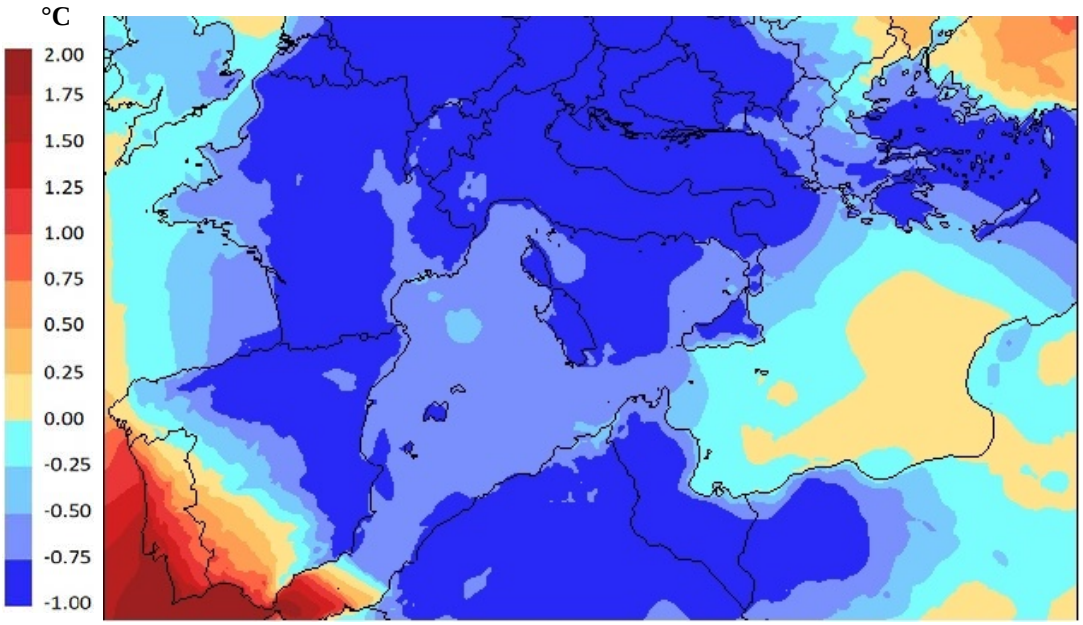
°C
2.00
1.75
1.50
1.25
1.00
0.75
0.50
0.25
0.00
-0.25
-0.50
-0.75
-1.00

July

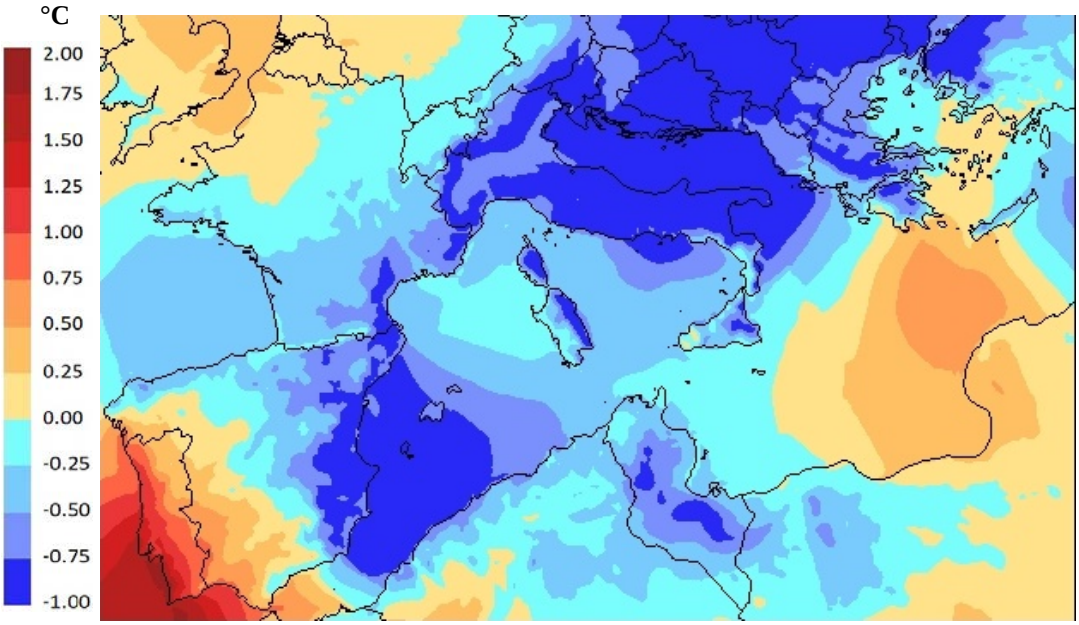
°C
2.00
1.75
1.50
1.25
1.00
0.75
0.50
0.25
0.00
-0.25
-0.50
-0.75
-1.00

August

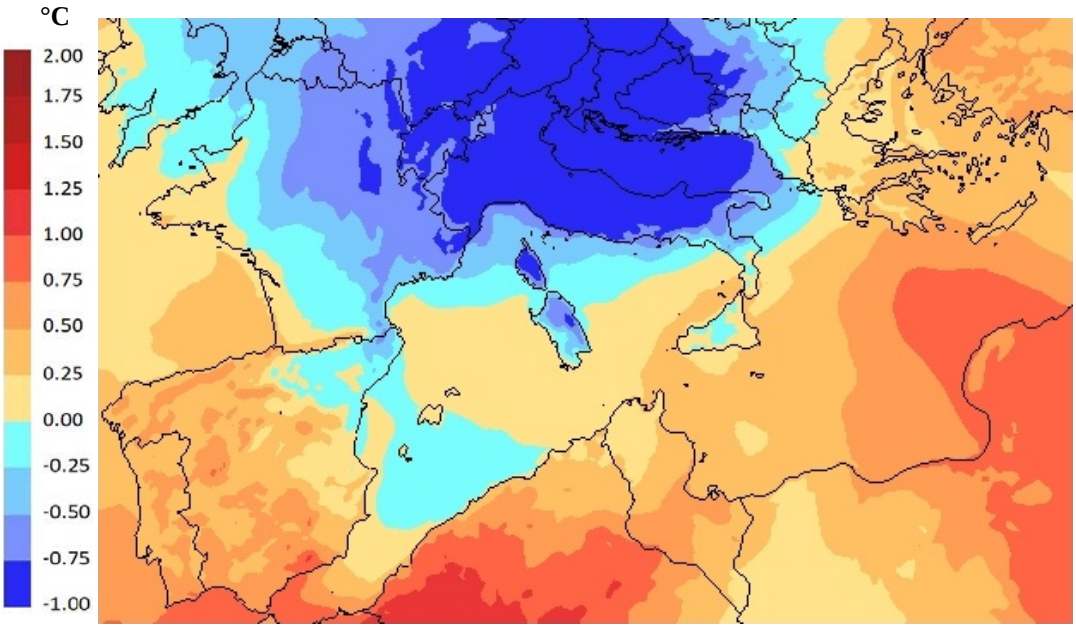
°C
2.00
1.75
1.50
1.25
1.00
0.75
0.50
0.25
0.00
-0.25
-0.50
-0.75
-1.00

September

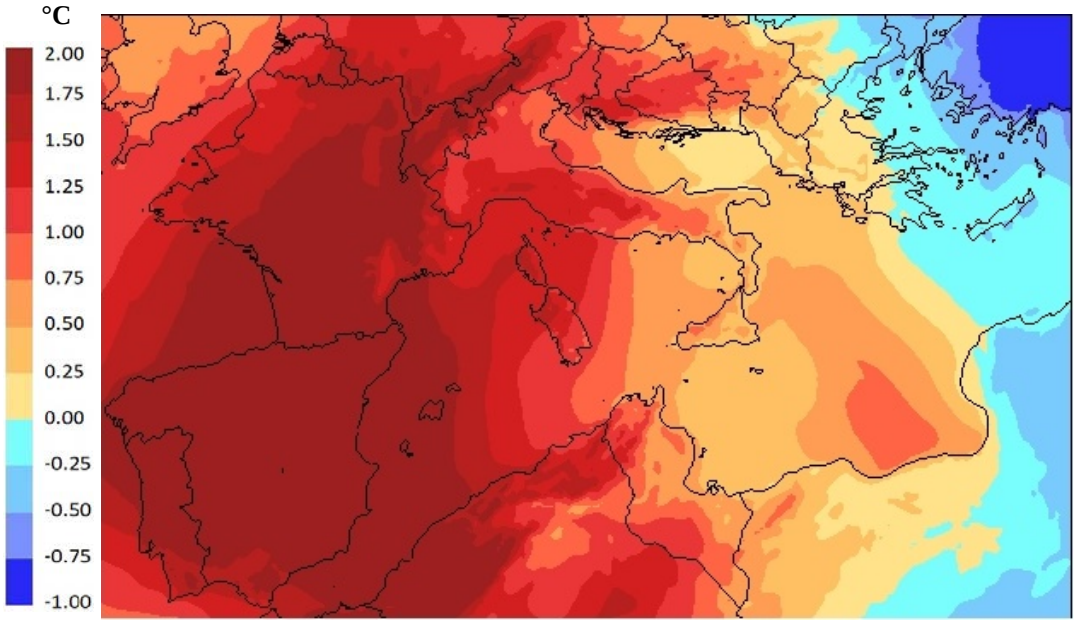

October

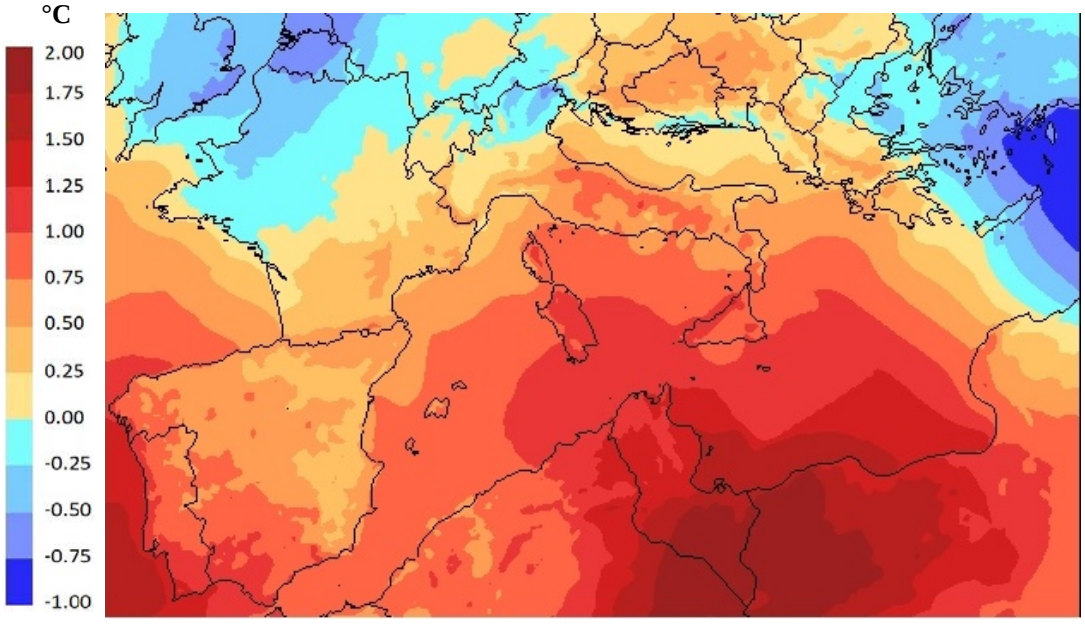

November

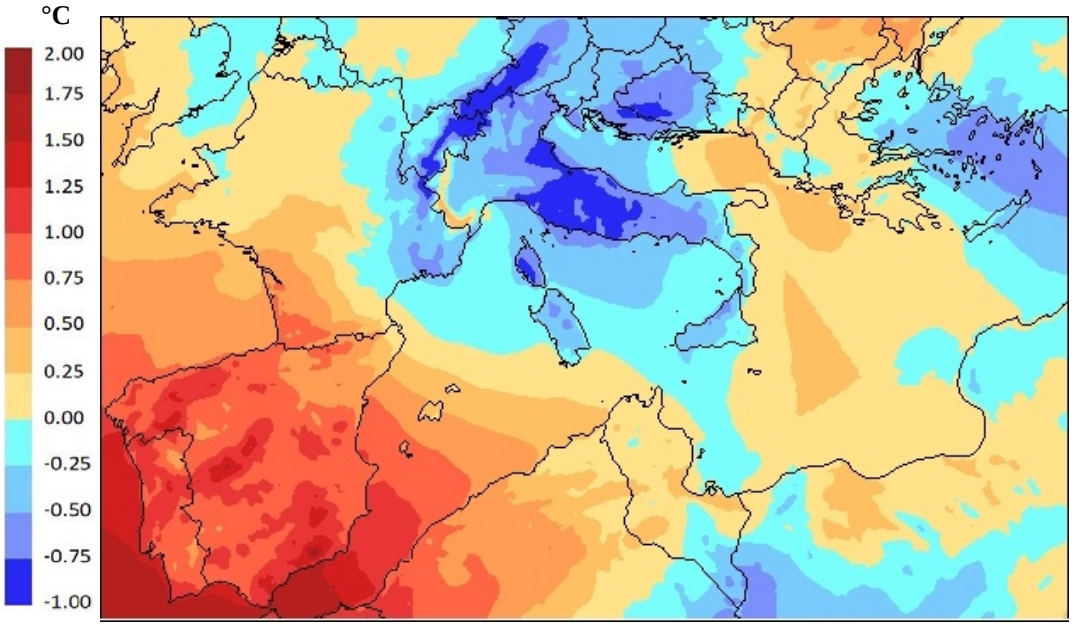

December

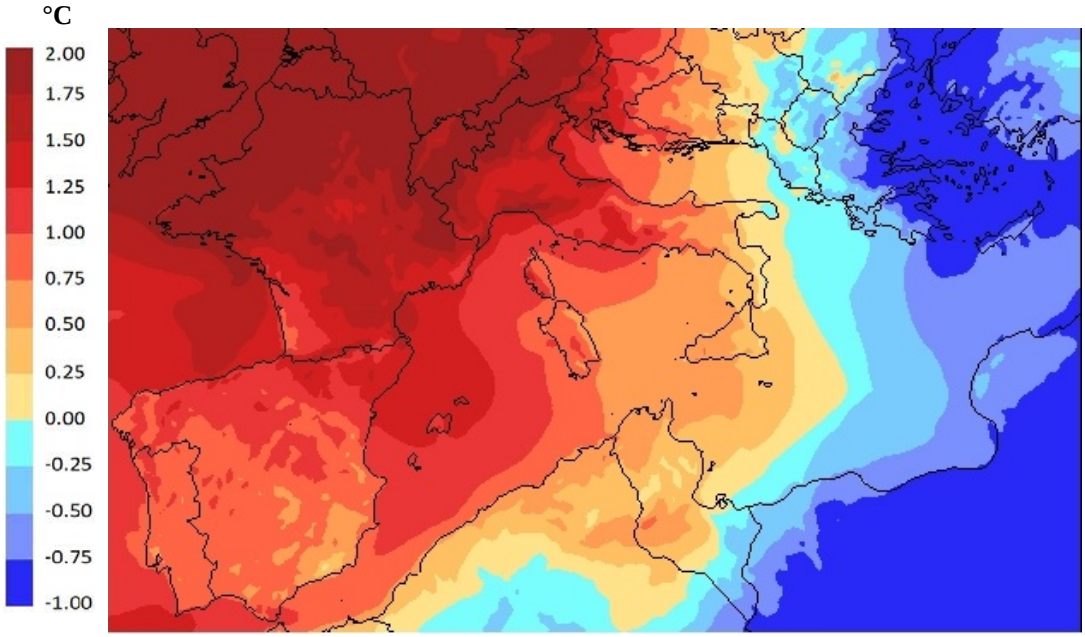

Annex 6: Monthly average precipitation change for RCP4.5

January

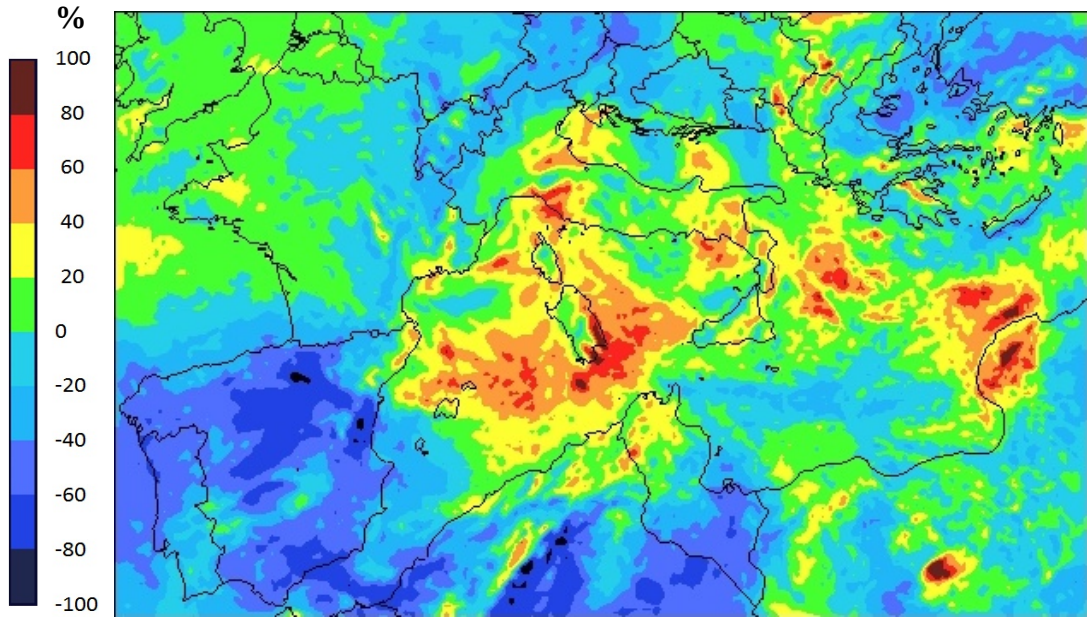

February

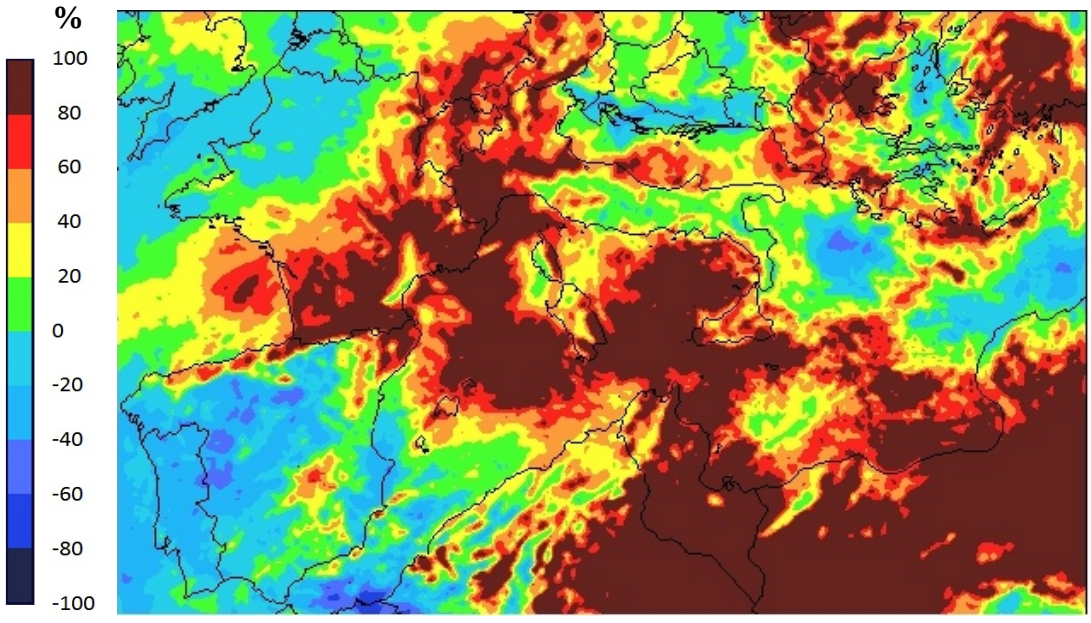

March

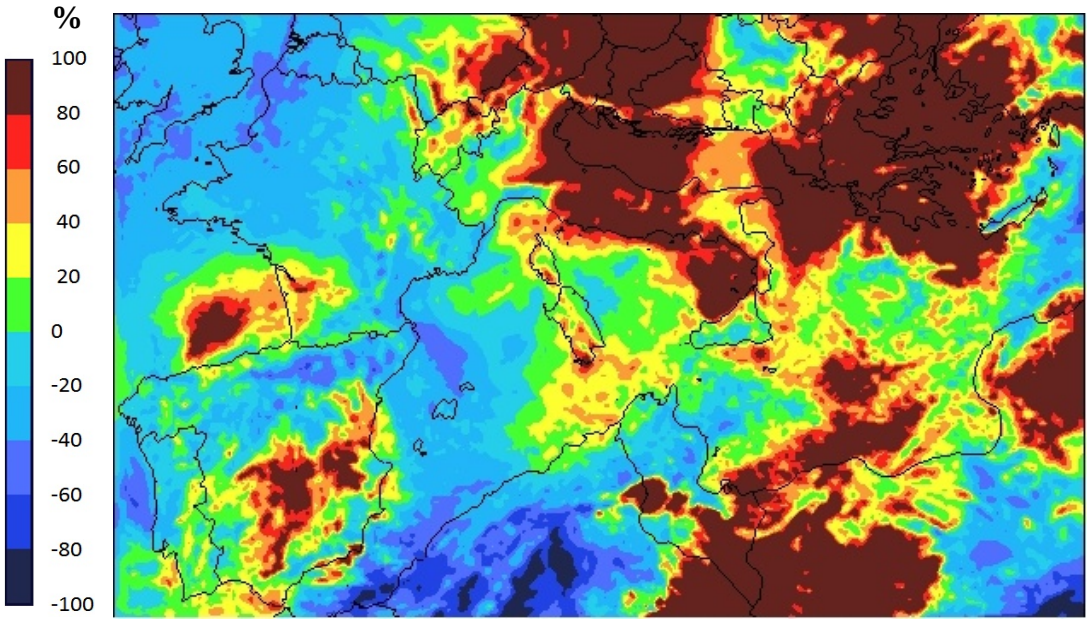

April

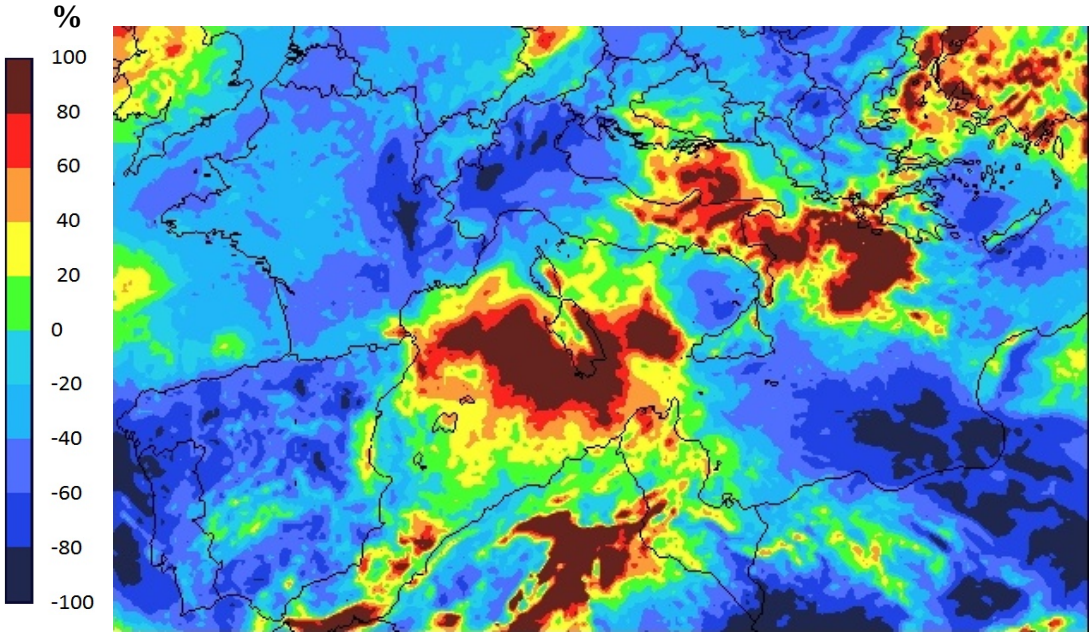

May

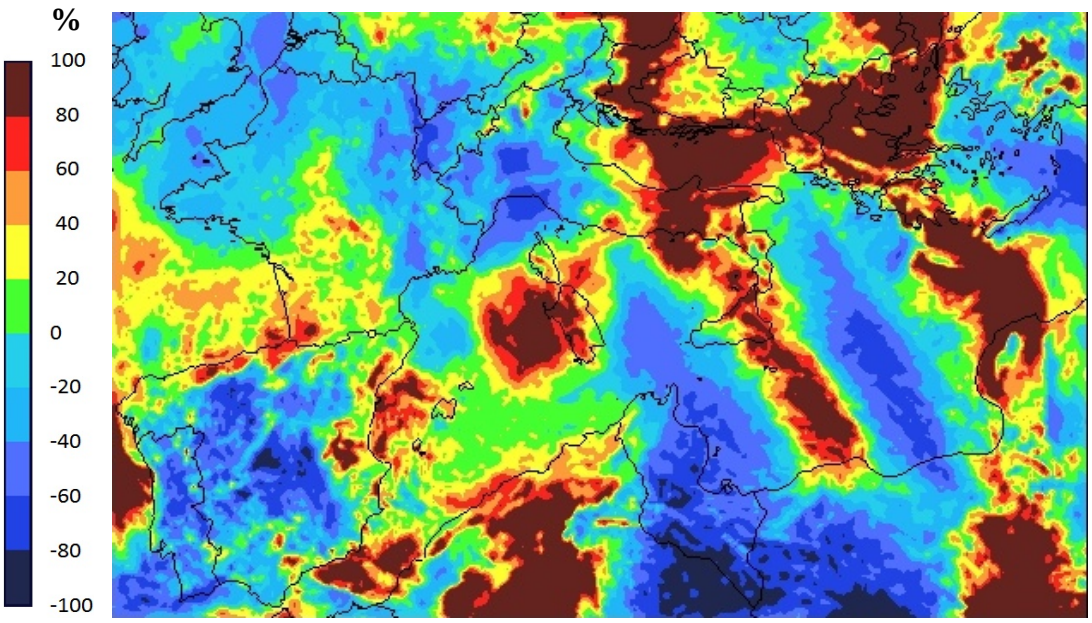

June

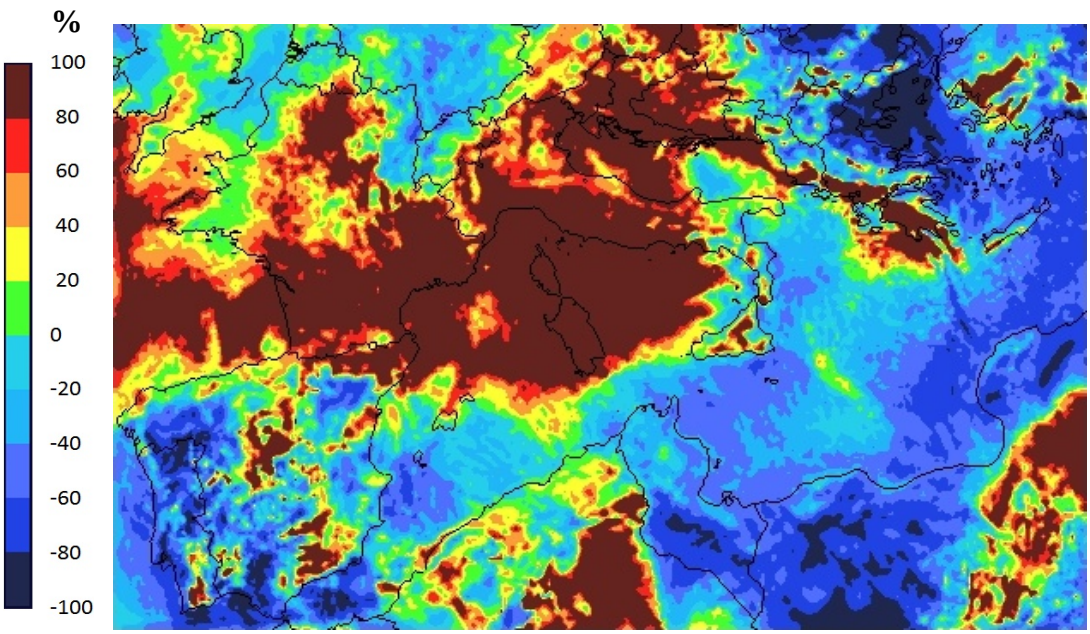

July

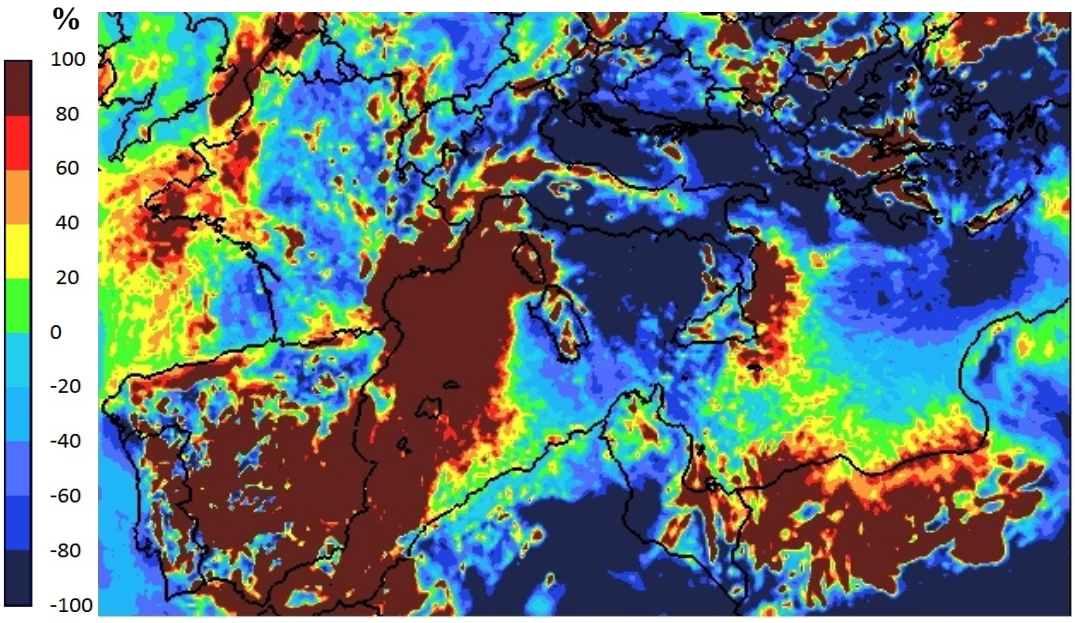

August

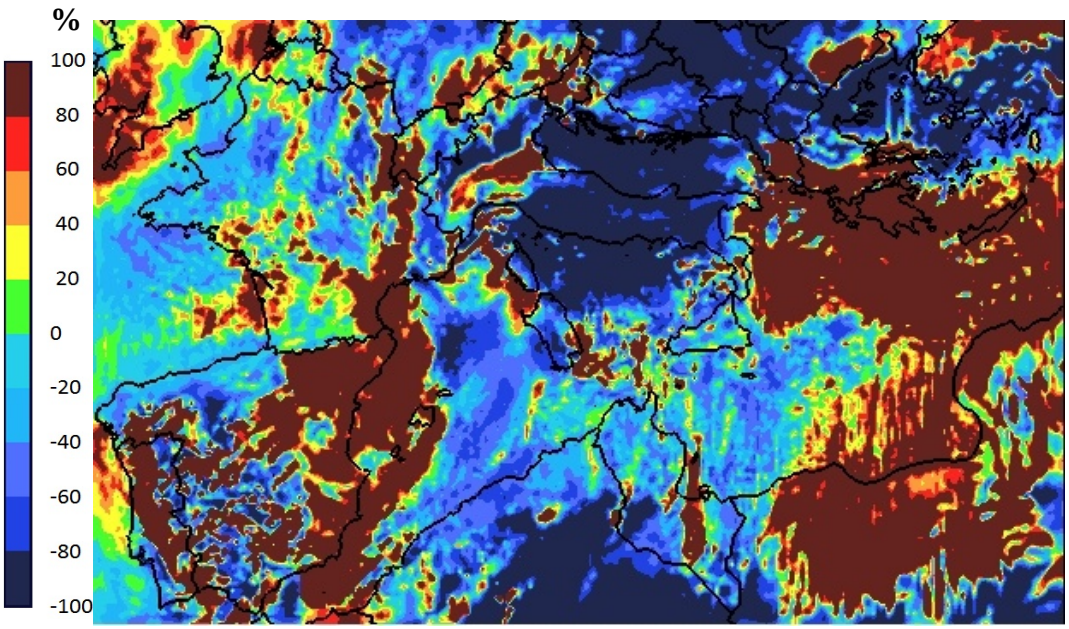

September

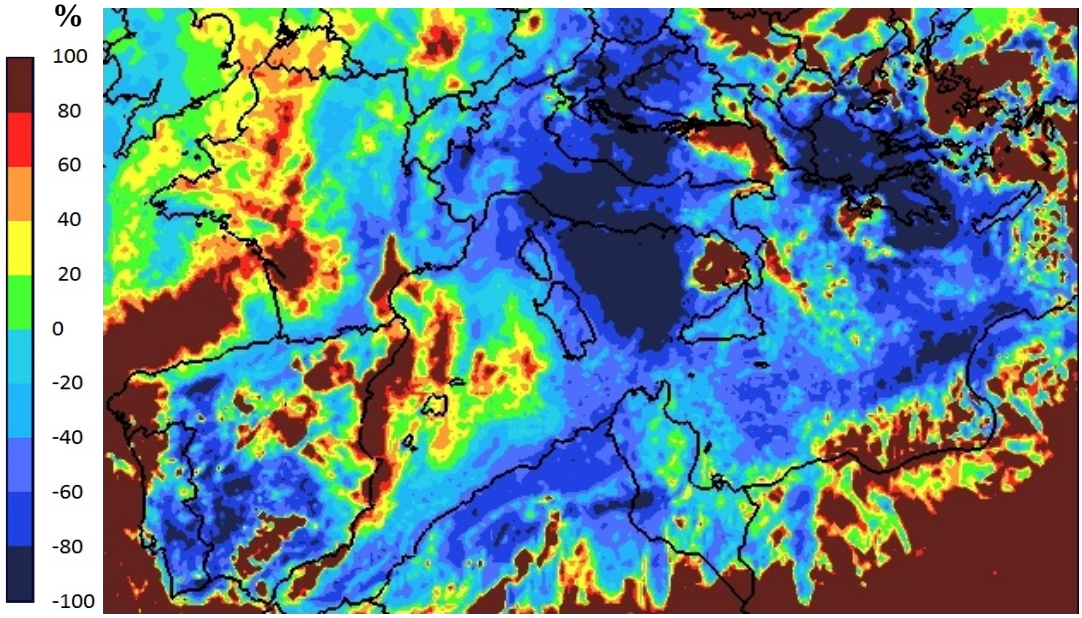

October

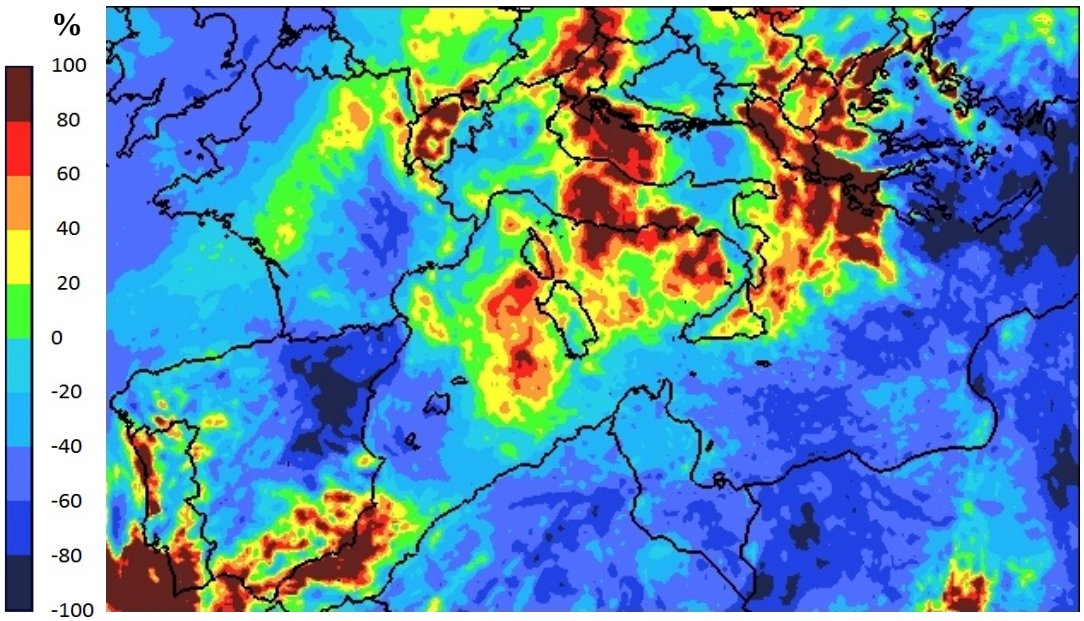

November

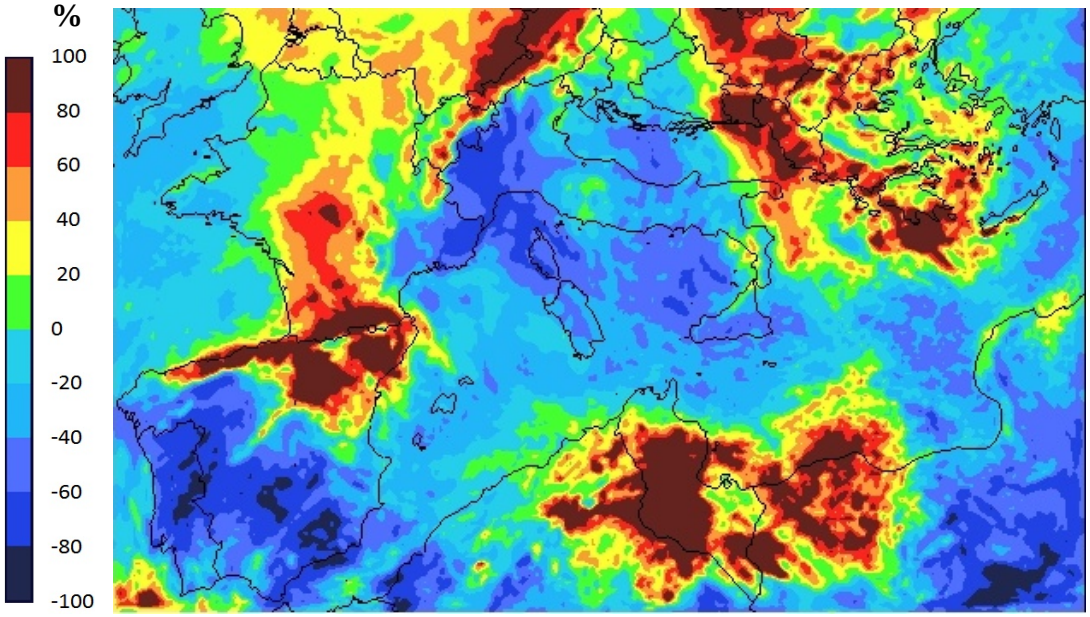
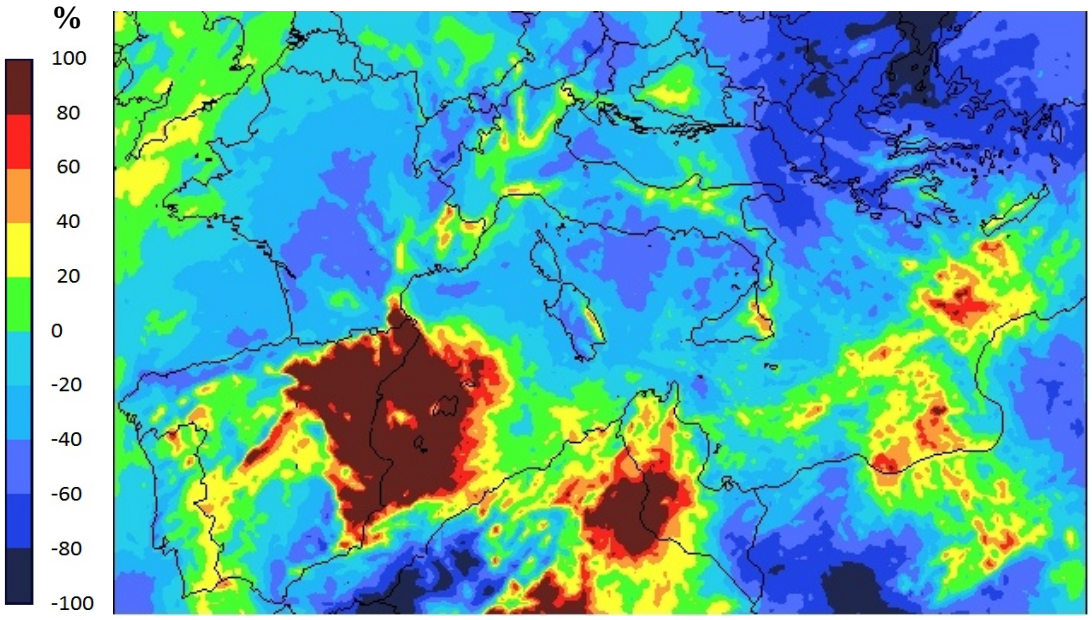
December